Studies on Specific Adsorption and Reaction Mechanism of Porphyrin Compounds at the Liquid-Liquid Interface

by

Hirohisa Nagatani

Department of Chemistry
Graduate School of Science
Osaka University

February, 1999

Contents

Chapter 1

General Introduction

The mechanism of bulk phase reactions, *e.g.*, acid-base equilibrium and metal complexation in an aqueous phase, has been widely studied up to the present and many methods to achieve the kinetic measurement have been developed.[1] On the other hand, the reaction which proceeds at the liquid-liquid interface has been less understood. The liquid-liquid interface is the specific reaction field and the investigation of its role and function is thought to be very important to understand the kinetics and mechanism of the solvent extraction[2,3] and the biochemical reaction.[4] Recently, the role of the liquid-liquid interface was demonstrated in the kinetic mechanisms of chelate, ion-association and synergistic extractions.[5,6] The researches concerning the chemical reaction at the liquid-liquid interface, however, have not been carried out extensively, since only limited numbers of methods and devices have been developed for the studies of the chemical reaction and the adsorption equilibrium at the liquid-liquid interface.

Previously, the interfacial adsorption and reaction had been studied by means of the stirred cell, the interfacial tension lowering, the electrochemical method.[7-9] However, each method has a few disadvantages, *i.e.*, low-sensitivity, indirect detection of the interfacial species and amount, limitation on the organic solvent, restricted time range in the kinetic measurement, etc. Thus, a new *in situ* method, which is sensitive to the interfacial species and available in the kinetic measurement, is in demand.

The porphyrins and their derivatives are one of the most important and valuable reagent in biochemistry and analytical chemistry. The porphyrin compounds have been well studied in the model system of biological reactions,[10,11] *i.e.* photoenergy conversion, enzymic reaction and mass transfer, and noted as an ionophore with anti-Hofmeister selectivity,[12-14] a sensitive reagent in the molecular recognition[15] and the trace determination of metal ions.[16,17] There are many reports relating equilibrium and kinetics of porphyrin compounds in the homogeneous system. Although many biological reactions *in vivo* occur in the heterogeneous system such as the surface and boundary of the biomembrane, studies on the reaction at the interface are less than those in the bulk phase. These situations suggest that the investigation towards the interfacial adsorption reaction of porphyrin compounds is of great value.

This thesis comprises the result from investigations towards the interfacial adsorption and reaction mechanism of hydrophobic porphyrin compounds in the immiscible two-phase

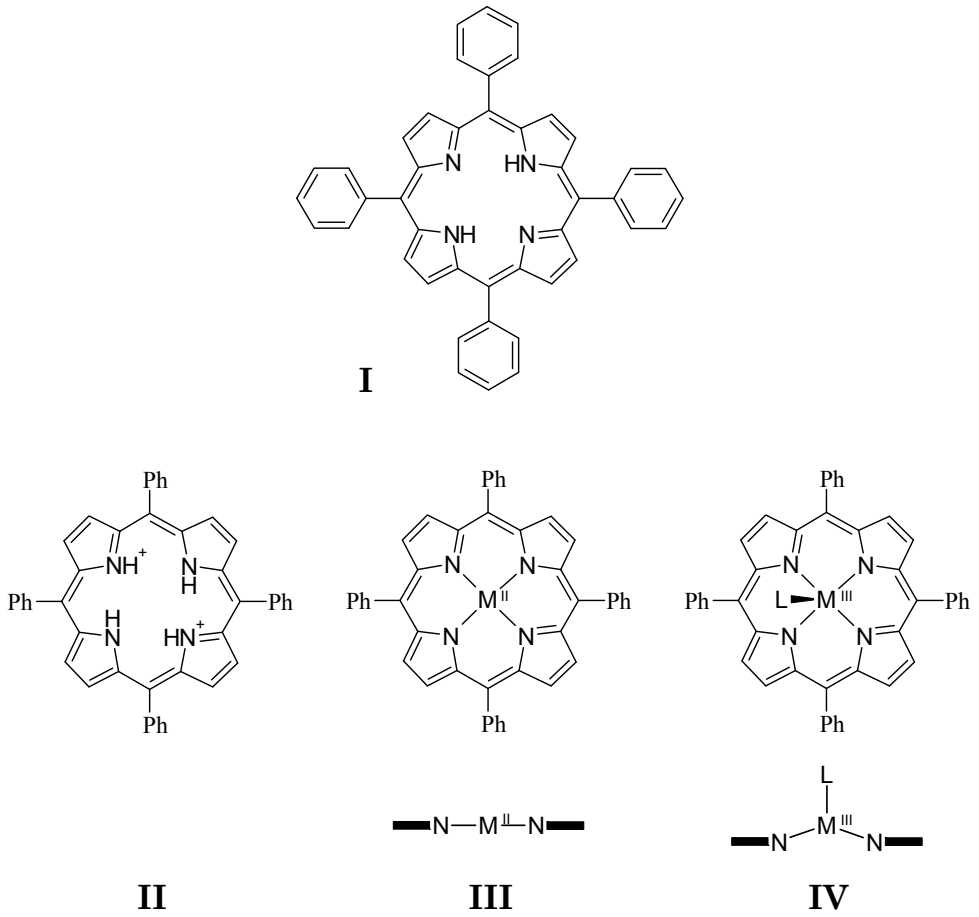

Figure 1.1. The molecular structures of 5,10,15,20-tetraphenylporphyrin and corresponding compounds studied in this thesis. (**I**) The free base (H_2TPP), (**II**) the diprotonated species (H_4TPP^{2+}), (**III**) the divalent and (**IV**) the trivalent metal complexes. M and L denote the central metal atom and the axial ligand such as chloride ion, respectively. In general, the divalent metal complex of TPP is almost a planar molecule and the central metal atom of the trivalent metal complex is displaced from the pyrrole ring plane towards the axial ligand.

system studied by various techniques including new *in situ* methods. In Chapters 2 and 3, the adsorption behavior and reaction mechanism of metal complexes of 5,10,15,20-tetraphenylporphyrin (H_2TPP) resulted from the high-speed stirring experiments are described in detail. The high-speed stirring method was developed in 1980's and it is very useful for the measurement of the interfacial adsorptivity of reagent dissolved in an organic phase.[5] The organic phase can be continuously separated from the dispersed liquid-liquid system by means of a Teflon® phase separator and the amount of interfacial adsorption is determined by evaluating the concentration change of bulk organic phase. In Chapter 2, the interfacial adsorptivity of divalent metalloporphyrins, *i.e.* cobalt(II), nickel(II), copper(II),

zinc(II) and vanadyl(IV), in the dodecane-water system is elucidated. The result of the investigation towards the interfacial adsorptivity of iron(III) complexes of TPP and the formation of μ-oxo-bis[(5,10,15,20-tetraphenylporphyrinato)iron(III)] ($(FeTPP)_2O$) at the dodecane-aqueous acid interface are expatiated in Chapter 3. The formation of $(FeTPP)_2O$ in the acidic condition was found out for the first time and the interfacial adsorption mechanism of iron(III) complexes was elucidated.

In Chapters 4-6, new *in situ* spectrophotometric methods, the two-phase stopped-flow method and the centrifugal liquid membrane method, which can determine the interfacial species directly, are invented and their applications to the kinetic measurement of the interfacial reaction are described. The two-phase stopped-flow method is one of the most sensitive methods against the interfacial species. It can produce the dispersed droplet system rapidly and be applied to a fast interfacial reaction for sub-second. In Chapter 4, the rate-determining step of the diprotonation of H_2TPP at the liquid-liquid interface is discussed in detail. The centrifugal liquid membrane (CLM) method in Chapters 5 and 6 can form a stable two-phase liquid membrane of tens μm thickness in a rotating optical cell. The two-phase liquid membrane system is produced by the centrifugal force and the interfacial area is kept constant throughout the experiment. The CLM method can also determine the interfacial species spectrophotometrically and it is available in a relatively slow reaction compared with the two-phase stopped-flow method. The equilibrium and kinetics of the protonation of the free base TPP and the demetallation of (5,10,15,20-tetraphenylporphyrinato)zinc(II) (ZnTPP) at the liquid-liquid interface are shown in Chapter 5. The rate-determining step of the interfacial demetallation is different from that of the bulk phase reaction and the specificity of the liquid-liquid interface as a reaction field is pronouncedly demonstrated. The fluorescence quenching reaction between ZnTPP in an organic phase and methylviologen as a quencher in an aqueous phase is described in Chapter 6. The quenching reaction is only proceeded at the interface in the presence of anionic surfactant, *i.e.* sodium dodecyl sulfate (SDS), since methylviologen dication in an aqueous phase can be provided to the interface by the ion-association adsorption with the negatively charged SDS^-.

References

(1) Batt, L.; Hague, D. N. In *Comprehensive Chemical Kinetics*, *Vol. 1*; Bamford, C. H., Tipper, C. F. H. Eds.; Elsevier: Amsterdam, 1969; Chapters 1 and 2.

(2) *Science and Practice of Liquid-Liquid Extraction*; Thornton, D. J. Ed.; Oxford University Press: New York, 1992.

(3) *Principles and Practices of Solvent Extraction*; Rydberg, J., Musikas, C., Choppin, R. G., Eds.; Marcel Dekker, Inc.: New York, 1992.

(4) Volkov, A. G.; Deamer, D. W.; Tanelian, D. L.; Markin, V. S. *Liquid Interfaces in Chemistry and Biology*; John Wiley & Sons, Inc.: New York, 1998.

(5) Watarai, H. *Trends Anal. Chem.*, **1993**, *12*, 313-318.

(6) Freiser, H. *Chem. Rev.*, **1988**, *88*, 611-616.

(7) Hanna, G. J.; Noble, R. D. *Chem. Rev.*, **1985**, *85*, 583-598.

(8) Danesi, P.R.; Chiarizia, R. *CRC Crit. Rev. Anal. Chem.*, **1980**, *10*, 1-126.

(9) *Liquid-Liquid Interfaces, Theory and Methods*; Volkov, A. G., Deamer, D. W., Eds.; CRC Press: Boca Raton, 1996.

(10) Falk, J. E. *Porphyrins and Metalloporphyrins*; Smith, K. M. Ed.; Elsevier: New York, 1975.

(11) Dolphin, D. *The Porphyrins*; Academic Press: New York, 1978.

(12) Ammann, D.; Huser, M.; Krautler, B.; Rusterholz, B.; Schulthess, P.; Lindemann, B.; Halder, E.; Simon, W. *Helv. Chim. Acta*, **1986**, *69*, 849-854.

(13) Chaniotakis, N. A.; Chasser, A. M.; Meyerhoff, M. E.; Groves, J. T. *Anal. Chem.*, **1988**, *60*, 185-191.

(14) Gao, D.; Li, J. Z.; Yu, R. Q.; Zheng, G. D. *Anal. Chem.*, **1994**, *66*, 2245-2249.

(15) Takeuchi, M.; Imada, T.; Shinkai, S. *Bull. Chem. Soc. Jpn.*, **1998**, *71*, 1117-1123.

(16) Tabata, M.; Tanaka, M. *Trends Anal. Chem.*, **1991**, *10*, 128-133.

(17) Ueno, K.; Imamura T.; Chang, K. L. *Hand Book of Organic Analytical Reagents* 2nd ed.; CRC Press: Boca Raton, 1992, pp 417-425.

Chapter 2

Specific Adsorption of Divalent Metalloporphyrins at Dodecane-Water Interface

Abstract

The interfacial adsorption of the divalent metal complexes of 5,10-15,20-tetraphenylporphyrin (H_2TPP) was found out in the dodecane-water system by means of the high-speed stirring method. Among metalloporphyrins of five metals examined, zinc(II) and vanadyl(IV) complexes showed appreciable adsorptivity at dodecane-water interface and the interfacial adsorption constants were determined by analyzing the adsorption isotherms with Langmuir isotherm. The interfacial adsorptivity of metalloporphyrins decreased in the order, Zn^{II}TPP > V^{IV}OTPP > Co^{II}TPP, Ni^{II}TPP, Cu^{II}TPP.

2.1 INTRODUCTION

The investigation of the adsorption behavior of metalloporphyrins at the liquid-liquid interface is thought to be very important to understand the roles of the interface in liquid-liquid separation as well as to understand the catalytic activities of porphyrin derivatives in liquid-membrane systems.

In the liquid-liquid system, the interfacial adsorptivity of a solute is usually measured by means of an interfacial tension lowering.[1,2] This method, however, can not be applied for the solute which is sparingly soluble and can not offer any information about chemical species which may be adsorbed at the liquid-liquid interface. On the contrary, a high-speed stirring method can be applied for a dilute solution provided that the concentration of the solute is measurable by spectrophotometry.[3] Furthermore, the chemical species responsible for the adsorption can also be determined. The metal complexes of 5,10,15,20-tetraphenylporphyrin (H_2TPP) are especially well suited for spectrophotometric studies, because they have large molar absorptivity at the Soret band. Since the metalloporphyrins derived from H_2TPP are highly hydrophobic, the dissolution into aqueous phase could be neglected in the present study. In this Chapter, the adsorption behavior of several metal complexes of TPP as a model compound of biological porphyrin derivatives from a bulk dodecane phase to dodecane-water interface was evaluated by employing the high-speed stirring method.

2.2 EXPERIMENTAL SECTION

Reagents. The complexes of cobalt(II), nickel(II), copper(II) and zinc(II) were prepared from 5,10,15,20-tetraphenylporphyrin (Dojindo Laboratories) (Figure 1.1) and the corresponding metal acetate by the method available in literature.[4] The hydrated metal acetates, *i.e.* Co(CH$_3$COO)2·4H2O, Ni(CH$_3$COO)$_2$·4H$_2$O, Cu(CH$_3$COO)$_2$·2H$_2$O and Zn(CH$_3$COO)$_2$·2H$_2$O, and (5,10,15,20-Tetraphenylporphyrinato)vanadyl(IV) (VOTPP) were obtained from Wako Chemicals and used without further purification. The absorption spectra of synthesized metalloporphyrins in dodecane are shown in Figure 2.2 and 2.3. 2-Hydroxy-5-nonyl-benzophenone oxime (LIX65N), which used to determine the interfacial area, was isolated as a sodium salt from the commercial extractant (Henkel Japan Ltd.) and purified by the copper-complex method.[5] Dodecane, nacalai tesque G.R., was purified by distillation after being washed with a mixture of fuming sulfuric acid and sulfuric acid and used as an organic solvent. The other reagents used in this work were nacalai tesque G.R. grade and the aqueous phase was prepared by using a distilled and deionized water purified by the use of a Milli-Q SP.TOC.(Millipore).

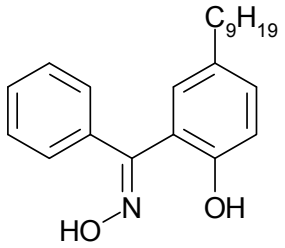

Figure 2.1. The molecular structure of LIX65N.

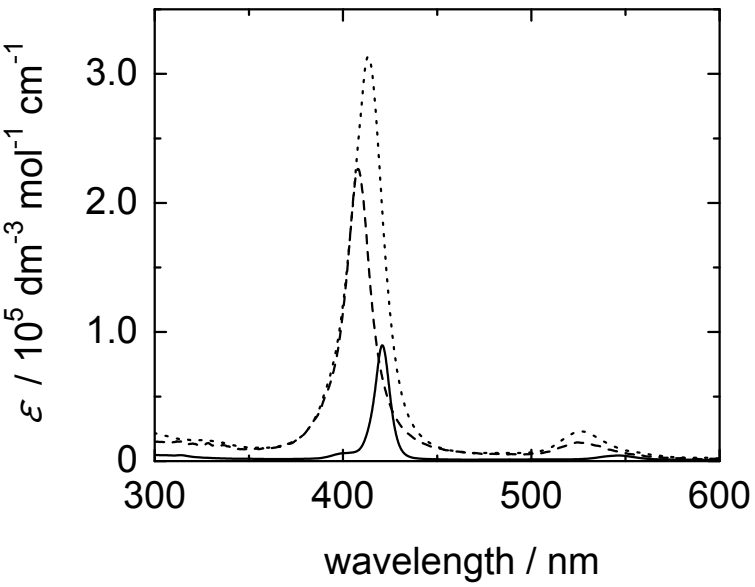

Figure 2.2. Absorption spectra of divalent metal complexes of TPP in dodecane. The solid line, broken line and dotted line denote V^{IV}OTPP, Co^{II}TPP and Ni^{II}TPP, respectively.

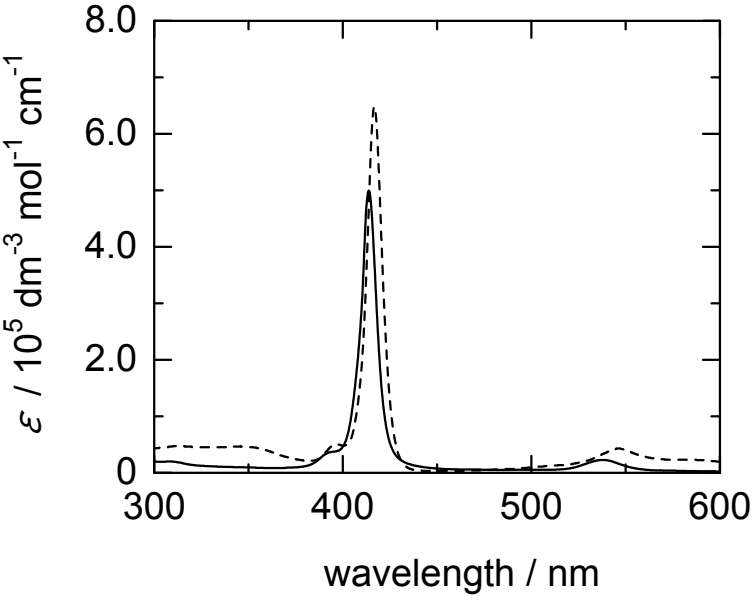

Figure 2.3. Absorption spectra of divalent metal complexes of TPP in dodecane. The solid line and broken line denote Zn^{II}TPP and Cu^{II}TPP, respectively.

High-Speed Stirring Experiments. The interfacial adsorption behavior of metalloporphyrins in the dispersed liquid-liquid system was observed by using the high-speed stirring apparatus shown in Figure 2.4. 50.0 cm^3 of dodecane phase containing a metalloporphyrin and the same volume of an aqueous phase were put into the stirring cell thermostated at 298±1 K. The extent of dispersion of the liquid-liquid system was controlled by changing the rotation rate of the stirrer made up of polychlorotrifluoroethylene resin (PCTFE), with a motor speed controller (Nikko Keisoku, SC-5), from 200 rpm to 5000 rpm. The change of the two-phase system between the high-speed stirring and the low-speed stirring is illustrated in Figure 2.5. The high-speed stirring (5000 rpm) produced an emulsion state, while in the low-speed stirring (200 rpm) the emulsion was promptly separated to the clear phase. The absorption spectrum of an organic phase, that was continuously separated from the dispersed liquid-liquid system by means of a Teflon® phase separator and circulated through a flow cell, was measured by a photodiode array UV/Vis detector (Shimadzu, SPD-M6A). Thus, we could determine the amount of interfacial complex by evaluating the difference between the absorbances of the bulk organic phase under the high-speed stirring (5000 rpm) and the low-speed stirring (200 rpm) at the absorption maximum wavelength as shown in Figure 2.6(b).

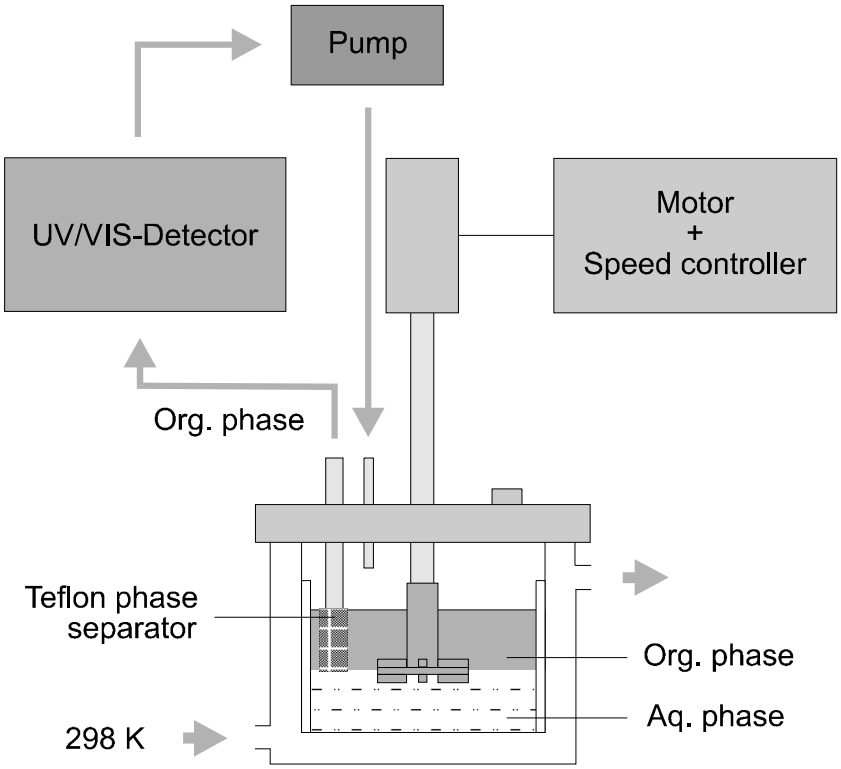

Figure 2.4. Schematic drawing of the high-speed stirring apparatus. An organic phase can be separated from the dispersed two-phase system by a Teflon® phase separator and continuously circulated in the instrument.

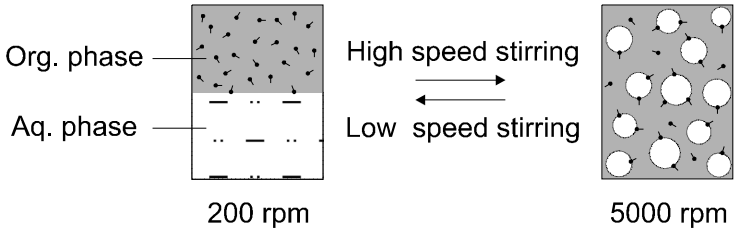

Figure 2.5. The change of the two-phase system between the low-speed stirring state and the high speed stirring state.

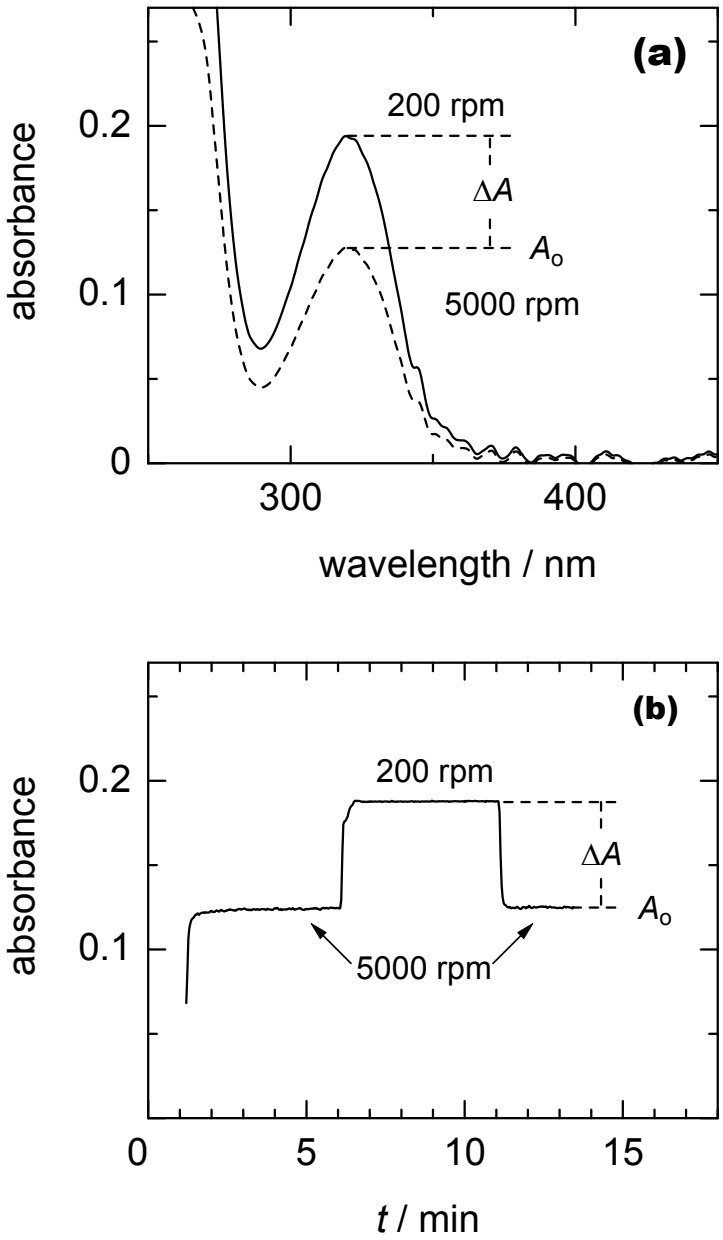

Figure 2.6. The spectral change (a) and the absorbance change (b) of the bulk organic phase in the high-speed stirring experiment for the LIX65N system. The absorbance change was measured at the absorption maximum wavelength of LIX65N, *i.e.*, 321 nm. The concentrations of LIX65N and perchloric acid were 4.94×10^{-5} mol dm^{-3} and 1.0×10^{-3} mol dm^{-3}, respectively.

Langmuir Isotherm. In the present system, Langmuir isotherm was given by

$$[\mathrm{MP}]_\mathrm{i} = \frac{aK'\,[\mathrm{MP}]_\mathrm{o}}{a + K'\,[\mathrm{MP}]_\mathrm{o}} \tag{2.1}$$

where $[\mathrm{MP}]_\mathrm{i}$ and $[\mathrm{MP}]_\mathrm{o}$ denote the concentrations of metalloporphyrin adsorbed at the liquid-liquid interface (mol dm^{-2}) and in the bulk organic phase (mol dm^{-3}), respectively. a is the saturated interfacial concentration (mol dm^{-2}) and K' is the interfacial adsorption constant (dm) defined under the condition of $a >> [\mathrm{MP}]_\mathrm{i}$,

$$K' = \frac{[\mathrm{MP}]_\mathrm{i}}{[\mathrm{MP}]_\mathrm{o}} \tag{2.2}$$

The difference between absorbances of the bulk organic phase under the high-speed stirring and the low-speed stirring, ΔA and the absorbance of the bulk organic phase under the high-speed stirring, A_o can be described as follows,

$$\Delta A = \varepsilon\, l\, [\mathrm{MP}]_\mathrm{i}\, S_\mathrm{i} / V_\mathrm{o} \tag{2.3}$$

$$A_\mathrm{o} = \varepsilon\, l\, [\mathrm{MP}]_\mathrm{o} \tag{2.4}$$

where ε, l, S_i and V_o are the molar absorptivity in dodecane, the optical path length (1.0 cm), the total interfacial area and the organic phase volume, respectively.

Interfacial Tension Measurements. The interfacial tension of the dodecane-water system was measured by employing a drop volume method with the automatic buret (Metrohm, Multi-Dosimat Model 655). The two phases were put into a water-jacketed vessel and thermostated at 298±0.1 K all through the measurement. The aqueous phase was perchloric acid solution of 1.0×10^{-3} mol dm^{-3} and the ionic strength was maintained at 0.10 by the addition of sodium perchlorate. The concentration of LIX65N in dodecane was changed from 8.4×10^{-7} mol dm^{-3} to 1.2×10^{-2} mol dm^{-3}.

2.3 RESULTS AND DISCUSSION

2.3.1 Determination of the Interfacial Area

The total interfacial area, S_i, in the dodecane-water system was evaluated from individual high-speed stirring experiments and interfacial tension measurements for the hydrophobic oxime, *i.e.*, LIX65N shown in Figure 2.1. The interfacial adsorptivity of β-hydroxyl oximes in the other solvent systems have been investigated by Watarai *et al*. and it was predicted that the adsorption resulted from the hydrophilic hydroxyl and oxime groups (=N-OH).[6-8] The adsorption isotherm of LIX65N was measured by the same apparatus used for the experiment of metalloporphyrins. The interfacial tension measurements were carried out in the dodecane-water system by employing a drop volume method. The adsorption isotherm and the plots of the interfacial tensions measured in dodecane-water system are shown in Figure 2.7 and 2.8, respectively. In both measurements, the aqueous phase was perchloric acid solution of 1.0×10^{-3} mol dm^{-3} and the ionic strength was maintained at 0.10. Since the pK_a value of LIX65N was reported as 8.70,[9] it can be expected that LIX65N is adsorbed at the liquid-liquid interface as the neutral form (Figure 2.1) in the present condition.

The interfacial tension was analyzed as a function of the concentration with Gibbs adsorption isotherm. Gibbs adsorption isotherm can be described as

$$\Gamma = -\frac{1}{2.303RT}\frac{\mathrm{d}\,\gamma}{\mathrm{d}\log[\mathrm{LIX65N}]} \qquad (2.5)$$

where Γ, R, T, γ and [LIX65N] are the interfacial excess (mol m^{-2}), the gas constant (8.31 N m^{-1} mol^{-1} K^{-1}), the absolute temperature (298 K), the interfacial tension (N m^{-1}) and the concentration of LIX65N (mol dm^{-3}). The saturated interfacial concentration, a, was given as 2.0×10^{-8} mol dm^{-2}, since Γ can be treated as a in the linear lowering region of the interfacial tension. Thus, we can determine the values of the total interfacial area, S_i, and the adsorption constant, K', as 1.9×10^{2} dm^2 and 1.5×10^{-4} dm, respectively, from the molar absorptivity at 320.8 nm in dodecane ($\varepsilon = 3.91\times10^{3}$ dm^3 mol^{-1} cm^{-1}) and the interfacial parameters, *i.e.* $S_i\,a$ and $S_i\,K'$, measured by the high-speed stirring experiments.

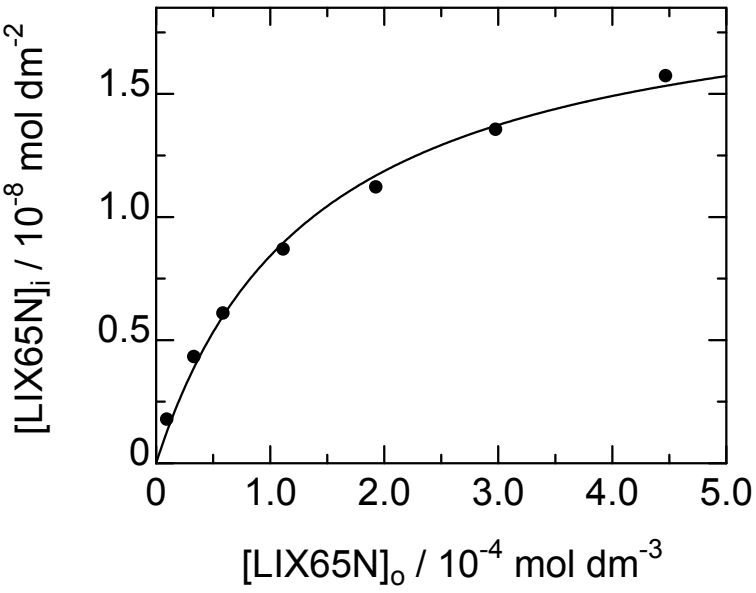

Figure 2.7. The adsorption isotherm of LIX65N measured by means of the high-speed stirring method in the dodecane-water system at 298 K. The solid line was obtained from the analysis with Langmuir isotherm described as equation 2.1.

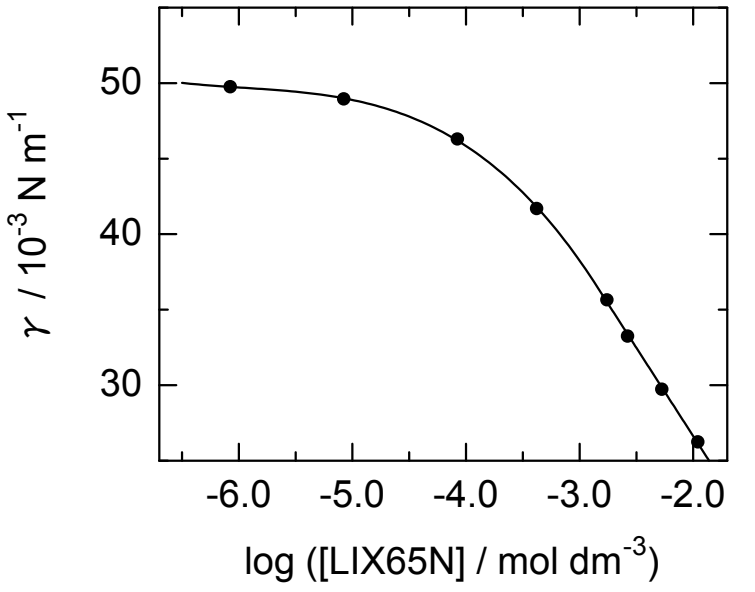

Figure 2.8. The plots of interfacial tension, *γ*, *vs.* logarithmic concentration of LIX65N in dodecane-water system at 298 K.

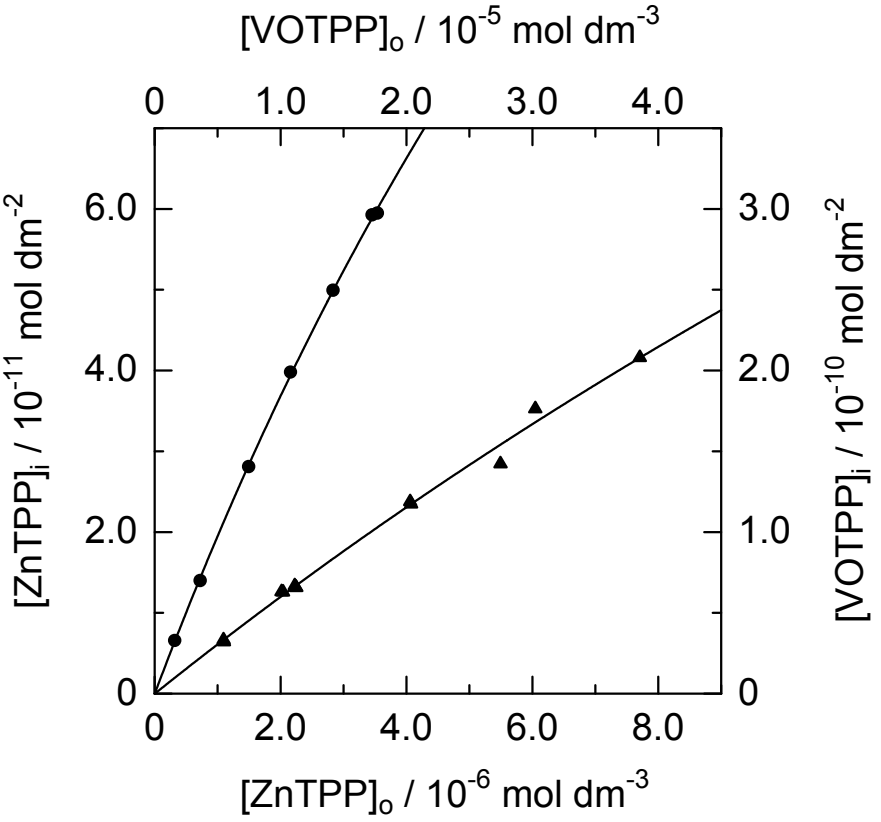

Figure 2.9. The adsorption isotherms of metal complexes of TPP at 298 K. The closed circle and triangle denote ZnTPP and VOTPP, respectively.

2.3.2 Interfacial Adsorptivity of Metalloporphyrins

In the dodecane-water system, ZnTPP and VOTPP showed appreciable adsorption to the interface in the high-speed stirring experiments and the other divalent metal complexes were not adsorbed. CoTPP was apparently adsorbed at the interface in the dodecane-water system, but the concentration in the bulk dodecane phase decreased gradually through the high-speed stirring experiment. The author thought that the cause of decrease of the bulk concentration was the oxidation of cobalt(II) to cobalt(III) at dodecane-water interface. The oxidation potentials of the divalent metal complex of TPP were reported as +0.52 V *vs*. SCE for $Co^{II} \rightarrow Co^{III}$ and +1.00 V *vs*. SCE for $Ni^{II} \rightarrow Ni^{III}$ in $(n\text{-}C_4H_9)_4NClO_4$/benzonitrile system, respectively.[10] Thus, CoTPP tends to be oxidized more readily than NiTPP. In the presence of ascorbic acid of 0.10 mol dm^{-3} as a reductant, CoTPP was not adsorbed at the liquid-liquid interface. Hence, it was suggested that the adsorption behavior of the cobalt complex results from the adsorption of the cationic cobalt(III) complex.

In this work, the adsorption isotherms for metalloporphyrins of zinc(II) and vanadyl(IV) were determined as shown in Figure 2.9. The measurements were made on the solutions ranging in concentration from 5.7×10^{-8} to 5.8×10^{-7} mol dm^{-3} for ZnTPP and from 6.7×10^{-7} to 4.6×10^{-6} mol dm^{-3} for VOTPP, respectively. Interfacial adsorption parameters obtained from the analysis of adsorption isotherms by equations 2.1-2.4 are summarized in Table 2.1. The value of K' for zinc(II) complex in the dodecane-water system is larger than vanadyl(IV) complex and LIX65N that has a relatively large value among oxime derivatives.[6] The adsorption constants for cobalt(II), nickel(II) and copper(II) complexes were estimated to be less than 10^{-6} dm from the detection limit of $\Delta A = 0.0005$. Therefore, the adsorptivity of TPP metal complexes decreased in the order, ZnTPP > VOTPP > CoTPP, NiTPP, CuTPP. The saturated interfacial concentrations of ZnTPP and VOTPP were calculated as 3.3×10^{-10} mol dm^{-2} and 1.5×10^{-9} mol dm^{-2}, respectively. These values are much lower than the reported values in other reagent systems,[6] in which a typical value of a is the order of 10^{-8} mol dm^{-2}. The values determined in the present system may contain some uncertainty, because of the low solubility of TPP complexes in dodecane.

The observed interfacial adsorption behavior of metal complexes of TPP agreed with the retention behavior observed in a reversed-phase HPLC[11-13] and TLC.[14,15] The chromatographic studies suggest that the hydrophilic property decreases in the order ZnTPP > VOTPP > NiTPP > CuTPP, namely zinc(II) and vanadyl(IV) complexes are more hydrophilic as compared with nickel(II) or copper(II). The hydrophile-lipophile balance (HLB) is important to consider the interfacial adsorption mechanism, since it is thought that the

Table 2.1. Interfacial adsorption constants at 298 K in the dodecane-water system

complex	λ_{max} / nm[a]	ε / dm^3 mol^{-1} cm^{-1} [b]	K' / dm[c]
CoTPP	408.2	2.04×10^5	$< 10^{-6}$
NiTPP	413.0	3.13×10^5	$< 10^{-6}$
CuTPP	413.8	6.50×10^5	$< 10^{-6}$
ZnTPP	416.6	4.98×10^5	2.1×10^{-4}
VOTPP	421.0	9.12×10^4	6.1×10^{-5}
LIX65N	320.8	3.91×10^3	1.5×10^{-4}

[a] The absorption maximum wavelength in dodecane. [b] The molar absorptivity at λ_{max} in dodecane. [c] The limit value of K' is evaluated from the detection limit of $\Delta A = 0.0005$.

adsorption of metal complexes results from the coordination of water molecule to the metal ion. Thus the more hydrophilic complex is more liable to be adsorbed at the dodecane-water interface. The large value of adsorption constant of ZnTPP can explain chromatographic results.

Table 2.2. The M-N bond lengths of metalloporphyrins[a]

complex	M-N bond length / pm
CoTPP	194.9
NiTPP	192.8
CuTPP	198.1
ZnTPP	203.6

[a] See references 16-19.

We can consider that the adsorptivity of VOTPP is due to the existence of the strong polar site (*i.e.*, vanadyl oxygen), and that of ZnTPP is the geometrical factor. The M-N bond length between zinc ion and nitrogen atoms of the pyrrole ring in the solid crystal state is reported as 203.6 pm by X-ray analysis.[16] The M-N bond lengths of several four-coordinate metalloporphyrins are summarized in Table 2.2. That of ZnTPP is the longest among the divalent metal complexes investigated in this work, and the long bond length will prefer to make the axially coordinated complex like a ZnTPP(H_2O) stable. The structure of five-coordinated monoaquo complex, ZnTPP(H_2O) has been confirmed in the solid state, in which the zinc(II) ion is displaced by 20 pm from the plane of the pyrrole ring towards the coordinated water molecule.[20] Thus, it can be expected that the zinc(II) complex is adsorbed as the form of ZnTPP(H_2O).

Recently, the partial molar volumes of the divalent metal complexes of TPP in benzene were reported, which decreased in the order, NiTPP > CuTPP > ZnTPP.[21] It suggested that ZnTPP has the strongest interaction with the solvent molecule, and the result also supported the highest adsorptivity of zinc(II) complex observed in this study.

2.4 REFERENCES

(1) Danesi, P. R. In *Principles and Practices of Solvent Extraction*; Rydberg, J., Musikas, C., Choppin, R. G., Eds.; Marcel Dekker: New York, 1992; Chapter 5.

(2) *Surface Adsorption and Surface Solubilization*; Sharma, R. Ed.; American Chemical Society: Washington, D.C., 1995; Chapters 18 and 19.

(3) Watarai, H. *Trends Anal. Chem.*, **1993**, *12*, 313-318.

(4) Banks, C. V.; Bisque, R. E. *Anal. Chem.*, **1957**, *29*, 522-526.

(5) Preston, J. S.; Whewell. R. J. *J. Inorg. Nucl. Chem.*, **1977**, *39*, 1675-1678.

(6) Watarai, H.; Satoh, K. *Langmuir*, **1994**, *10*, 3913-3915.

(7) Watarai, H.; Endoh, M. *Anal. Sci.*, **1991**, *7*, 137-140.

(8) Watarai, H.; Takahashi, M.; Shibata, K. *Bull. Chem. Soc. Jpn.*, **1986**, *59*, 3469-3473.

(9) Akiba, K.; Freiser, H. *Anal. Chim. Acta.*, **1982**, *136*, 329-337.

(10) Wolberg, A.; Manassen, J. *J. Am. Chem. Soc.*, **1970**, *92*, 2982-2991.

(11) Saitoh, K.; Kobayashi, M.; Suzuki, N. *J. Chromatogr.*, **1982**, *243*, 291-300.

(12) Saitoh, K.; Suzuki, N. *Anal. Chim. Acta.*, **1985**, *178*, 169-177.

(13) Suzuki, N.; Takeda, T.; Saitoh, K. *Chromatographia*, **1986**, *22*, 43-47.

(14) Sato, M.; Kwan, T. *Chem. Pharm. Bull.*, **1972**, *20*, 840-841.

(15) Saitoh, K.; Kobayashi, M.; Suzuki, N. *Anal. Chem.*, **1981**, *53*, 2309-2313.

(16) Scheidt, W. R.; Kastner, M. E.; Hatano, K. *Inorg. Chem.*, **1978**, *17*, 706-710.

(17) Stevens, E. D. *J. Am. Chem. Soc.*, **1981**, *103*, 5087-5095.

(18) Hoard, J. L. In *Porphyrins and Metalloporphyrins*; Smith, K. M. Ed.; Elsevier: New York, 1975; Chapter 8.

(19) Fleischer, E. B.; Miller, C. K.; Webb, L. E. *J. Am. Chem. Soc.*, **1964**, *86*, 2342-2347.

(20) Glick, M. D.; Cohen, G. H.; Hoard, J. L. *J. Am. Chem. Soc.*, **1967**, *89*, 1966-1988.

(21) Zielenkiewicz, W.; Perlovich, G. L.; Nikitina, G. E.; Semeykin, A. S. *J. Solution Chem.*, **1996**, *25*, 135-153.

Chapter 3

Formation and Interfacial Adsorption of $(Fe^{III}TPP)_2O$ in Dodecane-Aqueous Acid Systems

Abstract

The specific adsorption behavior of iron(III) complexes of 5,10,15,20-tetraphenylporphyrin (H_2TPP) at dodecane-water interface has been determined by means of the high-speed stirring method in the systems including hydrochloric acid, perchloric acid, nitric acid and sodium thiocyanate as the aqueous phases. In the systems of perchloric acid and nitric acid, FeTPPCl, which was initially dissolved in the dodecane phase, was transformed to the μ-oxo dimer, $(FeTPP)_2O$, after stirring. The adsorptivity of $(FeTPP)_2O$ is more pronounced in pH's lower than 4. It was postulated that the cationic dimer, $[(FeTPP)_2(OH)(H_2O)]^+$, was reversibly formed at the liquid-liquid interface by the reaction between $(FeTPP)_2O$ and H_3O^+ in the lower pH condition. The interfacial adsorptivity of the iron(III) porphyrin complexes decreased in the order, $[(FeTPP)_2(OH)(H_2O)]^+$ >> FeTPPCl > $(FeTPP)_2O$ > FeTPP(SCN). The interfacial adsorption constants of these species and the formation constants of $[(FeTPP)_2(OH)(H_2O)]^+$ were determined from the observed adsorption isotherms and the pH dependences.

3.1 INTRODUCTION

The investigation of the adsorption behavior of ligands and complexes at the liquid-liquid interfaces is very important to understand the role of interface in the solvent extraction mechanism of metal ions.[1] Since the ligands and complexes dissolved in a two-phase system can be concentrated by the adsorption at the liquid-liquid interface depending on the adsorptivity, specific reactions can proceed preferentially at the interface. Interfacial behavior of metal complexes is also interesting from the viewpoint of cell biology.

The investigation of adsorption behavior of metalloporphyrins at the liquid-liquid interface is particularly important to elucidate its biological functions *in vivo*,[2,3] *i.e.* photoenergy conversion, mass transfer, enzymic reaction, etc. The metalloporphyrins have been used for the trace determination of anions in analytical chemistry,[4-7] as a sensitive ionophore with anti-Hofmeister selectivity. In previous Chapter, the author described about the interfacial adsorption behavior of several metal complexes of 5,10,15,20-tetraphenylporphyrin (H_2TPP) at dodecane-water interface, the interfacial adsorptivity of them decreasing in the order, $Zn^{II}TPP$ > $V^{IV}OTPP$ > $Co^{II}TPP$, $Ni^{II}TPP$, $Cu^{II}TPP$.[8] We thought that the interfacial

adsorption of these metalloporphyrins resulted from the interaction between the central metal atom and the water molecule at the liquid-liquid interface. Moreover, the author studied preliminarily about the interfacial adsorption behavior of trivalent metal complexes of TPP with chromium(III), manganese(III), iron(III) and cobalt(III) as central metal ions and found that these trivalent metal complexes were highly adsorptive at the dodecane-water interface. In particular, the various reactivities of iron(III) complex of TPP, *i.e.* axial ligand substitution, μ-oxo dimerization and pronounced interfacial adsorptivity in acidic aqueous system, were very characteristic. The iron(III) complex of TPP has been extensively studied as a model compound of biological porphyrin derivatives, such as hemins and cytochrome P-450, and there have been many reports so far.[9-15] However, the interfacial adsorption behavior of iron(III) porphyrin in the liquid-liquid system has not been reported yet.

In this work, the adsorption behavior of (5,10,15,20-tetraphenylporphyrinato)iron(III) from a bulk dodecane phase to dodecane-water interface was examined in detail for the first time by employing the high-speed stirring method.

3.2 EXPERIMENTAL SECTION

Reagents. Chloro(5,10,15,20-tetraphenylporphyrinato)iron(III) (FeTPPCl) was obtained from Aldrich Chemical Company Inc. and used without purification. Dodecane, G.R., as the solvent was obtained from nacalai tesque and purified by distillation after being washed with a mixture of fuming sulfuric acid and sulfuric acid. The other organic solvents, *i.e.* hexane, benzene, toluene, chloroform and carbon tetrachloride, were nacalai tesque G.R. or S.P. reagent grade and used without further purification. The aqueous acids of various concentrations, *i.e.* hydrochloric acid, perchloric acid and nitric acid, in which the ionic strength was maintained at 0.10 by adding a corresponding sodium salt and 0.10 mol dm^{-3} sodium thiocyanate solution were used as aqueous phases. The pH of sodium thiocyanate solution was adjusted by the use of hydrochloric acid in lower pH region, the concentration of chloride ion being kept at 0.010 mol dm^{-3} and 0.010 mol dm^{-3} 2-[4-(2-hydroxylethyl)-1-piperazinyl]ethanesulfonic acid (HEPES) buffer was used in higher pH region. HEPES was purchased from Dojindo Laboratories and other reagents was nacalai tesque G.R. All of aqueous phase were prepared with a distilled and deionized water purified by using of a Milli-Q system (Millipore, Milli-Q SP.TOC.).

Dimerization Equilibrium. The dimerization equilibrium of FeTPPCl forming μ-oxo-bis[(5,10,15,20-tetraphenylporphyrinato)iron(III)], $(FeTPP)_2O$ was investigated by a batch technique in both the dodecane-hydrochloric acid and the dodecane-thiocyanate systems. The initial concentrations of FeTPPCl in dodecane were 2.6×10^{-6} mol dm^{-3} for the dodecane-hydrochloric acid system and 3.9×10^{-6} mol dm^{-3} for the dodecane-thiocyanate system, respectively. The dodecane phase containing FeTPPCl, 10 cm^3, was stirred with the same volume of aqueous phase for 24 h in a thermostated room at 298±1.5 K. After the equilibration, absorption spectra of bulk dodecane phase and pH values of the aqueous acid phase were measured by a JASCO V-550 UV/Vis spectrophotometer and a HORIBA pH meter F-14, respectively. In each pH condition, the dimer/monomer ratios of bulk species could be calculated from the regression analysis of absorption spectra.

High-Speed Stirring Experiments. The interfacial adsorption of iron(III) complexes of TPP at dodecane-water interface was observed by using the high-speed stirring apparatus as shown in Figure 2.4. The 50.0 cm^3 of dodecane phase containing an iron(III) complex and aqueous phase of the same volume were put into the stirring cell thermostated at 298±1.0 K. The extent of dispersion of the liquid-liquid system was controlled by changing the rotation rate of the

stirrer made up of polychlorotrifluoroethylene resin (PCTFE), with the motor speed controller (Nikko Keisoku, SC-5), from 200 rpm to 5000 rpm. The absorption spectrum from 195 nm to 600 nm of an organic phase, that was continuously separated from the dispersed liquid-liquid system by means of a Teflon® phase separator (Flon Industry, F-3010-R350) and circulated through the flow cell, was measured at 2.0 s intervals by a Shimadzu SPD-M6A photodiode array UV/Vis detector. The flow cell was a cylindrical quartz cell with the optical path length of 1.0 cm and the volume of 8×10^{-3} cm^3. The inner surface of the stirring cell and the flow cell were made hydrophobic by the treatment with benzene solution of dichlorodimethylsilane. Thus, we could determine the amount of interfacial adsorption evaluating the difference between the absorbances of the bulk organic phase containing a metalloporphyrin under high-speed stirring (5000 rpm) and low-speed stirring (200 rpm). The adsorption isotherm was determined by analyzing the absorbance change at the absorption maximum wavelength.

Measurements of Infrared Spectrum. The infrared spectra of iron(III) complexes of TPP were measured as KBr pellets on a JASCO FT/IR-8300 spectrometer. After the iron(III) complexes of TPP were prepared by mixing an organic phase containing FeTPPCl with an aqueous phase, the organic solvent was evaporated and the iron(III) complex was dried in a vacuum desiccator for 2 h at 333 K.

Transmission Spectrum of Ultra-Thin Two-Phase Systems. The dodecane phase containing 2.6×10^{-6} mol dm^{-3} of $(FeTPP)_2O$, 0.150 cm^3, and the aqueous phase, 0.250 cm^3, were put into the rotating cell that is cylindrical vial and stoppered by Teflon® plug as the rotation shaft connected to the high speed motor (HITACHI, GP 2SA).(*cf.* Chapter 5) 0.10 mol dm^{-3} hydrochloric acid solution or Milli-Q water were used as an aqueous phase. The inner diameter and inner height of the rotating cell were 19 mm and 29 mm, respectively. When the densities of an organic and an aqueous phases are different, the two-phase system is spread out on the inner wall of the rotating cell at the high speed rotation. In the present system, the densities of dodecane used as an organic solvent and water are 0.745 and 0.997 g cm^{-3} at 298 K, respectively. Thus, the dodecane and aqueous phases were spread as an inner liquid film of 79 μm thickness and an outer liquid film of 145 μm thickness, respectively. The ultra-thin two-phase liquid membrane system thus formed was stabilized in the range of *ca.* 6000 to 7500 rpm. The specific interfacial area was calculated as 114 cm^{-1}. The summation of the absorption spectra of interfacial and bulk organic phase species was measured from the perpendicular direction to the rotation axis by a JASCO V-550 UV/Vis spectrophotometer.

3.3 RESULTS AND DISCUSSION

3.3.1 Formation of the μ-Oxo Dimer

It was confirmed that the iron(III) complex of TPP is adsorbed at dodecane-water interface in all systems examined under the high-speed stirring conditions. From the absorption spectrum of the bulk dodecane phase measured by the high-speed stirring apparatus in the dodecane-water system, the author found that FeTPPCl initially dissolved in dodecane was completely changed to μ-oxo-bis[(5,10,15,20-tetraphenylporphyrinato)iron(III)], $(FeTPP)_2O$,[16-19] which is depicted in Figure 3.1. Figure 3.2 shows that the absorption spectra of the dodecane phase measured before and after the high-speed stirring with an aqueous phase. The absorption maximum wavelength of FeTPPCl changed from 419.0 nm to 407.0 nm. The Soret band and *Q* bands measured after stirring agreed with those of μ-oxo dimer available in the literature.[20] The absorption maximum wavelength and the molar absorptivity of the iron(III) complexes are summarized in Table 3.1. Therefore, it was concluded that the interfacial adsorption observed in the dodecane-water system should be related to the formation of $(FeTPP)_2O$. The change in the bulk species from FeTPPCl to $(FeTPP)_2O$ in the high-speed stirring experiment was also noticed in both the dodecane-perchloric acid system and the dodecane-nitric acid system without dissociation and demetallation. The infrared spectrum of the μ-oxo dimer was measured and the characteristic two peaks assigned to the antisymmetric Fe-O-Fe stretching vibration were confirmed at 890.5 cm^{-1} (medium) and 873.9 cm^{-1} (strong).[21,22]

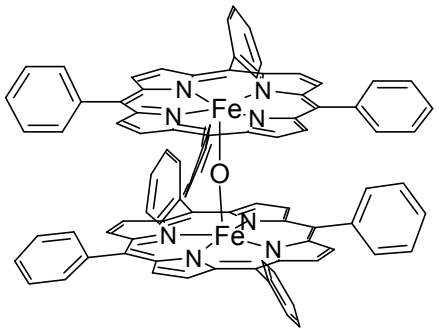

Figure 3.1. The molecular structure of the μ-oxo dimer, $(FeTPP)_2O$.

The formation of $(FeTPP)_2O$ under the acidic condition is very interesting, since the μ-oxo dimer is usually synthesized in alkaline conditions and decomposed to two monomer molecules in acidic conditions.[20,23] The formation of $(FeTPP)_2O$ in the dodecane phase by mixing with a perchloric acid solution occurred in the use of hexane as a solvent also, however it was not observed in chloroform, carbon tetrachloride, benzene and toluene systems. In the organic solvent systems such as chloroform and benzene, the chloride ion in FeTPPCl may be substituted with perchlorate ion which exists in excess in the aqueous phase and the ion-association complex, $FeTPP(ClO_4)$, could be extracted, whereas $FeTPP(ClO_4)$ is difficult

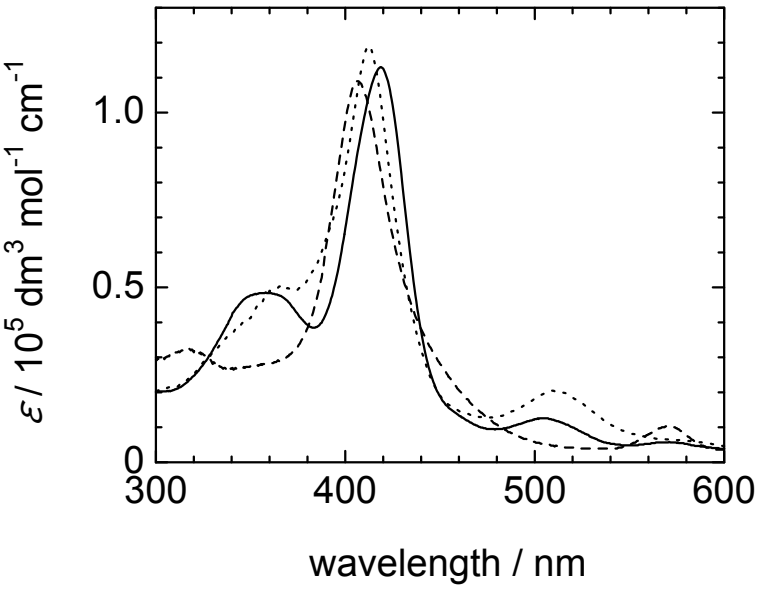

Figure 3.2. Absorption spectra of the bulk dodecane phase species. The solid line, broken line and dotted line denote FeTPPCl, $(FeTPP)_2O$ and FeTPP(SCN), respectively. The molar absorptivity of $(FeTPP)_2O$ is the half value to compare with other monomeric complexes.

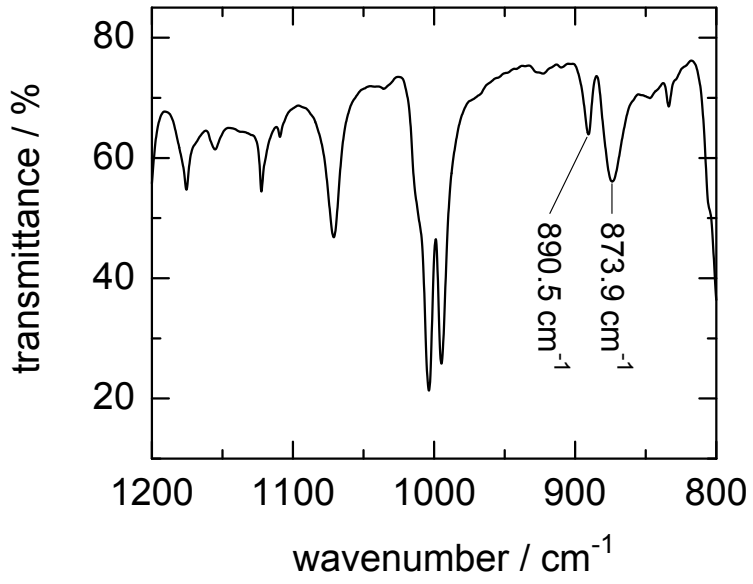

Figure 3.3. Infrared spectrum of $(FeTPP)_2O$ prepared by mixing the dodecane solution containing FeTPPCl with the perchlorate solution of 0.10 mol dm^{-3}. The two peaks at 890.5 cm^{-1} (m) and 873.9 cm^{-1} (s) are assigned to the antisymmetric vibration of Fe-O-Fe stretching.

Table 3.1. The molar absorptivity and the dimerization constant of iron(III) TPP complexes

compound	λ_{max} / nm	ε / dm^3 mol^{-1} cm^{-1} [a]	LogK_D [b]
FeTPPCl	419.0	1.13×10^5	-2.7±0.3
FeTPP(SCN)	412.0	1.19×10^5	-6.0±0.7
$(FeTPP)_2O$	407.0	2.18×10^5	—

[a] ε is the molar absorptivity at λ_{max}. [b] K_D (mol dm^{-3}) is the dimerization constant at 298 K defined as equation 3.3.

to be extracted into alkane solvents. Therefore, the formation of $(FeTPP)_2O$ could be favored in the dodecane and the hexane systems.

The organic phase species under acidic conditions in the dodecane-thiocyanate system was assigned to FeTPP(SCN), since the absorption maximum wavelength in dodecane changed from 419.0 nm of FeTPPCl to 412.0 nm. The axial ligand of FeTPPCl, *i.e.* chloride ion, was thought to be substituted to thiocyanate ion at the interface and FeTPP(SCN) was distributed into the bulk dodecane phase. The axial ligand substitution at the interface could occur in the presence of 0.10 mol dm^{-3} thiocyanate ion and 0.010 mol dm^{-3} chloride ion in an aqueous phase.

3.3.2 Dimerization Equilibrium

In the dodecane-hydrochloric acid system, the adsorbed amount of FeTPPCl was scarcely changed by the acid concentration. However, in the higher pH region than *ca.* 3.3, the bulk species could be gradually changed to $(FeTPP)_2O$ and then it can be assumed that the adsorbed species is the mixture of FeTPPCl and $(FeTPP)_2O$. The most of the species in the bulk dodecane phase changed to $(FeTPP)_2O$ in the higher pH region than *ca.* 4.7. Since chloride ion is extracted into the dodecane phase as an axial ligand, the μ-oxo dimer can be easily decomposed to two monomers, *i.e.* FeTPPCl, under acidic conditions. The formation equilibrium of $(FeTPP)_2O$ in the dodecane-hydrochloric acid system is written as,

$$2FeTPPCl_o + H_2O \rightleftharpoons (FeTPP)_2O_o + 2H^+ + 2Cl^- \qquad (3.1)$$

where the subscript o refers to the organic phase.

In the dodecane-thiocyanate system, the μ-oxo dimer began to increase in the higher pH than *ca.* 5.1 and the most of bulk species was changed to $(FeTPP)_2O$ in the higher pH than 6.6. The dimerization equilibrium in the dodecane-thiocyanate system is shown as,

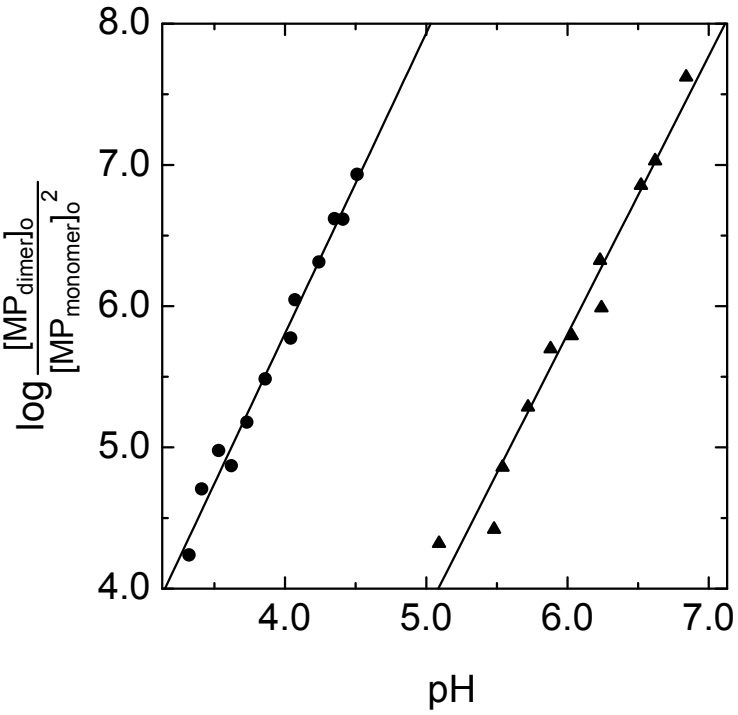

Figure 3.4. Logarithmic plot of $[MP_{dimer}]_o/[MP_{monomer}]_o^2$ *vs.* pH at 298 K. The circles and the triangles depict the dodecane-hydrochloric acid system and the dodecane-thiocyanate system, respectively. The slopes of both linear functions were approximately 2.

$$2FeTPP(SCN)_o + H_2O \rightleftharpoons (FeTPP)_2O_o + 2H^+ + 2SCN^- \qquad (3.2)$$

In both systems, the concentration of chloride ion or thiocyanate ion can be assumed as constant, 0.10 mol dm^{-3}, since their concentration was large excess relative to the iron(III) complex. The conditional dimerization constant, K_D (mol dm^{-3}), relating to the formation of the μ-oxo dimer can be defined as

$$K_D = \frac{[MP_{dimer}]_o[H^+]^2}{[MP_{monomer}]_o^2} \qquad (3.3)$$

where $[MP_{dimer}]_o$ and $[MP_{monomer}]_o$ denote the organic phase concentrations of the monomer, *i.e.* FeTPPCl or FeTPP(SCN), and the μ-oxo dimer, respectively. The ratio of $[MP_{dimer}]_o/[MP_{monomer}]_o^2$ could be calculated from the regression analysis of absorption spectra in each pH condition. The obtained values were plotted against pH value of the aqueous phase in Figure 3.4. The slopes of the linear functions obtained from the least-squares method were 2.1 for the dodecane-hydrochloric acid system and 2.0 for the dodecane-thiocyanate system, respectively, and the intercepts ($\log K_D$) were -2.7±0.3 and -6.0±0.7, respectively. Thus, the

two-proton process represented as the equations 3.1 and 3.2 was confirmed and the values of K_D suggested that the stability of FeTPP(SCN) is $10^{3.3}$ times higher than FeTPPCl. In addition, the separation factor (S.F.) described as equation 3.4 can be evaluated as 45 from the values of K_D determined in both systems, since thiocyanate ion can be preferentially extracted as an axial ligand from an aqueous phase in the presence of thiocyanate ion and chloride ion into an organic phase.

$$\text{S.F.} = \frac{[\text{FeTPP(SCN)}]_o}{[\text{FeTPPCl}]_o} = \sqrt{\frac{K_{D,\text{FeTPPCl}}}{K_{D,\text{FeTPP(SCN)}}}} \tag{3.4}$$

In the homogeneous system, the dimerization equilibrium of (5,10,15,20-tetra(*p*-sulfophenyl)porphyrinato)iron(III) (FeTPPS) was investigated by Fleischer *et al.* The value of logK_D for $(\text{FeTPPS})_2\text{O}$ in an aqueous solution, in which the ionic strength was maintained at 0.10, was reported as -8.1 at 298 K[23] and the μ-oxo dimer in the heterogeneous dodecane-water system is relatively stable against the proton attack in comparison with the homogeneous aqueous system.

3.3.3 Adsorption Isotherms

The adsorption isotherms determined in the dodecane-water, the dodecane-hydrochloric acid and the dodecane-thiocyanate systems were shown in Figure 3.5. In the dodecane-water system and the higher pH regions of the dodecane-hydrochloric acid and the dodecane-thiocyanate systems, the interfacially adsorbed species was $(\text{FeTPP})_2\text{O}$ and in the lower pH region of the dodecane-hydrochloric acid and the dodecane-thiocyanate system, they are FeTPPCl and FeTPP(SCN), respectively. It was assumed that the adsorbed species were the same as those in the bulk dodecane phase. The adsorption isotherms shown in Figure 3.5 were analyzed applying Langmuir isotherm,

$$[\text{MP}]_i = \frac{aK'[\text{MP}]_o}{a + K'[\text{MP}]_o} \tag{3.5}$$

where $[\text{MP}]_i$ and $[\text{MP}]_o$ denote the concentrations of metalloporphyrin adsorbed at the liquid-liquid interface and in the bulk organic phase, respectively. a is the saturated interfacial concentration (mol dm^{-2}) and K' is the interfacial adsorption constant (dm) defined under the condition of $a >> [\text{MP}]_i$,

$$K' = \frac{[\text{MP}]_i}{[\text{MP}]_o} \tag{3.6}$$

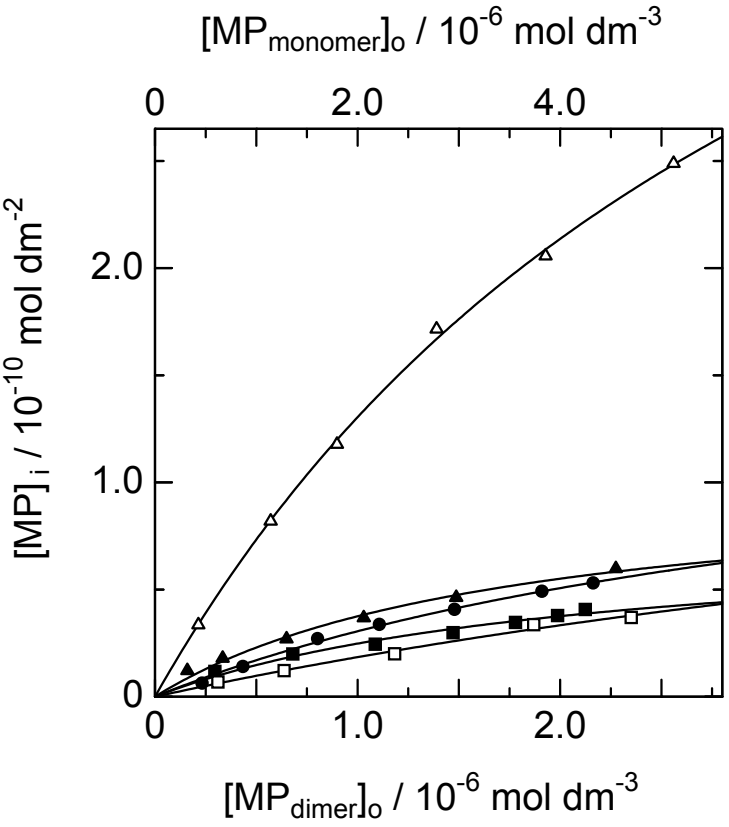

Figure 3.5. Langmuir plots determined by the high-speed stirring experiments at 298 K. (●) $(FeTPP)_2O$ in the dodecane-water system, (△) FeTPPCl in the dodecane-hydrochloric acid system(pH 2.96), (▲) $(FeTPP)_2O$ in the dodecane-hydrochloric acid system(pH 4.77), (□) FeTPP(SCN) in the dodecane-thiocyanate system(pH 2.11), (■) $(FeTPP)_2O$ in the dodecane-thiocyanate system(pH 7.73).

The difference between the absorbances of the bulk organic phase under high-speed stirring and low-speed stirring, ΔA, and the absorbance of the bulk organic phase under stirring, A_o, can be described as follows,

$$\Delta A = \varepsilon l [\mathrm{MP}]_i S_i / V_o \quad (3.7)$$

$$A_o = \varepsilon l [\mathrm{MP}]_o \quad (3.8)$$

where ε, l, S_i and V_o are the molar absorptivity at the absorption maximum wavelength in dodecane, the optical path length, the total interfacial area and the organic phase volume, respectively. As described in Chapter 2, the value of the total interfacial area in the dodecane-water system was evaluated as 1.9×10^4 cm^2 from the interfacial tension measurements and high-speed stirring experiments of 2-hydroxy-5-nonyl-benzophenone oxime (LIX65N).[8] Hence, the specific interfacial area, S_i / V_o, of the stirred system was

calculated as 380 cm^{-1}. The interfacial adsorption constants, K', obtained from the analysis with Langmuir isotherm are summarized in Table 3.2. The magnitude of K', which characterizes ease of interfacial adsorption, decreases in the order, FeTPPCl > $(FeTPP)_2O$ > FeTPP(SCN). This result suggests that FeTPP(SCN) is more hydrophobic than FeTPPCl and $(FeTPP)_2O$. The interfacial adsorption of them results in the interaction of the molecule of iron(III) complex and water at the interface, because the μ-oxo dimer and the monomers are neutral compound and an axial ligand coordination is stabilized by the presence of excess chloride ion or thiocyanate ion in each aqueous phase.

The values of the saturated interfacial concentration calculated for FeTPPCl, FeTPP(SCN) and $(FeTPP)_2O$ were much lower than reported values in other reagent systems, in which a typical value of a was the order of 10^{-8} mol dm^{-2}.[24] These values means that the unit area of a molecule was 3~100 times larger than those expected from the molecular size. Thus, the values of a determined in this work may contain some errors which attributes to Langmuir analysis without data in the high concentration region or other factor, *e.g.*, the lowering of activity coefficient of TPP complexes in dodecane phase, because of the solubility as low as 10^{-6} mol dm^{-3} in dodecane. Therefore, it may be difficult to determine the amount of the adsorbed complex at the saturated region of the interfacial adsorption.

It is expected that the pyrrole ring of the adsorbed metalloporphyrin molecule is probably parallel to the interface, because the molecule is a very hydrophobic and planar with a hydrophilic central metal ion. It can be assumed that the μ-oxo dimer has two axial coordination sites from its geometrical structure,[25,26] therefore, a water molecule can coordinate to either of two sites at dodecane-water interface.

3.3.4 pH Dependence in Adsorptivity

In the dodecane-perchloric acid system, the interfacial adsorptivity of the μ-oxo dimer changed depending upon pH of an aqueous phase and the interfacial adsorbed amount was increased in lower pH condition. The adsorption isotherms of the μ-oxo dimer in the dodecane-perchloric acid system were shown in Figure 3.6.

Since pH dependence in the adsorptivity of the μ-oxo dimer can not be explained by the hydration at the two axial coordination sites, other adsorption mechanism is required for the dodecane-perchloric acid system. The change in the interfacial adsorptivity with pH suggests the interfacial reaction of the μ-oxo dimer with hydronium ion at the liquid-liquid interface.

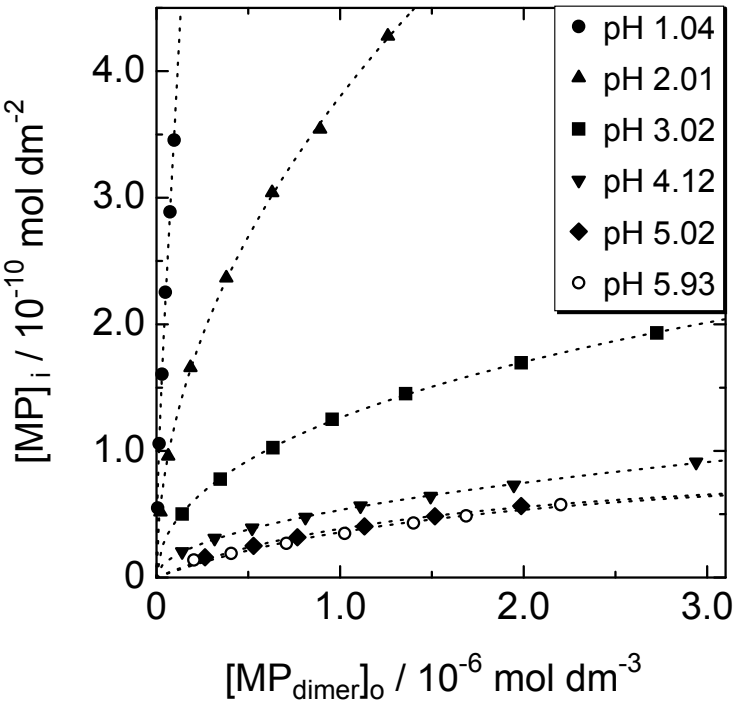

Figure 3.6. Adsorption isotherms of $(FeTPP)_2O$ in the dodecane-perchloric acid system determined in several pH conditions. The concentration of perchlorate ion was maintained at 0.10 mol dm^{-3} by the addition of sodium perchlorate.

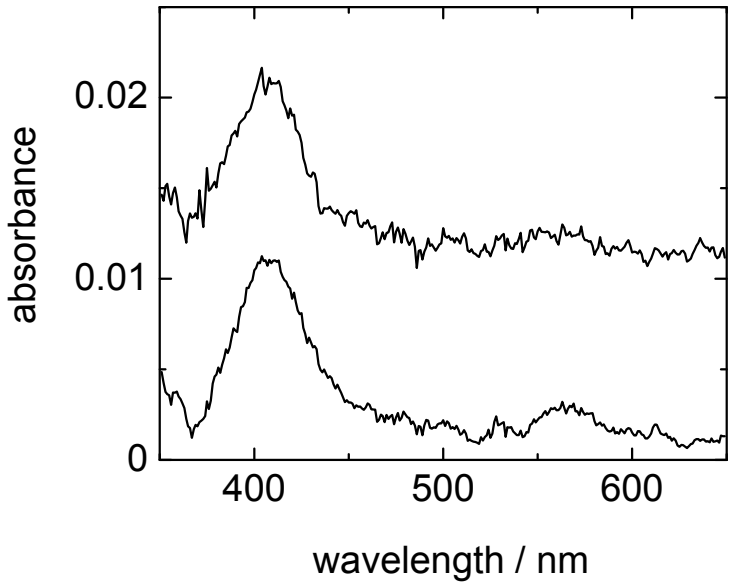

Figure 3.7. Transmission absorption spectra of $(FeTPP)_2O$ distributed between the interface and the organic phase (79 μm in thickness). Upper and lower spectra were measured in the dodecane-perchloric acid and the dodecane-water systems, respectively.

The absorption spectra of two-phase liquid membrane systems were determined by the rotating cell and shown in Figure 3.7. From the adsorption isotherm determined in the dodecane-perchloric acid system and the specific interfacial area of 114 cm^{-1}, the adsorptivity of the μ-oxo dimer in the rotating cell can be expected as *ca.* 30 %. This means that *ca.* 30 % of the transmission spectrum should be ascribable to the interfacial species. The interfacial spectrum in the dodecane-perchloric acid system shown in Figure 3.7 was scarcely changed from the spectrum of the μ-oxo dimer in the dodecane-water system, and hence the interfacial species in the dodecane-perchloric acid system was thought to be the species analogous to the μ-oxo dimer. It was also suggested that the interfacial species in lower pH region of the dodecane-hydrochloric acid system is the μ-oxo dimer and/or derivative of the μ-oxo dimer.

The author postulated that the interfacial adsorption mechanism of the μ-oxo dimer could be proceeded by the two steps. In the first step, the μ-oxo dimer distributes between the bulk dodecane phase and the interface.

$$(FeTPP)_2O_o \rightleftharpoons (FeTPP)_2O_i \tag{3.9}$$

$$K' = \frac{[(FeTPP)_2O]_i}{[(FeTPP)_2O]_o} \tag{3.10}$$

where the subscript i denotes the interface. If the aqueous phase is the acidic condition, the μ-oxo dimer tends to be protonated. Thus, in the second step, the μ-oxo dimer is changed to the cation, $[(FeTPP)_2(OH)(H_2O)]^+$ by reacting with a hydronium ion.

$$(FeTPP)_2O_i + H_3O^+ \rightleftharpoons [(FeTPP)_2(OH)(H_2O)]^+_i \tag{3.11}$$

$$K_f = \frac{[(FeTPP)_2(OH)(H_2O)]^+_i}{[(FeTPP)_2O]_i[H_3O^+]} \tag{3.12}$$

where K_f ($dm^3\ mol^{-1}$) is the formation constant of $[(FeTPP)_2(OH)(H_2O)]^+$ at the interface.

The interfacial adsorption mechanism of the iron(III) complexes in the dodecane-perchloric acid and the dodecane-nitric acid systems is illustrated in Figure 3.8. The cationic dimer, $[(FeTPP)_2(OH)(H_2O)]^+$, has been postulated as an intermediate in the decomposition process of the μ-oxo dimer of iron(III) porphyrins, *e.g.* deuteroporphyrins[27] and tetra(*p*-sulfophenyl)porphyrin[23] in acidic conditions. In the present study, the counter ion is a perchlorate ion and the cationic compound can be adsorbed at the interface as the ion pair, $[(FeTPP)_2(OH)(H_2O)]^+(ClO_4^-)$. The change in the bulk concentration of the μ-oxo dimer resulted from the interfacial adsorption of the μ-oxo dimer and the cationic dimer is represented by equations 3.7-3.12,

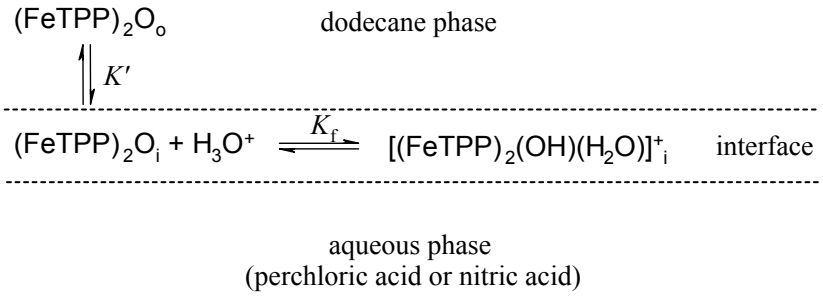

Figure 3.8. Proposed interfacial adsorption mechanism of $(FeTPP)_2O$ in the dodecane-perchloric acid system. Subscripts o and i denote the bulk dodecane phase and the interface, respectively. The interfacial adsorption could be proceeded by two steps. The first step is the distribution of $(FeTPP)_2O$ between the bulk dodecane phase and the interface. If the aqueous phase is the acidic condition, $(FeTPP)_2O$ tends to be protonated. Thus, in the second step, $(FeTPP)_2O$ is changed to $[(FeTPP)_2(OH)(H_2O)]^+$ by reacting with a hydronium ion at the interface.

$$\Delta[(FeTPP)_2O]_o = \left([(FeTPP)_2O]_i + [(FeTPP)_2(OH)(H_2O)]^+_i\right)\frac{S_i}{V_o}$$
$$= K'[(FeTPP)_2O]_o\left(1 + K_f[H_3O^+]\right)\frac{S_i}{V_o} \qquad (3.13)$$

Since the total concentration of iron(III) TPP compounds is the sum of the bulk concentration change and the bulk concentration of μ-oxo dimer,

$$[(FeTPP)_2O]_T = \Delta[(FeTPP)_2O]_o + [(FeTPP)_2O]_o \qquad (3.14)$$

equation 3.13 can be rewritten as follows,

$$\Delta[(FeTPP)_2O]_o = \frac{K'[(FeTPP)_2O]_T\left(1 + K_f[H_3O^+]\right)}{V_o/S_i + K'\left(1 + K_f[H_3O^+]\right)} \qquad (3.15)$$

The dependence of the interfacial amount in the dodecane-perchloric acid system upon pH is shown in Figure 3.9(a) the total concentration of the iron(III) complexes being maintained at 4.40×10^{-7} mol dm^{-3}. The acidity of a perchloric acid solution was changed from pH 5.93 to 1.04 and the concentration of perchlorate ion was kept constant at 0.10 mol dm^{-3}. The interfacially adsorbed amount became approximately constant in the regions of pH < 1 and 5 < pH. In this system, at least two species are adsorbed at the interface, *i.e.* the μ-oxo dimer, $(FeTPP)_2O$ and the cationic dimer, $[(FeTPP)_2(OH)(H_2O)]^+$. It is presumable that the interfacially adsorbed species is almost the cationic compound in the lower pH region and the μ-oxo dimer increases with the lowering of acidity of the aqueous phase. The dependence of

the interfacial amount upon pH was analyzed by applying equation 3.15. The values of adsorption constant of the μ-oxo dimer, K' and interfacial formation constant of the cationic compound, K_f were calculated as 7.3×10^{-5} dm and 2.8×10^{3} dm^3 mol^{-1}, respectively. The deviation of the fitting curve from the experimental points in the lower pH region in Figure 3.9(a) could be ascribable to the repulsive interaction between the adsorbed complexes at the liquid-liquid interface, because of the increase of the interfacial amount. At pH near 1, *ca*. 96 % of the total amount of the iron(III) complexes was adsorbed at the interface as the cationic dimer. The change in the interfacial adsorptivity with the pH of the aqueous phase was not only observed in the dodecane-perchloric acid system, but also in the dodecane-nitric acid system. The pH dependence of the interfacial adsorptivity in the dodecane-nitric acid system was measured in 3.67×10^{-7} mol dm^{-3} of $(FeTPP)_2O$ and pH 5.42 to 1.29. Since the bulk species was the μ-oxo dimer and pH dependence of the adsorptivity shown in Figure 3.9(b) was similar to the dodecane-perchloric acid system, the author considered that the adsorption mechanisms in both systems are the same and the adsorptivity change could be analyzed by equation 3.15. In the dodecane-nitric acid system, the values of adsorption constant of the μ-oxo dimer, K', and interfacial formation constant of the cationic dimer, K_f, were calculated as 5.1×10^{-5} dm and 2.2×10^{3} dm^3 mol^{-1}, respectively. The values of K' and K_f determined in both systems are approximately equal. The obtained interfacial parameters are summarized in Table 3.2 along with the previously reported values for divalent metal complexes.

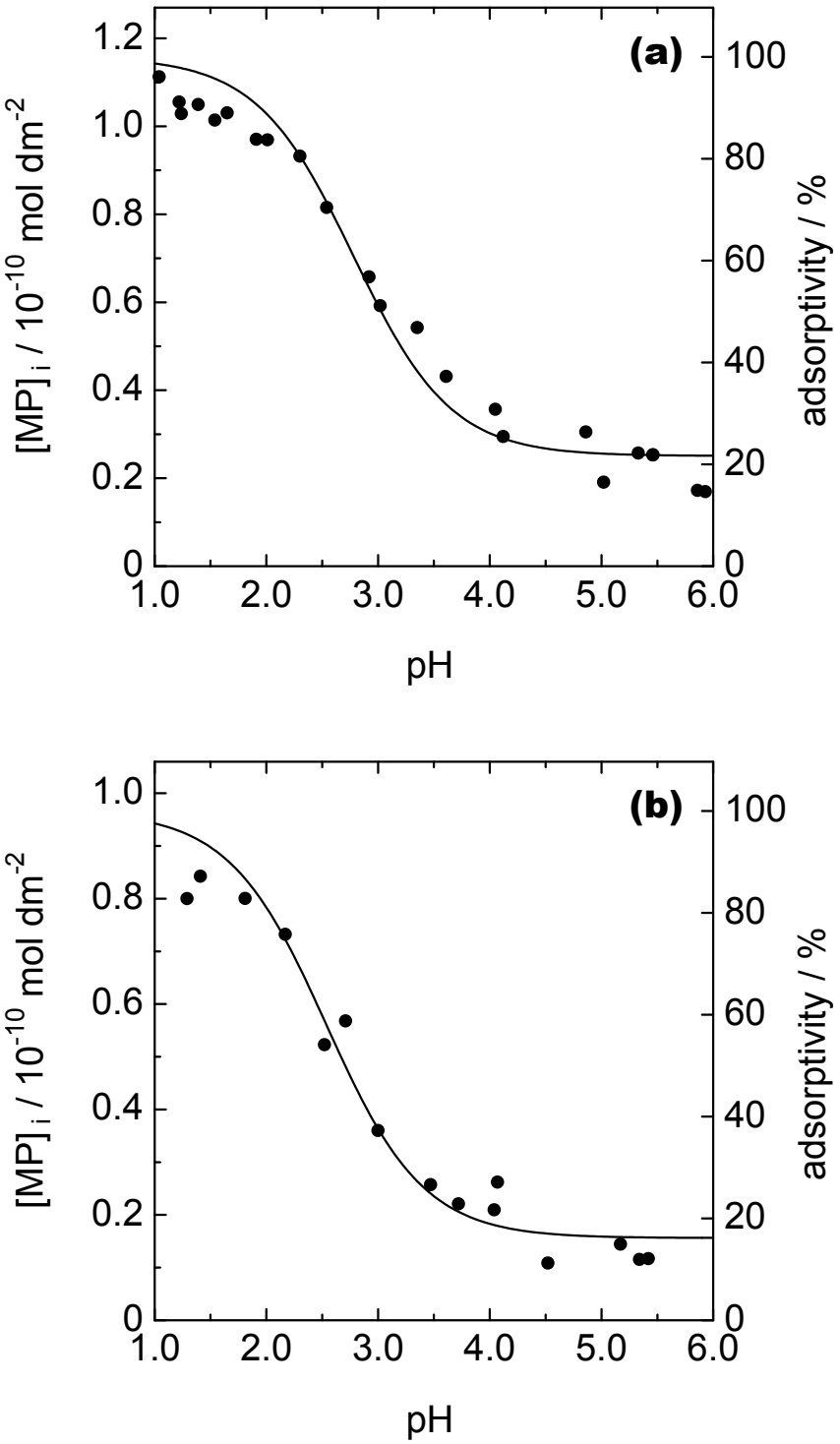

Figure 3.9. The pH dependence of the amount of iron(III) TPP complexes adsorbed at the interface determined in the dodecane-perchloric acid system (a), and in the dodecane-nitric acid system (b). Solid lines were obtained by the least-squares curve-fitting of the experimental data with equation 3.15. The adsorptivity (%) means the percentage of interfacial amount of the complex to the total amount.

Table 3.2. Interfacial adsorption constants of iron(III) complexes of TPP at 298 K

	conditions		species		interfacial parameters[a]	
	aqueous phase	pH	organic phase	interface	K' / dm	K_f / dm^3 mol^{-1}
divalent metal complex[b]	ascorbic acid	—	CoTPP		$< 10^{-6}$	
	H_2O	—	NiTPP		$< 10^{-6}$	
	H_2O	—	CuTPP		$< 10^{-6}$	
	H_2O	—	ZnTPP	ZnTPP	2.1×10^{-4}	
	H_2O	—	VOTPP	VOTPP	6.1×10^{-5}	
iron(III) complex	H_2O	—	$(FeTPP)_2O$	$(FeTPP)_2O$	3.8×10^{-5}	
	Cl^- [c]	≤ 3.3	FeTPPCl	FeTPPCl	8.4×10^{-5}	
		4.7 ≤	$(FeTPP)_2O$	$(FeTPP)_2O$	5.9×10^{-5}	
	SCN^- [d]	≤ 5.1	FeTPP(SCN)	FeTPP(SCN)	1.0×10^{-5}	
		6.6 ≤	$(FeTPP)_2O$	$(FeTPP)_2O$	3.6×10^{-5}	
	ClO_4^- [c]	1.04 - 5.93	$(FeTPP)_2O$	$(FeTPP)_2O$ $[(FeTPP)_2(OH)(H_2O)]^+$	7.3×10^{-5}	2.8×10^3
	NO_3^- [c]	1.29 - 5.42	$(FeTPP)_2O$	$(FeTPP)_2O$ $[(FeTPP)_2(OH)(H_2O)]^+$	5.1×10^{-5}	2.2×10^3

[a] K' and K_f are the interfacial adsorption constant and the formation constant of $[(FeTPP)_2(OH)(H_2O)]^+$ at dodecane-aqueous acid interface, respectively. [b] See Chapter 2. [c] The ionic strength of aqueous acid solutions was maintained at 0.10. [d] The concentration of thiocyanate ion was maintained at 0.10 mol dm^{-3}. The pH of aqueous phase was adjusted by adding hydrochloric acid or HEPES buffer.

3.4 CONCLUSIONS

It was concluded that the iron(III) complex of TPP was adsorbed at dodecane-water interface in all systems examined and the interfacial adsorption constant was determined in every system. The interfacial adsorptivity and the interfacial adsorbed species depended on the aqueous phase condition. The author found that FeTPPCl in dodecane converted to the μ-oxo dimer, $(FeTPP)_2O$, by the stirring with the acidic aqueous phase, *i.e.* perchloric acid or nitric acid. It was proposed that the interfacial species were $(FeTPP)_2O$ in the higher pH region and $[(FeTPP)_2(OH)(H_2O)]^+$ in the lower pH region. The interfacial adsorption constants of $(FeTPP)_2O$ determined in various aqueous systems were in the range between 3.6×10^{-5} and 7.3×10^{-5} dm. As for the monomers of FeTPPCl and FeTPP(SCN), the adsorption constants were 8.4×10^{-5} and 1.0×10^{-5} dm, respectively. The adsorptivity of the iron(III) complexes investigated in this work decreased in the order, $[(FeTPP)_2(OH)(H_2O)]^+$ >> FeTPPCl > $(FeTPP)_2O$ > FeTPP(SCN). The largest adsorptivity of $[(FeTPP)_2(OH)(H_2O)]^+$ formed under the acidic condition was ascribed to its positive charge. Usually, the cationic molecule is impossible to move into the organic phase from the liquid-liquid interface without forming the ion pair with an anion, *i.e.* ClO_4^- or NO_3^-. However, these ion pair do not tend to be extracted into the organic solvent such as dodecane. Thus, $[(FeTPP)_2(OH)(H_2O)]^+$ can exist only at the dodecane-water interface.

In a comparison of the interfacial adsorptivity with previously reported divalent metal complexes of TPP, the adsorptivity in the dodecane-water system decreases in the order, $[(FeTPP)_2(OH)(H_2O)]^+$ >> ZnTPP > FeTPPCl > VOTPP, $(FeTPP)_2O$ > FeTPP(SCN) > CoTPP, NiTPP, CuTPP. Furthermore, the author has found that the other trivalent metal complexes of TPP, *i.e.* chromium(III), manganese(III) and cobalt(III), are also adsorbed at the dodecane-water interface. For example, *ca.* 99 % of the bulk MnTPPCl (3.5×10^{-7} mol dm^{-3}) was adsorbed at the interface under the high-speed stirring condition. The interfacial adsorptivity of these trivalent metalloporphyrins result from the reactivity of the axial ligand, in contrast with the divalent metal complex systems described in Chapter 2.

3.5 REFERENCES

(1) Watarai, H. *Trends Anal. Chem.*, **1993**, *12*, 313-318.

(2) Falk, J. E. In *Porphyrins and Metalloporphyrins*; Smith, K. M. Ed.; Elsevier: New York, 1975; Section B.

(3) Dolphin, D. *The Porphyrins*; Academic Press: New York, 1978; Vol. VI and VII.

(4) Ammann, D.; Huser, M.; Krautler, B.; Rusterholz, B.; Schulthess, P.; Lindemann, B.; Halder, E.; Simon, W. *Helv. Chim. Acta*, **1986**, *69*, 849-854.

(5) Chaniotakis, N. A.; Chasser, A. M.; Meyerhoff, M. E.; Groves, J. T. *Anal. Chem.*, **1988**, *60*, 185-188.

(6) Abe, H.; Kokufuta, E. *Bull. Chem. Soc. Jpn.*, **1990**, *63*, 1360-1364.

(7) Gao, D.; Li, J. Z.; Yu, R. Q.; Zheng, G. D. *Anal. Chem.*, **1994**, *66*, 2245-2249.

(8) Nagatani, H.; Watarai, H. *Chem. Lett.*, **1997**, 167-168.

(9) Groves, J. T.; Nemo, T. E.; Myers, R. S. *J. Am. Chem. Soc.*, **1979**, *101*, 1032-1033.

(10) Mansuy, D.; Bartoli, J. F.; Chottard, J. C.; Lange, M. *Angew. Chem.*, **1980**, *92*, 938-939.

(11) Shannon, P.; Bruice, T. C. *J. Am. Chem. Soc.*, **1981**, *103*, 4580-4582.

(12) Smith, J. R. L.; Sleath, P. R. *J. Chem. Soc.*, *Perkin Trans 2*, **1982**,1009-1015.

(13) Dicken, C. M.; Lu, F. L.; Nee, M. W.; Bruice, T. C. *J. Am. Chem. Soc.*, **1985**, *107*, 5776-5789.

(14) Collman, J. P.; Sorrell, T. N.; Hoffman, B. M. *J. Am. Chem. Soc.*, **1975**, *97*, 913-914.

(15) Higuchi, T.; Uzu, S.; Hirobe, M. *J. Am. Chem. Soc.*, **1990**, *112*, 7051-7053.

(16) Hoffman, A. B.; Collins, D. M.; Day, V. W.; Fleischer, E. B.; Srivastava, T. S.; Hoard, J. L. *J. Am. Chem. Soc.*, **1972**, *94*, 3620-3626.

(17) Murray, K. S. *Coord. Chem. Rev.*, **1974**, *12*, 1-35.

(18) Kurtz, Jr. D. M. *Chem. Rev.*, **1990**, *90*, 585-606.

(19) West, B. O. *Polyhedron*, **1989**, *8*, 219-274.

(20) Fleischer, E. B.; Srivastava, T. S. *J. Am. Chem. Soc.*, **1969**, *91*, 2403-2405.

(21) Saxton, R. J.; Olson, L. W.; Wilson, L. J. *J. Chem. Soc.*, *Chem. Commun.*, **1982**, 984-986.

(22) Choen, I. A. *J. Am. Chem. Soc.*, **1969**, *91*, 1980-1983.

(23) Fleischer, E. B.; Palmer, J. M.; Srivastava, T. S.; Chatterjee, A. *J. Am. Chem. Soc.*, **1971**, *93*, 3162-3166.

(24) Watarai, H.; Satoh, K. *Langmuir*, **1994**, *10*, 3913-3915.

(25) Strauss, S. H.; Pawlik, M. J.; Skowyra, J.; Kennedy, J. R.; Anderson, O. P.; Spartalian, K.; Dye, J. L. *Inorg. Chem.*, **1987**, *26*, 724-730.

(26) Swepston, P. N.; Ibers, J. A. *Acta Cryst.*, **1985**, *C41*, 671-673.

(27) Sadasivan, N.; Eberspaecher, H. I.; Fuchsman, W. H.; Caughey, W. S. *Biochemistry*, **1969**, *8*, 534-541.

Chapter 4

Two-Phase Stopped-Flow Method Applied to Kinetic Measurement of Protonation of H_2TPP at the Liquid-Liquid Interface

Abstract

The protonation mechanism of 5,10,15,20-tetraphenylporphyrin (H_2TPP) in the dispersed two-phase system composed of a dodecane and an aqueous acid phases was studied by means of a stopped-flow method. The protonation reaction took place at the liquid-liquid interface, and the diprotonated product, H_4TPP^{2+}, was adsorbed there. The interfacially adsorbed species are existed as the diprotonated monomer in the dodecane-trichloroacetic acid system and the J-aggregate in the dodecane-hydrochloric acid system, respectively. In order to determine the detailed mechanism of the protonation in the dodecane-trichloroacetic acid system, the changes in absorbance at the absorption maximum wavelengths of H_2TPP and H_4TPP^{2+} were analyzed. The obtained rate constant for the decrease of H_2TPP in the organic phase, 21 ± 2 s^{-1}, was in agreement with that for the increase of H_4TPP^{2+} at the interface, 20 ± 3 s^{-1}. The observed rate constants did not show any dependence on both concentrations of H_2TPP and the acid. The experimental results suggested the rate-determining step to be the molecular diffusion process of H_2TPP in the stagnant layer in the organic phase side at the liquid-liquid interface and the thickness of the stagnant layer was estimated as 1.4×10^{-4} cm according to a two-film model. In the dodecane-hydrochloric acid, the effect of the addition of nonionic surfactant, Triton-X100, was investigated and the excess surfactant in the two-phase system prevented the interfacial reaction.

4.1 INTRODUCTION

The kinetic mechanism of solvent extraction includes, in general, bulk phase reactions and interfacial reactions. The bulk phase reactions have been extensively studied by applying various kinetic methods, *e.g.,* the flow injection method, the stopped-flow method, the relaxation methods etc.[1,2] The interfacial reactions, however, have been less understood in comparison with the bulk phase reactions.

Recently, the role of interfacial reaction in metal extraction kinetics was demonstrated by means of the high-speed stirring method employing various extraction systems including chelate extraction, ion-association extraction and synergic extraction.[3,4] It has been shown in the previous studies, for example, that the ion-association extraction rate of Fe(II) with a hydrophobic 1,10-phenanthroline is governed by the formation rate of 1:1 complex at the

liquid-liquid interface,[5] while the ion-association extraction rate of tetrabutylammonium picrate is controlled by the diffusional mass transfer rate rather than the ion pairing chemical reaction itself.[6] Now, it is highly required to find any kinetic criteria to distinguish between a mass transfer regime and a chemical reaction regime.

Stopped-flow method has widely been employed for the kinetic studies not only in homogeneous system, but also in micellar[7,8] and microemulsion systems.[9,10] However, it has rarely been applied to the study of reaction mechanisms at the liquid-liquid interface in relevance to the solvent extraction. This method has potential capabilities to produce a dispersed two-phase system by mixing rapidly an aqueous solution with an organic solution, and then to detect the rapid reactions in the dispersed system which may attain equilibria within a few hundred milliseconds. Furthermore, the reaction at the liquid-liquid interface must be directly measured by the two-phase stopped-flow spectrophotometry, provided that the reaction is accompanied by a sufficient spectral change for the detection.

5,10,15,20-Tetraphenylporphyrin (H_2TPP) is a highly hydrophobic chelate reagent with a very large molar absorptivity, hence it has a bright prospect of using as an extraction-spectrophotometric reagent. H_2TPP is known to be protonated by the attack of hydrogen ions,[11,12] and to produce the diprotonated species (H_4TPP^{2+}) which is sparingly soluble in water.

$$H_2TPP + 2H^+ \rightarrow H_4TPP^{2+} \qquad (4.1)$$

When an organic solution containing H_2TPP and an aqueous acid solution are put into contact, the protonation reaction takes place at the liquid-liquid interface, and the diprotonated species is adsorbed there.[13] The heterogeneous reaction will proceed through two steps : the molecular diffusion process of H_2TPP from the organic phase and hydrogen ions from the aqueous phase to the liquid-liquid interface, and the chemical reaction between H_2TPP and hydrogen ions at the interface. In this case, it is not necessary to consider the distribution of H_2TPP into an aqueous phase, since H_2TPP is not soluble in water. The protonation is accompanied by the distinctive spectral shift at the Soret band from 416.0 nm (H_2TPP) to 438.0 nm (H_4TPP^{2+}). The large molar absorptivity of H_2TPP and the large spectral shift in the protonation are thought well suited for an *in situ* spectrophotometric study of the protonation reaction at liquid-liquid interface.

In this work, the kinetics of the formation of the diprotonated species in the dispersed dodecane-aqueous acid system was studied by means of the two-phase stopped-flow spectrophotometry, in order to clarify the rate-determining step in the interfacial protonation.

4.2 EXPERIMENTAL SECTION

Reagents. 5,10,15,20-Tetraphenylporphyrin (H_2TPP) was obtained from Dojindo Laboratories and dissolved in dodecane at concentrations ranging from 1.48×10^{-6} to 3.78×10^{-5} mol dm^{-3}. The absorption spectrum of H_2TPP in dodecane is shown in Figure 4.1. The absorption maximum wavelength, λ_{max}, and the molar absorptivity at λ_{max} in dodecane, ε, are 416.0 nm and 4.33×10^{5} dm^3 mol^{-1} cm^{-1}, respectively. Dodecane, G.R., used as an organic solvent was purchased from nacalai tesque and was highly purified by distilling after the treatment with the mixture of fuming sulfuric acid and sulfuric acid. Trichloroacetic acid (TCA) and hydrochloric acid, G.R., were obtained from nacalai tesque and used to prepare aqueous acid phases. The concentration of trichloroacetic acid was changed from 1.0×10^{-3} to 0.10 mol dm^{-3}. The ionic strengths of trichloroacetic acid and hydrochloric acid systems were maintained at 0.10 and 1.0 by the addition of sodium trichloroacetate or sodium chloride, since the dispersion state of the mixture may be influenced by the ionic strength of the aqueous solution. In this condition, the dissociation constant of trichloroacetic acid, pK_a is 0.66.[14] Therefore, the concentration of hydrogen ion in an aqueous solution was calculated from pK_a. In the hydrochloric acid system, polyoxyethylene(10)octhylphenyl ether (Triton-X100), Wako chemical Pr.Gr, was used to stabilize the dispersed two-phase system.

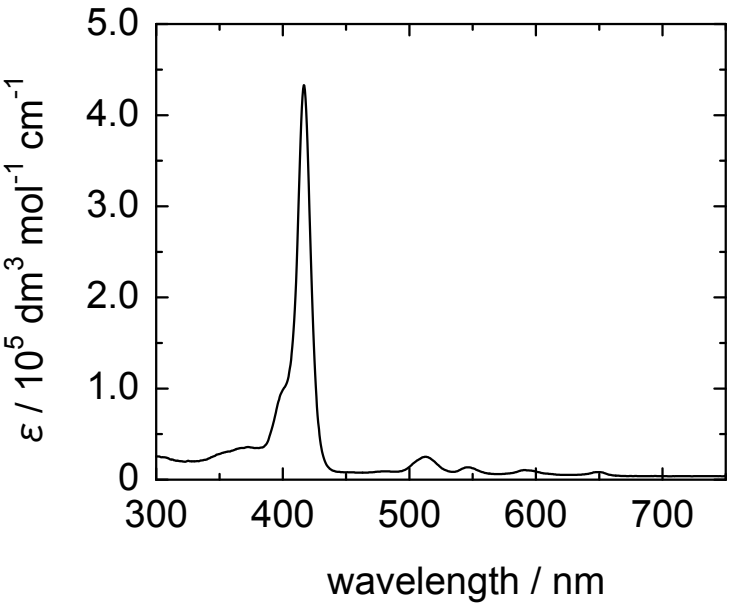

Figure 4.1. The absorption spectrum of H_2TPP in dodecane. The Soret band at 416.0 nm as the absorption maximum wavelength and four peaks of the *Q* band between 500 nm and 700 nm were observed.

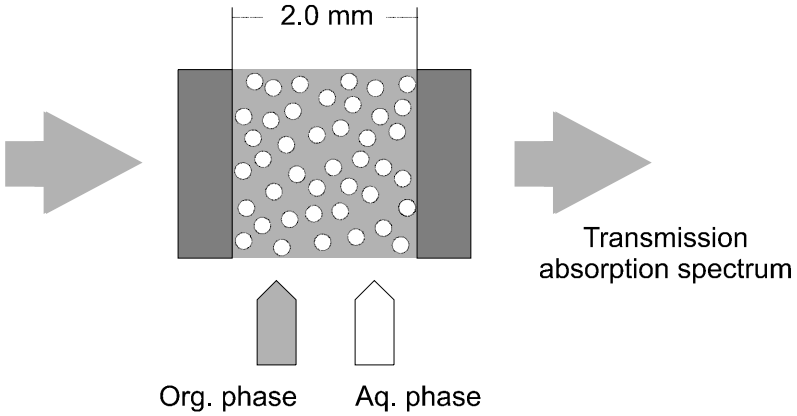

Figure 4.2. Schematic drawing of the dispersed two-phase system formed in the cylindrical quartz cell. In the dodecane-trichloroacetic acid system, an aqueous phase is dispersed as droplets. The progress of the interfacial reaction can be followed by acquiring the transmission absorption spectrum at 5.0 ms intervals.

All of aqueous solutions were prepared by using a distilled and deionized water through a Milli-Q system (Millipore, Milli-Q SP. TOC.).

Apparatus. A conventional stopped-flow spectrophotometer (Unisoku, RSP-601) was used to measure the protonation of H_2TPP in the dispersed two-phase systems as illustrated in Figure 4.2. The optical cell used for the stopped-flow measurements was a cylindrical quartz cell of 2.0 mm i.d. (*i.e.*, 2.0 mm maximum optical path length) and 6.0 mm o.d. and was thermostated at 298.2±0.1 K. A photodiode array UV/Vis detector was used to observe the change in the absorption spectrum. The radii of the dispersed droplets in the dodecane-trichloroacetic acid system were measured by an optical microscope (Nikon, LABPHOTO YF) installed with a CCD video system. In the present experiment, the dodecane phase was the continuous phase and the aqueous phase was the dispersed droplet phase. The averaged radius of the dispersed aqueous droplets in the dodecane-trichloroacetic acid system, r_0, was estimated as $(3.3 \pm 0.9) \times 10^{-3}$ cm from the video pictures.

Kinetic measurements. A dodecane solution containing H_2TPP and an aqueous acid solution containing TCA in a couple of gas-drive syringes were mixed in a volume ratio of 1 to 1 by a two-jet mixer. The total volume of the mixture was 0.2 cm^3 for each kinetic run. The dispersed droplet system of dodecane and trichloroacetic acid solution was so rapidly produced in the optical cell that it was sufficiently agitated for more than *ca.*1000 ms by the initial mixing energy without using any surfactant. After a long time standing, the droplets gradually coagulated and finally separated into two phases. The progress of the protonation at

the liquid-liquid interface was followed by acquiring the transmission absorption spectrum ranging from 346.0 to 554.0 nm at 5.0 ms intervals. The apparent first-order rate constants for the decrease of H_2TPP and the increase of H_4TPP^{2+} were obtained by analyzing the absorbance changes at each absorption maximum wavelength. A series of experiments to examine the dependence of the apparent reaction rate constants on concentrations of H_2TPP and trichloroacetic acid was carried out by using 1.0×10^{-2} mol dm^{-3} trichloroacetic acid in aqueous solution and 1.90×10^{-5} mol dm^{-3} H_2TPP in dodecane, respectively.

4.3 RESULTS AND DISCUSSION

4.3.1 Protonation Equilibrium

The spectral change in Figure 4.3 shows the decrease of H_2TPP in dodecane phase and the increase of H_4TPP^{2+} adsorbed at the interface after the mixing in the dodecane-trichloroacetic acid system. The absorption maximum wavelengths (λ_{max}) of the free base and the diprotonated species were 416.0 nm and 438.0 nm, respectively, and the isosbestic point was 423.5 nm. Beer's law was examined in the dispersed two-phase system produced by mixing H_2TPP in dodecane with 0.10 mol dm^{-3} sodium trichloroacetate solution or 1.0×10^{-2} mol dm^{-3} TCA solution. A linear relationship was obtained between absorbances and concentrations ranging from 1.48×10^{-6} to 3.78×10^{-5} mol dm^{-3}. Thus, Beer's law was confirmed and the apparent molar absorptivities for H_2TPP and the diprotonated species, H_4TPP^{2+}, in the dispersed two-phase system were determined as 5.85×10^{5} dm^3 mol^{-1} cm^{-1} and 5.71×10^{5} dm^3 mol^{-1} cm^{-1}, respectively.

The protonation equilibrium of H_2TPP at the dodecane-water interface is written as

$$H_2TPP_o + 2H^+ \rightleftharpoons H_4TPP^{2+}{}_i \qquad (4.2)$$

where the subscripts o and i denote the bulk dodecane phase and the interface, respectively.

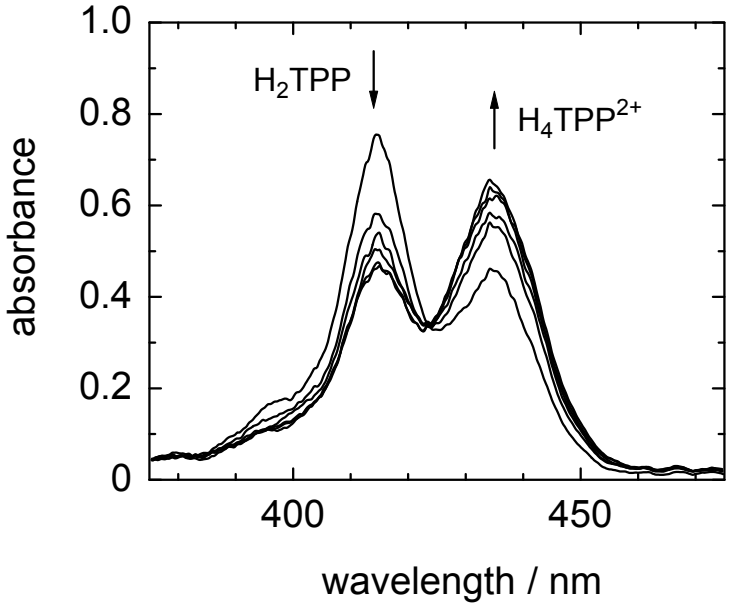

Figure 4.3. A typical spectral change measured at 50 ms intervals in the dodecane-trichloroacetic acid system. The concentrations of H_2TPP and TCA were 1.90×10^{-5} mol dm^{-3} and 1.0×10^{-2} mol dm^{-3}, respectively. The total concentration of trichloroacetate ion was 0.10 mol dm^{-3}.

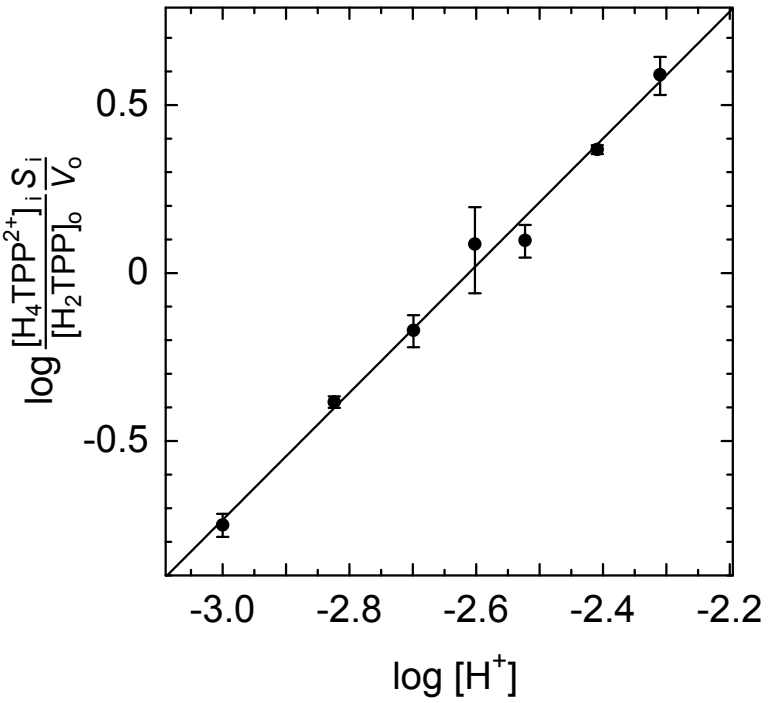

Figure 4.4. Logarithmic plot of $[H_4TPP^{2+}]_iS_i/[TPP]_oV_o$ *vs.* the concentration of hydrogen ion in an aqueous phase. The concentration of H_2TPP in dodecane was 7.6×10^{-6} mol dm^{-3} and the total concentration of trichloroacetate was kept at 0.10 mol dm^{-3}.

The protonated species is adsorbed as an ion pair with anions, *i.e.* trichloroacetate ion (TCA^-) in the present system, at the interface. The protonation equilibrium was reached at *ca.* 500 ms. The equilibrium constant, K_e, for equation 4.2 can be defined by

$$K_e = \frac{[H_4TPP^{2+}]_i S_i/V_o}{[H_2TPP]_o[H^+]^2} \qquad (4.3)$$

where $[H_2TPP]_o$ (mol dm^{-3}) and $[H_4TPP^{2+}]_i$ (mol dm^{-2}) are the bulk concentration of H_2TPP in a dodecane phase and the interfacial concentration of H_4TPP^{2+} at the equilibrium state, respectively, and S_i is the total area of the dodecane-water interface and V_o is the volume of the dodecane phase. The values of $([H_4TPP^{2+}]_i/[H_2TPP]_o)(S_i/V_o)$ could be calculated from the absorbances of both species at 1000.0 ms and the molar absorptivities. The obtained values of the concentration ratio were plotted in Figure 4.4 as a function of the hydrogen ion concentration. The slope of the linear plot was 1.9, as expected from equation 4.2, confirming the formation of H_4TPP^{2+}. From the intercept, the value of equilibrium constant was obtained as 8×10^4 mol^{-2} dm^6. This value is larger than 7.7×10^3 mol^{-2} dm^6 determined in DMSO-H_2O mixture,[12] suggesting the preferential stabilization of H_4TPP^{2+} at the dodecane-water

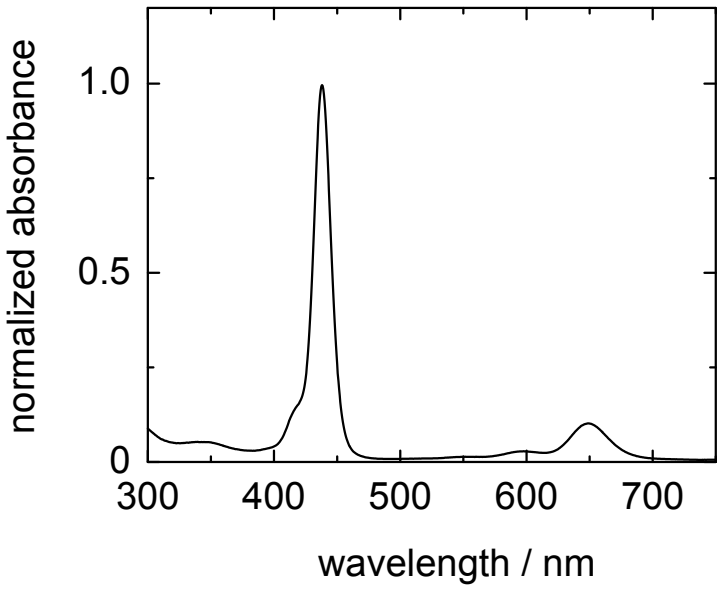

Figure 4.5. The absorption spectrum of $H_4TPP(TCA)_2$ extracted into dodecane in the strongly acidic condition. The Soret band as the absorption maximum wavelength and the *Q* band appeared at 438.0 nm and 649.0 nm, respectively. The concentration of TCA was 1.0 mol dm^{-3}.

interface.

Recently, the interfacial adsorption and the ion-association extraction of H_4TPP^{2+} described in equation 4.4 was investigated by means of the high-speed stirring method in the toluene-aqueous acid system.[15]

$$H_4TPP^{2+}{}_i + 2TCA^- \rightarrow H_4TPP(TCA)_{2\,o} \qquad (4.4)$$

In the toluene-TCA system, the ion-association extraction of the diprotonated species could occur in the low concentration of TCA, *i.e.* 0.010 mol dm^{-3}, compared with the present system. The ion-association extraction of $H_4TPP(TCA)_2$ in the dodecane-TCA system do not take place, even if 0.10 mol dm^{-3} TCA aqueous solution is used. Thus, the distribution of H_4TPP^{2+} between the liquid-liquid interface and the bulk dodecane phase is negligible in this study. It suggests that the interfacial species, H_4TPP^{2+}, can be much more stabilized at the interface in the dodecane-TCA system, since toluene is more hydrophilic than dodecane. In the strongly acidic condition with 1.0 mol dm^{-3} TCA aqueous solution, the absorption spectrum of $H_4TPP(TCA)_2$ extracted into the bulk dodecane phase could be measured and is shown in Figure 4.5.

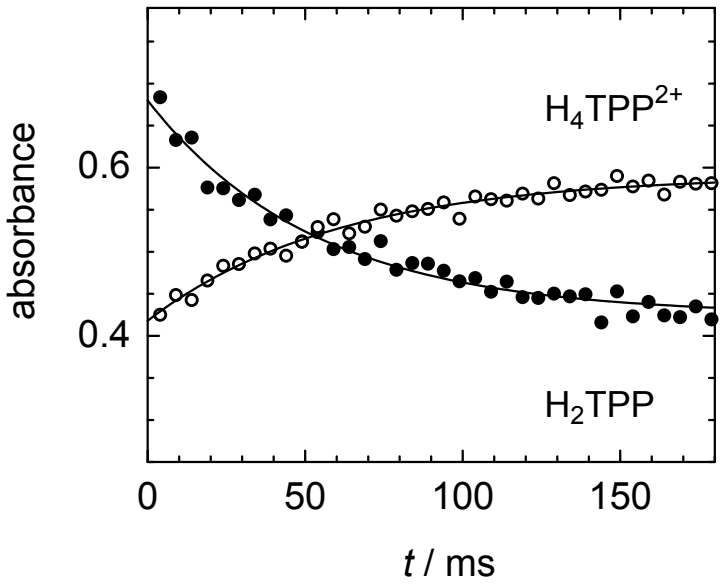

Figure 4.6. First-order kinetic profiles at the absorption maximum wavelengths, λ_{max} = 416.0 nm for H_2TPP and λ_{max} = 438.0 nm for H_4TPP^{2+}. Solid lines are the fitting curves obtained by the first-order analysis.

4.3.2 Interfacial Protonation Kinetics

In order to determine the increasing rate constants of H_4TPP^{2+}, the changes in absorbance at λ_{max} , 416.0 nm for H_2TPP and 438.0 nm for H_4TPP^{2+} were analyzed. Figure 4.6 shows the changes in absorbance at each λ_{max} after subtracting the base line drift. The absorbance changes obeyed pseudo-first-order kinetics, since the concentration of hydrogen ion in the aqueous phase was in large excess. The rate law can be written as

$$-\frac{\mathrm{d}[\mathrm{H_2TPP}]_\mathrm{o}}{\mathrm{d}t} = \frac{\mathrm{d}[\mathrm{H_4TPP^{2+}}]_\mathrm{i}}{\mathrm{d}t}\frac{S_\mathrm{i}}{V_\mathrm{o}} = k[\mathrm{H_2TPP}]_\mathrm{o} \qquad (4.5)$$

where k (s^{-1}) is the observed rate constant.

The values of the rate constant were evaluated by a curve-fitting of the absorbance data from 4.0 to 154.0 ms. The observed rate constants for the decrease of H_2TPP and for the increase of H_4TPP^{2+} under the various concentrations of H_2TPP or hydrogen ion are summarized in Table 4.1. The results show that the values of the observed rate constants depended on neither concentration of H_2TPP nor hydrogen ion. From the experiments varying the concentration of hydrogen ion, the averaged values of rate constants were 21±2 s^{-1} for the consumption of H_2TPP and 20±3 s^{-1} for the formation of H_4TPP^{2+}, fairly consistent with each

Table 4.1. Dependences of the rate constants on the concentrations of H_2TPP and hydrogen ion at 298 K in the dodecane-TCA system

dependence on concentration of H_2TPP [a]			dependence on concentration of hydrogen ion [b]		
$[H_2TPP]$ / mol dm^{-3}	rate constant[c]		$[H^+]$ / mol dm^{-3}	rate constant[c]	
	k_d / s^{-1}	k_i / s^{-1}		k_d / s^{-1}	k_i / s^{-1}
1.5×10^{-6}	14.2±2.4	23.6±4.1	2.0×10^{-3}	20.9±6.6	19.2±3.3
2.2×10^{-6}	20.1±7.8	14.3±3.5	3.0×10^{-3}	25.0±5.2	22.9±0.2
2.9×10^{-6}	23.0±3.5	13.7±3.6	4.9×10^{-3}	19.8±1.0	17.1±1.5
4.2×10^{-6}	19.3±1.9	15.8±1.4	6.8×10^{-3}	18.6±0.3	16.9±1.1
5.2×10^{-6}	19.9±2.0	14.6±0.6	9.6×10^{-2}	20.4±0.3	20.5±1.2
7.6×10^{-6}	21.3±2.0	21.6±2.3	1.8×10^{-2}	17.0±1.7	16.6±0.5
1.9×10^{-5}	20.4±0.3	20.5±1.2	4.2×10^{-2}	21.6±1.5	22.3±2.0
2.7×10^{-5}	16.9±0.6	15.2±1.1	5.6×10^{-2}	20.0±2.0	22.6±2.9
3.8×10^{-5}	16.5±1.4	15.8±1.7	7.5×10^{-2}	22.1±4.3	25.9±5.1
mean	19 ± 3	17 ± 4	mean	21 ± 2	20 ± 3

[a] The concentration of TCA was held at 1.0×10^{-2} mol dm^{-3}. [b] The concentration of H_2TPP was held at 1.90×10^{-5} mol dm^{-3}, and that of hydrogen ion was calculated from pK_a of TCA, 0.66. [c] k_d and k_i denote the rate constants for the decrease of H_2TPP and the increase of H_4TPP^{2+}, respectively.

other. A consistency between the values of 19±3 s^{-1} and 17±4 s^{-1} is also acceptable, regarding the poor reproducibility in the kinetic measurements under the various H_2TPP concentrations. The averaged value for all data listed in Table 4.1 was 19±3 s^{-1}. These results suggest the rate-determining step of the formation of H_4TPP^{2+} in the two-phase system to be the molecular diffusion process rather than the chemical reaction process. The reaction rate constants between porphyrins and hydrogen ion were reported to be larger than 10^6 dm^3 mol^{-1} s^{-1} in homogeneous systems.[12,16]

In this dispersed two-phase system, we have to consider two types of diffusion process. The diffusion of hydrogen ions in the aqueous droplet phase to the dodecane-water interface is governed by a spontaneous diffusion. On the other hand, the transport of H_2TPP molecules in the dodecane phase is attained by a turbulent flow, since the continuous dodecane phase is vigorously stirred by the mixing energy. However, even when the mixture was efficiently stirred, a stagnant layer of finite thickness located on the dodecane side of the aqueous droplet surface can be assumed. Therefore, the one-dimensional random walk model was applied to the diffusion of hydrogen ion in the aqueous phase and the two-film theory to the diffusion of H_2TPP in the stagnant layer, respectively, in order to estimate the time necessary for their

diffusion to the interface.

According to the one-dimensional random walk model, the diffusion of hydrogen ions from the aqueous phase to the interface is represented by[17]

$$\Delta = \sqrt{2D_a t} \tag{4.6}$$

where Δ, D_a and t are the diffusion distance, the diffusion coefficient in an aqueous phase and diffusion time, respectively. The devoted time in the transport process can be estimated by using equation 4.6 and a few assumptions. If we denote that the saturated interfacial concentration of H_4TPP^{2+} on the interface of an aqueous droplet is a, multiplication of $2a$ by the surface area of a droplet gives the amount of hydrogen ion required for the protonation of all H_2TPP molecules adsorbed at the interface. Then, the relationship between the hydrogen ion concentration in the aqueous phase, c_{H^+}, and the amount of the hydrogen ion supplied to the interface for the protonation of H_2TPP can be described as follows,

$$c_{H^+} \int_r^{r_0} 4\pi r^2 \mathrm{d}r = (2a)(4\pi r_0^{\,2}) \tag{4.7}$$

where r_0 and r are the radius of a droplet and a distance from a center, respectively. A maximum diffusion distance of the hydrogen ion required for the interfacial protonation can be calculated from equation 4.7. A typical value of a for interfacially adsorbed species is 10^{-8} mol dm^{-2}.[18] The minimum value of c_{H^+} and radius of the aqueous droplet in this work are 1.0×10^{-3} mol dm^{-3} and 3.3×10^{-3} cm, respectively. Thus, Δ (*i.e.*, r_0 - r) can be calculated as 2×10^{-4} cm. If we assume that D_a is the same value as the diffusion coefficient of acetic acid in 0.1 mol dm^{-3} aqueous solution at 298 K, 1.20×10^{-5} cm^2 s^{-1},[19] the devoted time in the transport process is obtained as *ca.* 2 ms. This value is vanishingly shorter than the time for achieving the protonation equilibrium. As a consideration from these estimation, we do not have to consider the diffusion of hydrogen ions from the bulk aqueous phase to the interface as the rate-determining step.

In the liquid-liquid system, the two-film theory by Lewis and Whitman has proved to be useful for dealing with a diffusion process.[20] This theory predicts that two stagnant layers exist in stirred liquid-liquid systems, one on either side of the interface with a thickness of δ. In the present system, however, the stagnant layer model is not applied to the aqueous phase side, since the interior of the aqueous droplet phase is not stirred. In the stagnant layer on the organic phase, mass transfer occurs with only molecular diffusion of species, and Fick's first law for diffusion can be applied for the rate analysis. Then, the rate equation for the diffusion of H_2TPP to the interface is written as,

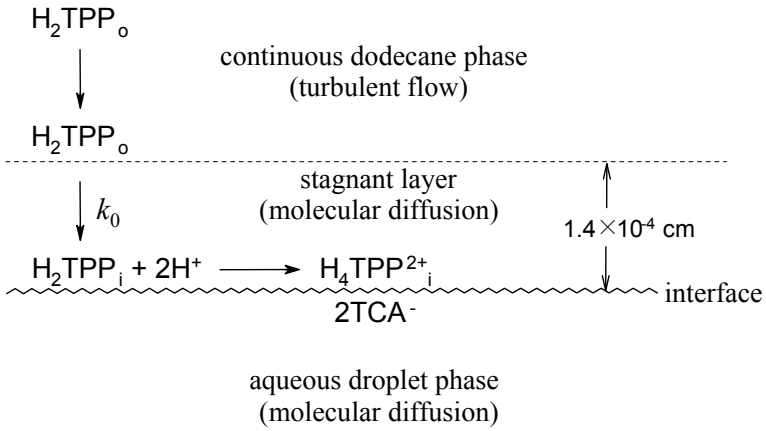

Figure 4.7. Schematic drawing of the protonation mechanism of H_2TPP at the dodecane-trichloroacetic acid interface. The molecule in the stagnant layer is provided from the continuous dodecane phase by the turbulent flow. The transport of H_2TPP to the dodecane-water interface is dominated by only the molecular diffusion. The protonation of H_2TPP proceeds at the interface and the diprotonated species, H_4TPP^{2+}, is adsorbed as the ion pair with two trichloroacetate ions.

$$-\frac{\mathrm{d}[\mathrm{H_2TPP}]_\mathrm{o}}{\mathrm{d}\,t} = \frac{D_\mathrm{o}}{\delta_\mathrm{o}}\frac{S_\mathrm{i}}{V_\mathrm{o}}[\mathrm{H_2TPP}]_\mathrm{o} \tag{4.8}$$

where D_o is the diffusion coefficient of H_2TPP in a dodecane phase. Equation 4.8 has the same form as the pseudo-first-order rate equation 4.5 in which the term (D_oS_i/δ_oV_o) is equal to the rate constant k. The thickness of the stagnant layer can be evaluated from the values of k, D_o, and S_i/V_o. The specific interfacial area, S_i/V_o, can be calculated by using the droplet radii of the dispersed phase, in which the volume of a dodecane phase is the same as that of an aqueous phase. If we assume that the distribution of droplet sizes is uniform over the whole system in the optical cell, the value of S_i/V_o can be estimated by dividing the sum of interfacial area by the sum of each droplet volume and was calculated as 777 cm^{-1} from equation 4.9.

$$\frac{S_\mathrm{i}}{V_\mathrm{o}} = \frac{\sum_i 4\pi r_i^{\,2}}{\sum_i (4\pi r_i^{\,3}/3)} \tag{4.9}$$

The averaged droplet radius in the present system was $(3.3\pm0.9)\times10^{-3}$ cm. The diffusion coefficient of H_2TPP in a dodecane phase is extrapolated from the values in several alkanes measured by Tominaga *et al.*,[21] as 3.5×10^{-6} cm^2 s^{-1}. The rate constant of 19 s^{-1}, which is the averaged value for all data in Table 4.1, yields 1.4×10^{-4} cm as the thickness of the stagnant

layer. The values of the thickness of the stagnant layer previously reported range from 1×10^{-4} to 1×10^{-2} cm.[22] Because the present system is vigorously agitated for at least 1000 ms, the stagnant layer is thought to become very thin. The mechanism of the protonation of H_2TPP at the dodecane-water interface is schematically shown in Figure 4.7.

4.3.3 Effect of the Addition of Nonionic Surfactant

The nonionic surfactant, Triton-X100, was added into an aqueous phase in the dodecane-hydrochloric acid system to stabilize the dispersed system, because the rate of the protonation of H_2TPP in this system was slower than that of the trichloroacetic acid system. The dispersed two-phase system without adding any surfactant is stable for *ca.* 1000 ms, however, the protonation equilibrium in the hydrochloric acid system is reached at a few thousands milliseconds.

Figure 4.8 shows a typical spectral change of the protonation of H_2TPP in the dodecane-hydrochloric acid system without any surfactant. We could find a difference of the protonation product between trichloroacetic acid and hydrochloric acid systems. The protonation product adsorbed at the interface in the trichloroacetic acid system was only the diprotonated monomer, H_4TPP^{2+}. However, in the hydrochloric acid system, two species were

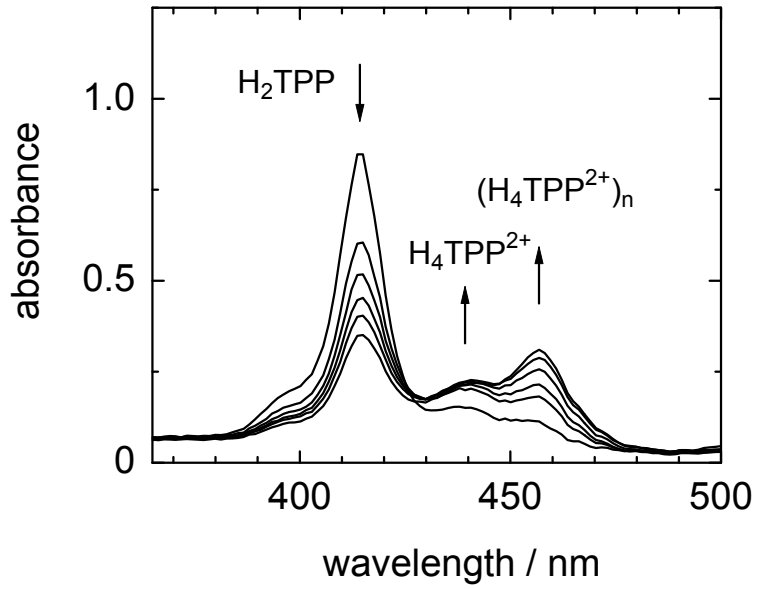

Figure 4.8. A typical spectral change from 4 ms to 1004 ms at 200 ms intervals measured in the dodecane-hydrochloric acid system without any surfactant. The concentrations of H_2TPP and hydrochloric acid were 1.90×10^{-5} mol dm^{-3} and 1.0 mol dm^{-3}, respectively. The ionic strength was 1.0.

formed at the interface and they had two absorption maximum wavelengths at 438 nm and 457 nm. After the formation of a species at 438 nm in the initial reaction stage, the red-shifted one at 457 nm increased. It suggests that the formation rate of a species at 457 nm is slower than that of the preceded reaction shown in equation 4.2. The species at 438 nm can be assigned as the diprotonated monomer from the result in the trichloroacetic acid system and other one is the J-aggregate of the diprotonated species described as $(H_4TPP^{2+})_n$.

$$n H_4TPP^{2+}{}_i \rightarrow (H_4TPP^{2+})_{ni} \qquad (4.10)$$

The red-shifted J-aggregate relating to several diprotonated porphyrins was reported in the heterogeneous system[23-26] and at the liquid-liquid interface.[13]

The shift of the absorption frequency (cm^{-1}), which is attributable to the aggregation, is represented by[27,28]

$$\Delta\nu_{nm} = \frac{1}{4\pi\varepsilon_0}\frac{2}{h}\frac{(n-1)}{n}\frac{\langle M^2\rangle}{r_{nm}{}^3}(1-3\cos^2\alpha) \qquad (4.11)$$

where ε_0, h, $\langle M^2\rangle$ and r_{nm} are the dielectric constant in vacuum, Plank constant, the mean square of the transition dipole moment of the monomer and the center-to-center distance between monomers, respectively. If the angle, α, between the transition dipole moment of monomers and the center-to-center axis is less than 54.7 °, the difference between the absorption frequencies of the aggregate and the monomer, $\Delta\nu_{nm}$, is a negative value which means the red-shift of the absorption frequency. As shown in Figure 4.9, the red-shift and the blue-shift expect the formation of the J-aggregate ($0° < \alpha < 54.7°$) and the H-aggregate ($54.7° < \alpha < 90°$), respectively. Thus, the red-shift of the Soret band of the diprotonated species from 438 nm to 457 nm obtained in the present system suggests the formation of the J-aggregate at the liquid-liquid interface. The reaction mechanism in the

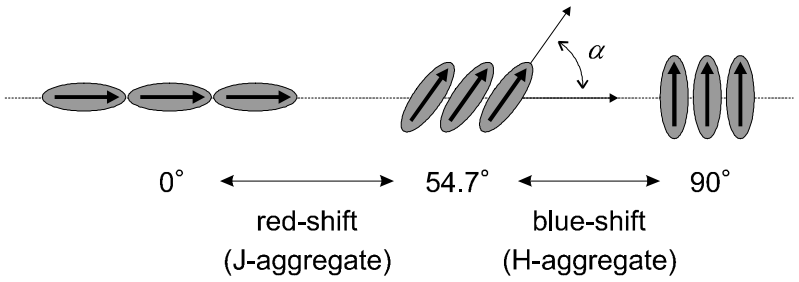

Figure 4.9. Schematic drawing of the arrangement of H_4TPP^{2+} molecules. The red-shift and the blue-shift of the Soret band expect the formation of the J-aggregate ($0° < \alpha < 54.7°$) and the H-aggregate ($54.7° < \alpha < 90°$), respectively.

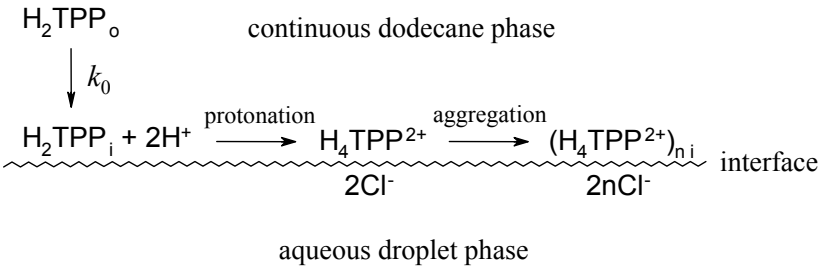

Figure 4.10. Schematic drawing of the protonation mechanism of H_2TPP in the dodecane-hydrochloric acid system. After the interfacial protonation, the J-aggregate, $(H_4TPP^{2+})_n$, is slowly transformed from the diprotonated monomers.

dodecane-hydrochloric acid system is illustrated in Figure 4.10. The protonation and aggregation of H_4TPP^{2+} in the dodecane-hydrochloric acid system is also described in Chapter 5.

The spectrum changes measured in the dodecane-hydrochloric acid systems containing Triton-X100 are shown in Figure 4.12(a) and (b). The addition of Triton-X100 made the dispersed system stable. However, the interfacial amount of the diprotonated monomer at 438 nm was decreased by the addition of the surfactant, although the total interfacial area of the dispersed droplet system was increased, and the equilibrium was reached at *ca.* 500 ms. In this condition, the diprotonated monomer as an initial product at 438 nm was decreased with the elapse of time and the aggregate was increased. In contrast to the case in the absence of Triton-X100, the production of H_4TPP^{2+} at the interface was not continued. It suggested that the surfactant molecule was preferentially adsorbed at the liquid-liquid interface and the interfacial reaction between the free base in a bulk organic phase and hydrogen ions in an aqueous phase was depressed by the surfactant layer. Since the unit area consumed by the adsorption of the J-aggregate is smaller than the diprotonated monomer, it was predicted that

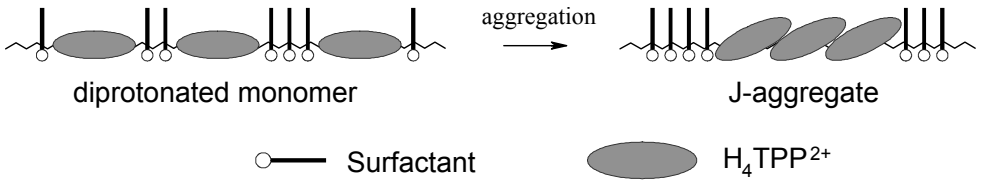

Figure 4.11. Schematic drawing of the transformation from the diprotonated monomer to the J-aggregate at the liquid-liquid interface in the presence of surfactant molecules. The interfacial area occupied by the molecules constructing the J-aggregate is smaller than that of free monomers.

the aggregation was promoted by the increase of the interfacial area occupied by products and surfactants.(Figure 4.11) In the presence of Triton-X100 of 7×10^{-4} mol dm^{-3} and more, the interfacial protonation was completely inhibited. These effects of the addition of Triton-X100 could be observed in both the dodecane-hydrochloric acid and the dodecane- trichloroacetic acid systems.

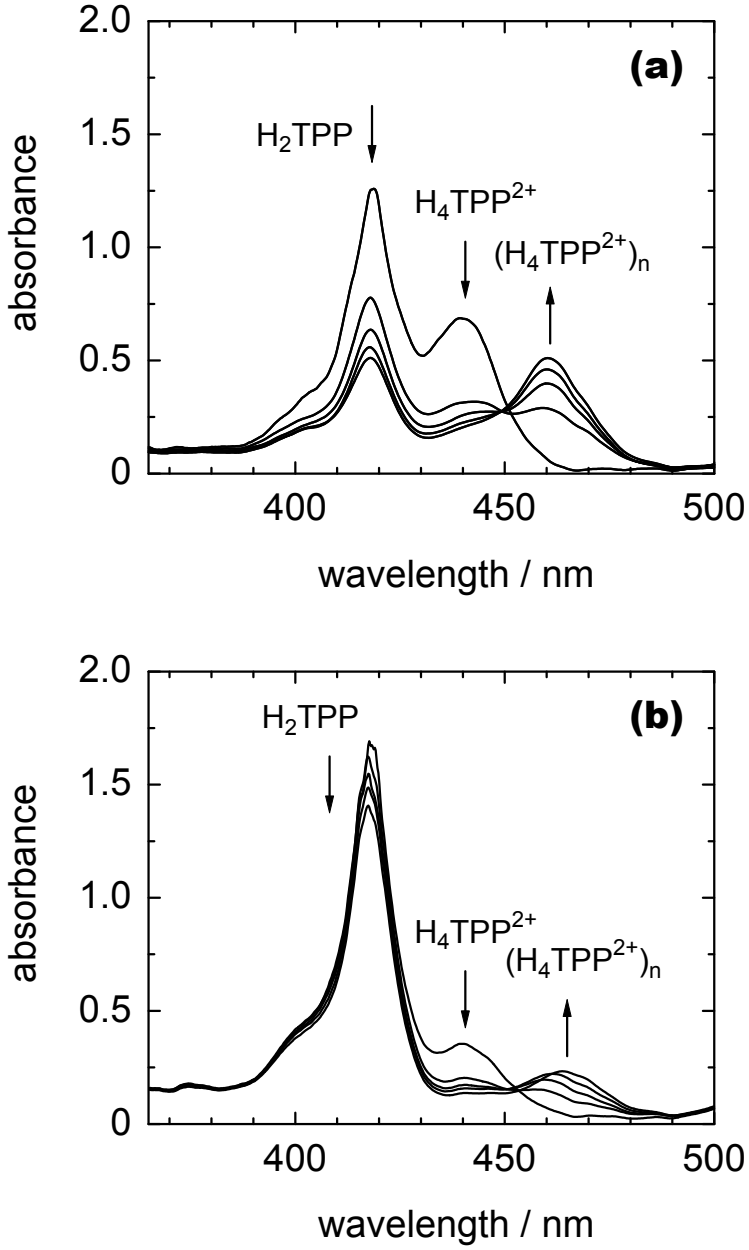

Figure 4.12. Typical spectral changes in the presence of nonionic surfactant, Triton-X100, from 4 ms to 504 ms. The concentrations of Triton-X100 in an aqueous solution were 1.3×10^{-4} mol dm^{-3} (a) and 4.1×10^{-4} mol dm^{-3} (b), respectively. The concentrations of H_2TPP in dodecane and hydrochloric acid in an aqueous solution were 3.80×10^{-5} mol dm^{-3} and 1.0 mol dm^{-3}, respectively.

4.4 CONCLUSIONS

The two-phase stopped-flow method was applied to the protonation of H_2TPP in the dodecane-trichloroacetic acid system. The sensitivity of this method to the interfacial species is very high and the specific interfacial area, S_i/V_o was evaluated as 777 cm^{-1}. It was revealed that the rate-determining step of the protonation of H_2TPP in the present system is a molecular diffusion process of H_2TPP within the stagnant layer in a dodecane phase. The averaged mass transport rate constant within the stagnant layer was measured as 19±3 s^{-1} and the thickness was estimated as 1.4×10^{-4} cm from the analysis with the two-film theory. This value can be thought as a limiting maximum value for the solvent extraction rate constant in a dodecane-water system. In other words, the interfacial reaction with larger rate constant than 19 s^{-1} must be leveled off in this system and only slower reaction can be assigned to the "true" interfacial chemical reaction.

In the dodecane-hydrochloric acid system, the nonionic surfactant, *i.e.* Triton-X100, was added into the aqueous phase to stabilize the dispersed two-phase system and the influence for the interfacial reaction was investigated. Two interfacial species, which were H_4TPP^{2+} and the J-aggregate, were detected in this system, whereas the progress of the protonation of H_2TPP was prevented by Triton-X100 molecules which could be preferentially adsorbed at the interface.

In addition, we also have to develop a method to study the interfacial kinetics of much slower reaction such as the aggregation of H_4TPP^{2+} in the dodecane-hydrochloric acid system.

4.5 REFERENCES

(1) Batt, L.; Hague, D. N. In *Comprehensive Chemical Kinetics*, *Vol. 1*; Bamford, C. H., Tipper, C. F. H. Eds.; Elsevier: Amsterdam, 1969; Chapters 1 and 2.

(2) *Techniques and Applications of Fast Reactions in Solution*; Gettins, W. J., Wyn-Jones, E. Eds.; D. Reidel Publishing Company: Holland, 1978.

(3) Watarai, H. *Trends Anal. Chem.*, **1993**, *12*, 313-318.

(4) Freiser, H. *Bull. Chem. Soc. Jpn.*,**1988**,*61*, 39-45.

(5) Watarai, H.; Sasaki, K.; Sasaki, N. *Bull. Chem. Soc. Jpn.*, **1990**, *63*, 2797-2802.

(6) Cantwell, F. F.; Freiser, H. *Anal. Chem.*, **1988**, *60*, 226-230.

(7) Robinson, B. H.; White, N. C.; Mateo, C. *Adv. Mol. Relax. Processes*, **1975**, *7*, 321-338.

(8) James, A. D.; Robinson, B. H. *J. Chem. Soc.*, *Faraday Trans. 1*, **1978**, *74*, 10-21.

(9) Fletcher, P. D.; Howe, A. M.; Robinson, B. H. *J. Chem. Soc.*, *Faraday Trans. 1*, **1987**, *83*, 985-1006.

(10) Fletcher, P. D.; Robinson, B. H. *J. Chem. Soc.*, *Faraday Trans. 1*, **1984**, *80*, 2417-2437.

(11) Hibbert, F.; Hunte, P. P. K. *J. Chem. Soc.*, *Chem. Comm.*, **1975**, 728-729.

(12) Hibbert, F.; Hunte, P. P. K. *J. Chem. Soc.*, *Perkin Trans. 2*, **1977**, 1624-1628.

(13) Watarai, H.; Chida, Y. *Anal. Sci.*, **1994**, *10*, 105-107.

(14) Martell, A. E.; Smith, R. M. *Critical Stability Constants Vol. 3*; Plenum Press: New York, 1977; p 19.

(15) Chida, Y.; Watarai, H. *Bull. Chem. Soc. Jpn.*, **1996**, *69*, 341-347.

(16) Pasternack, F. R.; Sutin, N.; Turner, H. D. *J. Am. Chem. Soc.*, **1976**, *98*, 1908-1913.

(17) Bard, A. J.; Faulkner, L. R. *Electrochemical Method*; John Wiley & Sons: New York, 1980; Chapter 5.

(18) Watarai, H.; Satoh, K. *Langmuir*, **1994**, *10*, 3913-3915.

(19) *Landolt-Börnstein* II Band, 5 Teil; Springer-Verlag: Berlin, 1968; pp 639-653

(20) Danesi, P. R. In *Principles and Practices of Solvent Extraction*; Rydberg, J., Musikas, C., Choppin, R. G., Eds.; Marcel Dekker: New York, 1992; Chapter 5.

(21) Takami, K.; Saiki, H.; Tominaga, T.; Hirayama, S.; Scully, A. In *Proceedings of 18th Symposium on Solution Chemistry of Japan*; 1995; pp 126-127.

(22) Skelland, A. H. P. In *Science and Practice of Liquid-Liquid Extraction*, *Vol. 1*; Thornton, D. J. Ed.; Oxford University Press: New York, 1992; Chapter 2.
(23) Barber, D. C.; Freitag, R. A.; Whitten, D. G. *J. Phys. Chem.*, **1991**, *95*, 4074-4086.
(24) Ohno, O.; Kaizu, Y.; Kobayashi, H. *J. Chem. Phys.*, **1993**, *99*, 4128-4139.
(25) Jin, R.-H.; Aoki, S.; Shima, K. *J. Chem. Soc.*, *Faraday Trans.*, **1997**, *93*, 3945-3953.
(26) Akins, D. L.; Zhu, H.-R.; Guo, C. *J. Phys. Chem.*, **1996**, *100*, 5420-5425.
(27) Maiti, N. C.; Mazumdar, S.; Periasamy, N. *J. Phys. Chem. B*, **1998**, *102*, 1528-1538.
(28) Bohn, P. W. *Annu. Rev. Phys. Chem.*, **1993**, *44*, 37-60.

Chapter 5

Centrifugal Liquid Membrane Method Applied to Kinetic Measurement of Demetallation of $Zn^{II}TPP$ at the Liquid-Liquid Interface

Abstract

The equilibrium and kinetics of the protonation of 5,10,15,20-tetraphenylporphyrin (H_2TPP) and the demetallation of (5,10,15,20-tetraphenylporphyrinato)zinc(II) (ZnTPP) at the dodecane-aqueous acid interface were investigated by means of a new *in situ* spectrophotometric method, the centrifugal liquid membrane (CLM) method, which can provide the thin two-phase liquid membrane system in a rotating glass cell. The consumption of H_2TPP or ZnTPP in the bulk dodecane phase and the production of the diprotonated aggregate, $(H_4TPP^{2+})_n$, adsorbed at the liquid-liquid interface were directly measured from the spectral change. The equilibrium constants of the interfacial aggregation of H_4TPP^{2+} and the demetallation of ZnTPP were determined as $\log(K_{e1} / dm^6\ mol^{-2}) = 2.14\pm0.07$ and $\log(K_{e2} / dm^9\ mol^{-3}) = -6.05\pm0.04$ at 298 K, respectively. The observed rate constant of the demetallation of ZnTPP depended upon the first-order of the acidity function and it was suggested that the rate-determining step is the formation of the monoprotonated intermediate, $[ZnTPPH]^+$, at the liquid-liquid interface. The demetallation rate constant of ZnTPP was determined as $k_1 = (8.6\pm1.3)\times10^{-5}$ $dm^3\ mol^{-1}\ s^{-1}$ at 298 K. In the aggregation of H_4TPP^{2+}, the rate-determining step was controlled by the molecular diffusion of H_2TPP in the bulk dodecane phase.

5.1 INTRODUCTION

There have been developed only a limited number of methods and devices to study interfacial reactions and interfacial adsorption at the liquid-liquid interface. Most of those methods are indirect in that the interfacial phenomena must be estimated from concentration changes in the bulk phases, *i.e.* the high-speed stirring method,[1] or from changes in interfacial energy, *i.e.* the interfacial tension methods.[2] The assignment of an interfacial species by these methods, therefore, is rather ambiguous. In Chapter 4, the author described about the direct stopped-flow spectroscopic measurement of the diprotonation of 5,10,15,20-tetraphenylporphyrin (H_2TPP) at a liquid-liquid interface.[3] The two-phase stopped-flow spectrometry was very sensitive to detect the interfacial species and applicable to a fast interfacial reaction of sub-second, but the dispersed two-phase system formed was stable only for *ca.* 1000 ms. Thus, in order to establish the direct spectroscopic method of the

interfacial kinetics, several requirements have to be resolved, including the stability of the two-phase system, the discrimination of overlapped absorption spectra of the bulk phase species and the large specific interfacial area.

In this Chapter, we proposes a new *in situ* spectrophotometric method to study liquid-liquid interfacial reaction kinetics. The ultra-thin two liquid membranes were made in a rotating optical cell, and the spectral change was directly observed.

The kinetics of the demetallation of metalloporphyrin are well studied in homogeneous systems.[4-6] However, the kinetics and liquid-liquid interfacial reaction mechanism of the metalloporphyrin have not been reported. As described in Chapters 2 and 3, the author studied about the adsorption behavior and reaction mechanism of several metalloporphyrins at the liquid-liquid interface.[7,8] (5,10,15,20-Ttetraphenylporphyrinato)zinc(II) (ZnTPP) is specifically adsorbed at the liquid-liquid interface, compared with other divalent metal complexes, *e.g.*, cobalt(II), nickel(II), copper(II) and vanadyl(IV). In this work, the kinetics and mechanism of demetallation of ZnTPP at the dodecane-aqueous acid interface were investigated to demonstrate the advantages of the new method.

5.2 EXPERIMENTAL SECTION

Reagents. (5,10,15,20-tetraphenylporphyrinato)zinc(II) (ZnTPP) was prepared from 5,10,15,20-tetraphenylporphyrin (Dojindo Laboratories) and zinc(II) acetate dihydrate (Wako Chemicals, > 99.9 %) in acetic acid by according to the literature.[9] ZnTPP prepared in acetic acid was extracted into dodecane and washed several times with Milli-Q water. Dodecane as an organic solvent was obtained from nacalai tesque, G.R. and purified by distillation after being washed with a mixture of fuming sulfuric acid (nacalai tesque, E.P., 25 %) and sulfuric acid. The hydrochloric acid solution of various concentrations was used as an aqueous phase, and the ionic strength was kept at 2.0 by the addition of sodium chloride. All of the acids and sodium chloride were G.R. grade of nacalai tesque. The aqueous solutions used for the experiments were all prepared in Milli-Q water purified with a Millipore Milli-Q SP.TOC.

Centrifugal Liquid Membrane Method. The centrifugal liquid membrane (CLM) method can form the stable ultra-thin two-phase liquid membrane by the centrifugal force produced by the rotation. The CLM apparatus is schematically shown in Figure 5.1. The organic phase and the aqueous phase (0.250 cm^3) were put into the cylindrical glass cell and stoppered by a Teflon® plug attached to the rotation shaft of the high-speed motor (HITACHI, GP 2SA).

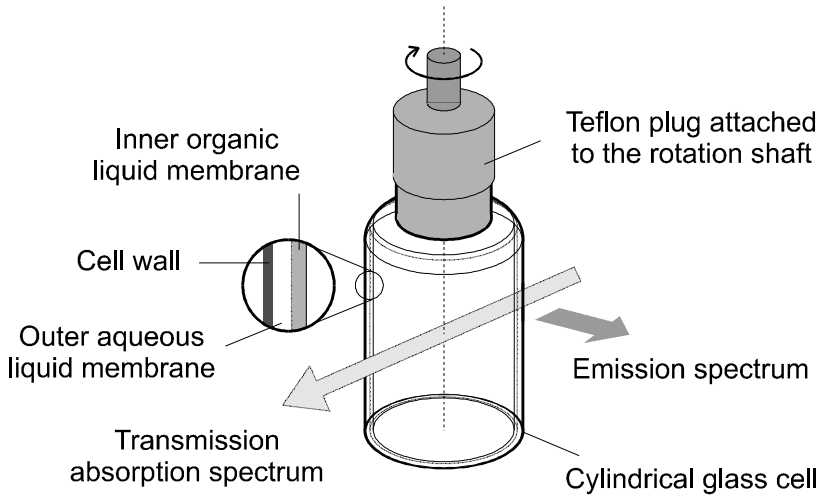

Figure 5.1. Schematic drawing of the centrifugal liquid membrane apparatus. The thin two-phase liquid membrane system was stable in the rotation speed ranging from 6000 to 7500 rpm. In the present system, the organic phase, 0.150 cm^3, and the aqueous phase, 0.250 cm^3, were spread as an inner liquid membrane of 79 μm film thickness and an outer liquid membrane of 145 μm thickness, respectively. The transmission absorption spectrum was measured from the perpendicular direction to the rotation axis by the diode array spectrophotometer.

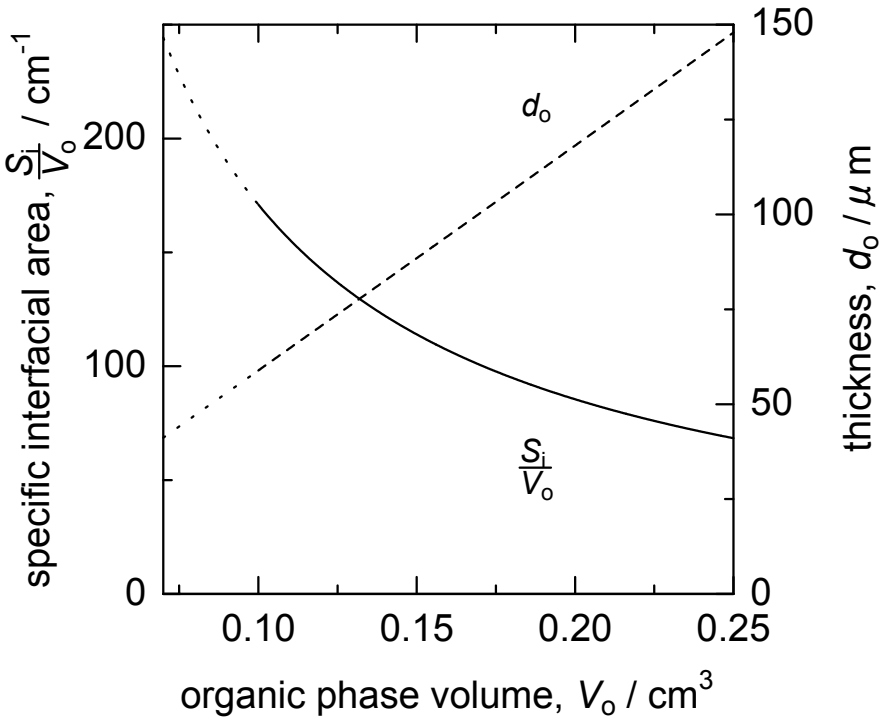

Figure 5.2. The relationships of the specific interfacial area, S_i/V_o, and the film thickness of an organic phase, d_o, *vs.* the organic phase volume, V_o, in the CLM apparatus. The solid line and broken line refer to S_i/V_o and d_o, respectively. The stable two-phase liquid membrane system could be formed within 68 cm^{-1} ≤ S_i/V_o ≤ 170 cm^{-1} and 53 μm ≤ d_o ≤ 132 μm, respectively.

The volume of the organic phase, V_o, was available in 0.100 cm^3 ≤ V_o ≤ 0.250 cm^3, and it used in each measurement was 0.150 cm^3 unless otherwise noted. The rotation speed of the cylindrical cell was regulated by a TOSHIBA SLIDAC SD105 and monitored by a digital tachometer (ONO SOKKI, HT-431). The inner diameter and inner height of the cylindrical cell were 19 mm and 29 mm, respectively. When the densities of an organic and an aqueous phases are different, the two-phase system is spread out at the inner wall of the cylindrical glass cell by the high-speed rotation. The produced two-phase liquid membrane system was stable in the rotation speed range of *ca.* 6000 to 7500 rpm and could be regarded just as coated liquid films. In the present system, the densities of dodecane used as an organic solvent and water at 298 K are 0.745 and 0.997 g cm^{-3}, respectively.[10] Thus, the dodecane was spread as an inner liquid membrane of 79 μm film thickness and the aqueous phase as an outer liquid membrane of 145 μm thickness which was sandwiched between the dodecane layer and the cell wall. Since the interfacial area between the two phases, S_i, was 17 cm^2, the specific

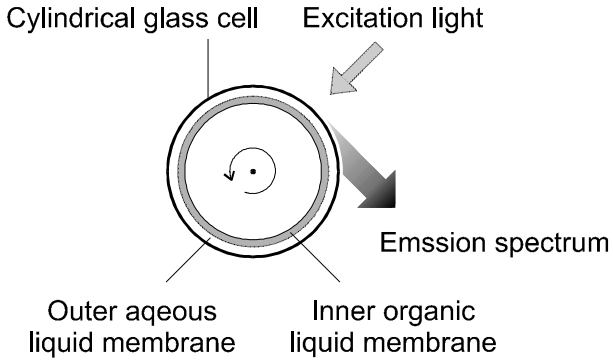

Figure 5.3. The layout of an optical cell and a detector in the fluorescence measurement. The excitation wavelength was the absorption maximum wavelength of each porphyrin compound.

interfacial area, S_i/V_o, and the organic film thickness, d_o, can be shown in Figure 5.2.

The species in the bulk phase and at the interface were measured by the absorption spectroscopy and the fluorescence spectroscopy. The summation of both absorption spectrum of interfacial and bulk organic phase species were measured from the perpendicular direction to the rotation axis with a Hewlett-Packard HP8452A diode array spectrophotometer. Thus, the light beam passed through twice the liquid-liquid interface and both bulk phases in the rotating optical cell. The emission spectrum of corresponding species was measured by a Perkin Elmer LS50B luminescence spectrometer with the layout of an optical cell and a detector, which is illustrated in Figure 5.3. The excitation wavelengths used in the fluorescence measurement were the absorption maximum wavelengths of porphyrin compounds. The typical transmission absorption and emission spectra of the two-phase liquid membrane system are shown in Figure 5.4 and 5.5, respectively.

Equilibrium Measurements. The equilibrium constants of the interfacial protonation of H_2TPP and the demetallation of ZnTPP in the dodecane-hydrochloric acid system were determined by analyzing the transmission absorption spectra, which were measured in a thermostated room at 298±2 K. The concentrations of H_2TPP and ZnTPP were 1.71×10^{-5} mol dm^{-3} and 9.7×10^{-6} mol dm^{-3}, respectively.

Kinetic Measurements. A stable two-phase liquid membrane system in the rotating optical cell was established at *ca.* 4 s after the beginning of the rotation. The kinetic measurement of protonation and aggregation of H_2TPP in the dodecane-hydrochloric acid system was carried out by using the dodecane solution of H_2TPP ranging in the concentration from 3.23×10^{-5} to

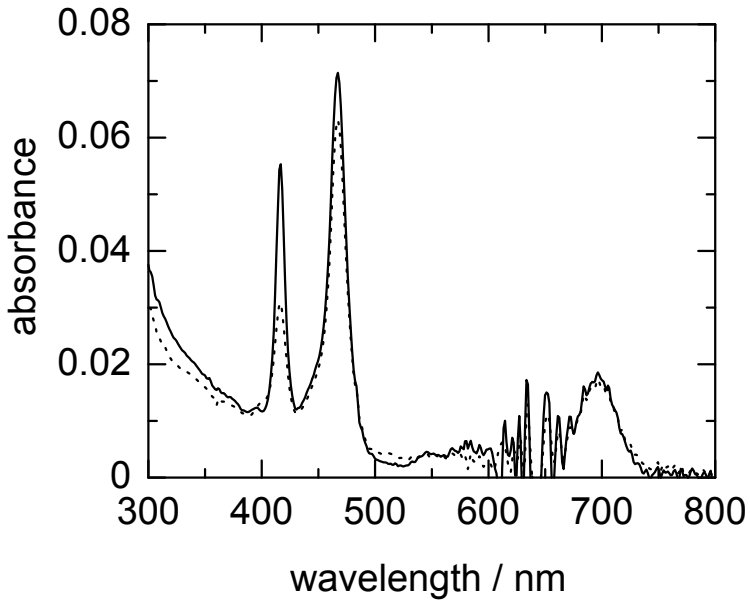

Figure 5.4. Typical transmission absorption spectra of the two-phase liquid membrane system. The solid and dotted lines refer to the demetallation of ZnTPP and the protonation of H_2TPP, respectively. The absorption maximum wavelengths were 416 nm for ZnTPP and H_2TPP in dodecane and 466 nm for $(H_4TPP^{2+})_n$ at the interface, respectively. The initial concentrations in dodecane of ZnTPP and H_2TPP were 1.86×10^{-5} mol dm^{-3} and 1.71×10^{-5} mol dm^{-3}, respectively. The concentrations of hydrochloric acid were 2.0 mol dm^{-3} for the demetallation of ZnTPP and 0.17 mol dm^{-3} for the protonation of H_2TPP, respectively.

5.9×10^{-6} mol dm^{-3} and the demetallation of ZnTPP was studied by using 8.9×10^{-6} mol dm^{-3} ZnTPP in dodecane. The changes of absorbance at the absorption maximum wavelengths and the emission intensity at the emission maximum wavelength were recorded at 1.0 s intervals with the integration time of 1.0 s. The kinetic measurements were carried out in a thermostated room at 298±2 K.

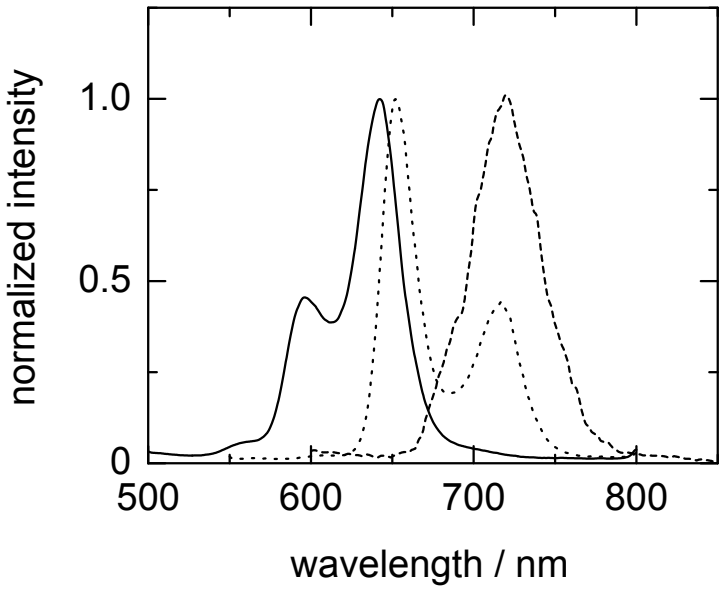

Figure 5.5. Normalized emission spectra measured in the two-phase liquid membrane system. The solid, dotted and broken lines refer to ZnTPP in dodecane, H_2TPP in dodecane and $(H_4TPP^{2+})_n$ at dodecane-water interface, respectively. The excitation wavelengths were 416 nm for ZnTPP and H_2TPP, and 466 nm for $(H_4TPP^{2+})_n$, respectively.

5.3 RESULTS AND DISCUSSION

5.3.1 Protonation and Aggregation of H_2TPP

The kinetic measurement of protonation and aggregation of H_2TPP in the dodecane-hydrochloric acid system was carried out by applying the centrifugal liquid membrane method. When the dodecane solution of H_2TPP was contacted with the aqueous acidic solution, H_2TPP was protonated and hardly stabilized at the interface, and the diprotonated product, H_4TPP^{2+}, was changed to the aggregate, $(H_4TPP^{2+})_n$, at the interface,

$$H_2TPP_o + 2H^+ \rightarrow H_4TPP^{2+}{}_i \quad (5.1)$$

$$nH_4TPP^{2+}{}_i \rightarrow (H_4TPP^{2+})_{ni} \quad (5.2)$$

where the subscripts o and i refer to the bulk organic phase and the interface, respectively. The overall reaction was represented by

$$H_2TPP_o + 2H^+ \xrightarrow{k_0} (H_4TPP^{2+})_{ni} \quad (5.3)$$

where k_0 (s^{-1}) is the pseudo-first-order rate constant. This aggregate existed only at the interface and the counter ions for the diprotonated species were postulated as chloride ions.

These reactions could be confirmed from remarkable changes in both the transmission absorption spectrum and emission spectrum. The diprotonation and aggregation were indicated by the large red-shift of the Soret band as shown in Figure 5.4, in which the transmission absorption spectra of H_2TPP in the dodecane phase and $(H_4TPP^{2+})_n$ at the dodecane-water interface were depicted. The isosbestic point was observed at *ca.* 430 nm and the absorption maximum wavelength, λ_{max}, was 416 nm for H_2TPP in dodecane and 466 nm for $(H_4TPP^{2+})_n$, respectively. The diprotonated monomer, H_4TPP^{2+}, at the interface was obtained at 440 nm in the initial stage of the aggregation, however, it disappeared rapidly

Table 5.1. Spectrometric parameters of TPP compounds

	absorption		emission[c]	
	λ_{max} / nm[a]	ε / $dm^3\ mol^{-1}\ cm^{-1}$ [b]	$Q(0, 0)$ / nm	$Q(0, 1)$ / nm
H_2TPP	416	4.33×10^5	651 (s)	716 (m)
ZnTPP	416	4.98×10^5	596 (m)	642 (s)
$(H_4TPP^{2+})_n$	466	3.06×10^5		720 (w)

[a] The Soret band as the absorption maximum wavelength. [b] The molar absorptivity at λ_{max}. [c] The excitation wavelength was λ_{max} of each compound.

accompanying by the formation of $(H_4TPP^{2+})_n$ at 466 nm. The broad absorption peak at 698 nm is the *Q* band of $(H_4TPP^{2+})_n$. The molar absorptivities of each species, ε, at λ_{max} were 4.33×10^5 dm^3 mol^{-1} cm^{-1} for H_2TPP in dodecane and 3.06×10^5 dm^3 mol^{-1} cm^{-1} for H_4TPP^{2+} forming the aggregate at the dodecane-water interface, respectively. These values are summarized in Table 5.1.

As described in Chapter 4, the author has studied about the interfacial diprotonation and aggregation of H_2TPP by means of the two-phase stopped-flow method in the dispersed dodecane-hydrochloric acid system. It was concluded that the diprotonation process from H_2TPP to H_4TPP^{2+} is faster than the aggregation process from H_4TPP^{2+} to $(H_4TPP^{2+})_n$ and λ_{max} are 440 nm for H_4TPP^{2+} and 457 nm for $(H_4TPP^{2+})_n$, respectively. It is noted that the λ_{max} for $(H_4TPP^{2+})_n$ is not consistent between the two-phase stopped-flow experiment, 457 nm, and the CLM experiment, 466 nm.(*cf.* Chapter 4) This disagreement may be attributable to the difference of conditions of the interface, *i.e.* the interface of droplets in the stopped-flow system is appreciably perturbed during the measurement, but the interface in the CLM system is not perturbed. Since the larger red-shift of the Soret band in the J-aggregation of H_4TPP^{2+} corresponds to the larger aggregation number,[11-15] it can be concluded that the aggregation of H_4TPP^{2+} in the stopped-flow system is less proceeded than that in the CLM system.

The equilibrium constant of the interfacial diprotonation of H_2TPP, K_{e1} (dm^6 mol^{-2}), was defined as

$$H_2TPP_o + 2H^+ \rightleftharpoons (H_4TPP^{2+})_{ni} \tag{5.4}$$

$$K_{e1} = \frac{[(H_4TPP^{2+})_n]_i S_i/V_o}{[H_2TPP]_o[H^+]^2} \tag{5.5}$$

The value of logK_{e1} was determined as 2.14±0.07 from the intercept of the logarithmic linear function shown in Figure 5.6 and the slope, which means the reaction order of hydrogen ion, was 2.29±0.08.

Since the concentration of hydrogen ion in the aqueous acid phase was in large excess over that of H_2TPP, the absorbance changes at λ_{max} of H_2TPP and $(H_4TPP^{2+})_n$ were analyzed by a pseudo-first-order rate law written as follows,

$$-\frac{d[H_2TPP]_o}{dt} = \frac{d[(H_4TPP^{2+})_n]_i}{dt}\frac{S_i}{V_o} = k_0[H_2TPP]_o \tag{5.6}$$

The typical first-order kinetic profiles are shown in Figure 5.7(a) and the rate constant, k_0 (s^{-1}), were determined by a least-square curve-fitting of the absorbance change at each λ_{max}. The diprotonation and aggregation attained equilibrium after *ca.* 100 s and the values of k_0 did not

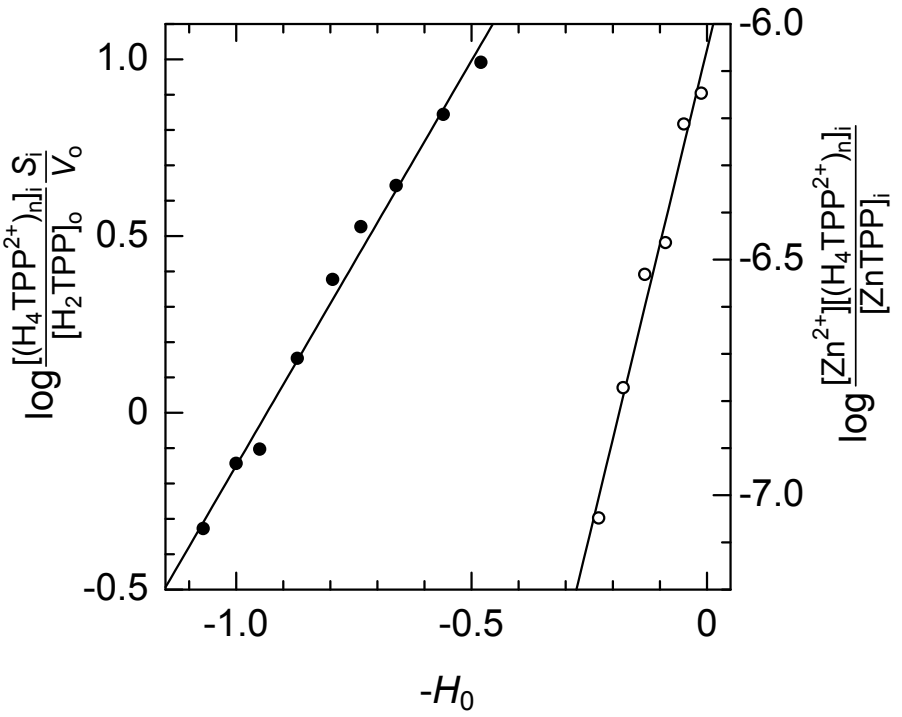

Figure 5.6. Logarithmic plot of $[(H_4TPP^{2+})_n]_i S_i/[H_2TPP]_o V_o$ and $[Zn^{2+}][(H_4TPP^{2+})_n]_i/[ZnTPP]_i$ against acidity function of hydrochloric acid, $-H_0$. The closed and open circles refer to the diprotonation of H_2TPP and the demetallation of ZnTPP, respectively. The slopes of the straight lines were 2.3 for the protonation and 4.1 for the demetallation systems, respectively. The equilibrium measurements were carried out in the thermostated room at 298±2 K.

depend upon both concentrations of H_2TPP in dodecane phase and hydrogen ion in the aqueous phase. The values of the observed rate constants were $(3.9\pm0.4)\times10^{-2}$ s^{-1} for the decrease of H_2TPP and $(4.4\pm0.4)\times10^{-2}$ s^{-1} for the increase of $(H_4TPP^{2+})_n$, respectively, and the averaged value was $(4.1\pm0.5)\times10^{-2}$ s^{-1}. Thus, it was suggested that the interfacial diprotonation of H_2TPP in the present system was proceeded by the diffusion controlled mechanism as concluded in the two-phase stopped-flow experiments.

The rate law for the diffusion controlled protonation of H_2TPP at the interface is derived from Fick's first law as follows,[16]

$$-\frac{dC_\delta}{dt} = \frac{D_o}{\delta_o}\frac{S_i}{V_o}(C_\delta - C_i) \qquad (5.7)$$

where C_δ, C_i, D_o and δ_o are the concentration of H_2TPP in dodecane at the distance of δ_o from

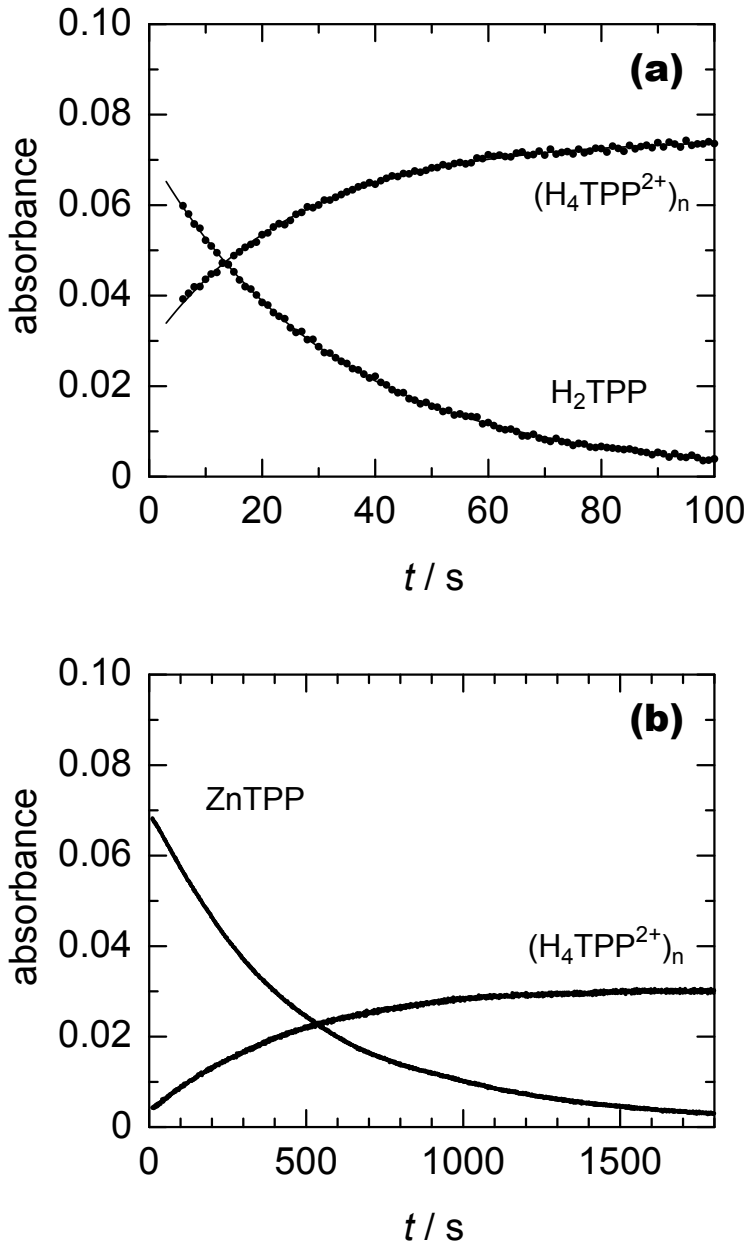

Figure 5.7. The first-order kinetic profiles observed from the CLM measurements in the diprotonation of H_2TPP (a) and the demetallation of ZnTPP (b). The solid lines are the fitting curves obtained by the first-order analysis. The initial concentrations of H_2TPP and ZnTPP in dodecane were 1.71×10^{-5} mol dm^{-3} and 8.9×10^{-6} mol dm^{-3}, respectively. The concentration of hydrochloric acid was 2.0 mol dm^{-3}.

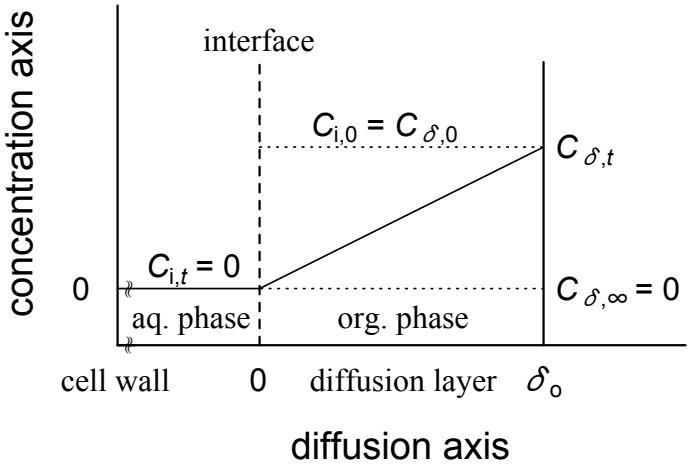

Figure 5.8. Concentration profile of a solute in an organic phase assumed by the model containing a diffusion layer. C_δ and C_i denote the concentrations of solute at the distance δ from the interface and at the interface, respectively. C_i is equal to C_δ in the initial situation, however, it decreases to zero with the progress of the interfacial reaction in which the solute is consumed after the arbitrary time.(*i.e.*, a few seconds) Then, the concentration of solute in the organic phase decreases from C_δ to zero with a linear gradient.

the liquid-liquid interface, the concentration of H_2TPP at the interface, the diffusion coefficient of H_2TPP in dodecane (3.5×10^{-6} cm^2 s^{-1}) and the thickness of diffusion layer in dodecane with a linear concentration gradient, respectively.[3] The concentration profile assumed by the diffusion model is shown in Figure 5.8. The thickness of diffusion layer is assumed to be equal to that of the organic liquid membrane, d_o (cm), in the present system, because the two-phase liquid membrane system formed by the CLM method is the ultra-thin unstirred system and the mass transfer is expected to be carried out by only molecular diffusion. For t = 0 s, the initial concentrations are all same, $C_\delta = C_i$. Since the intrinsic protonation rate of H_2TPP is much faster than the mass transfer rate, the value of C_i becomes to zero soon after the start of the reaction and the concentration of H_2TPP in the organic layer decreases from C_δ to zero with a linear gradient. In this situation, the concentration of H_2TPP observed in the CLM measurement is a mean concentration of the organic layer,

$$[H_2TPP]_o = \frac{C_\delta + C_i}{2} \cong \frac{C_\delta}{2} \qquad (5.8)$$

From equations 5.6-5.8, the rate constant, k_0, is expressed as

Table 5.2. Rate constants for the diprotonation of H_2TPP determined at several V_o conditions[a]

conditions			rate constants	
V_o / 10^{-3} cm^3 [b]	S_i/V_o / cm^{-1} [c]	d_o / 10^{-4} cm[d]	k_0 / 10^{-2} s^{-1} [e]	k_{calc} / 10^{-2} s^{-1} [f]
100	170	53	9.9±3.4	11.3
150	113	79	4.4±0.7	5.0
200	85	100	2.1±0.1	3.0
250	68	132	1.5±0.3	1.8

[a] The kinetic measurements were carried out in a constant aqueous phase volume ,0.250 cm^3. The concentration of HCl and the ionic strength were 1.0 mol dm^{-3} and 2.0, respectively. [b] The organic phase volume introduced into the rotating glass cell. [c] S_i is constant value, 17 cm^2. [d] The thickness of an organic liquid membrane. [e] Experimental rate constants at 298 K. [f] Calculated mass transport constants from equation 5.9.

$$k_0 = \frac{D_o}{\delta_o}\frac{S_i}{V_o} \tag{5.9}$$

where D_o and S_i are constant value. Equation 5.9 shows that k_0 is a function of V_o and δ_o (= d_o). When V_o is decreased, k_0 should be increased according to equation 5.9. The values of k_0 and d_o were determined in several conditions of V_o with a constant aqueous phase volume, 0.250 cm^3. The calculated mass transport constant, k_{calc} (s^{-1}), was obtained from equation 5.9 replacing δ_o by d_o. The values of k_0 and k_{calc} are summarized in Table 5.2. The values of k_0 are *ca.* 10-30 % smaller than k_{calc}, however, it is thought that k_0 agreed with k_{calc} within experimental errors. Thus, it was confirmed that the diprotonation of H_2TPP in the two-phase liquid membrane system is dominated by the diffusion controlled mechanism and k_0 is mass transport constant. It was also shown that the thickness of diffusion layer can be easily regulated by changing an organic phase volume and the values of k_0 mean the limiting value of mass transfer rate in the present two-phase liquid membrane systems. On the other hands, these results also suggest that the diffusion coefficient of a solute can be determined by the CLM experiment. Further, it may be possible that solutes with the different value of the diffusion coefficient are kinetically distinguished.

5.3.2 Demetallation Kinetics of Zn^{II}TPP

The typical kinetic profiles obtained in the CLM measurements are shown in Figure

5.7(b). In the acidic systems, ZnTPP adsorbed at the interface was decomposed to zinc ion and the free base porphyrin by the attack of hydrogen ions.

$$ZnTPP_o \rightarrow ZnTPP_i \quad (5.10)$$

$$ZnTPP_i + 2H^+ \rightarrow Zn^{2+} + H_2TPP_i \quad (5.11)$$

Immediately, H_2TPP was diprotonated and the aggregate of H_4TPP^{2+} was produced at the interface (*c.f.* equations 5.1 and 5.2). The overall demetallation of ZnTPP can be written,

$$ZnTPP_o + 4H^+ \rightarrow Zn^{2+} + (H_4TPP^{2+})_{ni} \quad (5.12)$$

where $(H_4TPP^{2+})_{ni}$ means the unit molecule constructing the aggregate.

In preliminary experiments, the author has confirmed that the demetallation of CoTPP, NiTPP and CuTPP, which do not show the adsorptivity at dodecane-water interface, can not take place in the present condition. The resistance of metalloporphyrin towards protic acids in the homogeneous system is classified into five groups according to its stability[17-19] and the assignment of stability classes is summarized in Table 5.3. The monometallic metalloporphyrins of cobalt(II), nickel(II) and copper(II) are grouped into *class II* and zinc(II) is *class III*.[20] It suggests that metalloporphyrin of cobalt(II), nickel(II) and copper(II) are more stable towards a protic acid than that of zinc(II). The stability class was explained by Buchler with a so-called "stability index" which was defined as $100 \times E_N Z/r_i$. In this index, the Pauling electronegativity, E_N, and the charge-to-radius ratio of the metal ion, Z/r_i, relate to the covalent bonding tendency of a central metal and the electrostatic contribution to the bonding energy, respectively. A small radius and the large values of a electronegativity and a charge number suggest the high stability, *e.g.*, the stability indexes are 6.8 for nickel(II), 6.1 for copper(II), 5.8 for cobalt(II) and 4.5 for zinc(II), respectively.[17,19] The typical stability of divalent metalloporphyrins decreases in the order, Pt > Pd > Ni > Co > Ag > Cu > Fe > Zn >

Table 5.3. Assignment of stability classes to metalloporphyrins towards protic acids[a]

stability class	condition (298 K, 2 h)	behavior	metal[b]
I	100 % H_2SO_4	not completely demetallated	Pd^{II}, Al^{III}, Au^{III}, V^{IV}, Sn^{IV}
II	100 % H_2SO_4	completely demetallated	Co^{II}, Ni^{II}, Cu^{II}, Mn^{III}, Fe^{III}
III	HCl/H_2O-CH_2Cl_2	demetallated	Fe^{II}, Zn^{II}, In^{III}, Bi^{III}
IV	100 % CH_3COOH	demetallated	Mg^{II}, Mn^{II}, Cd^{II}, Hg^{II}, Pb^{II}
V	H_2O-CH_2Cl_2	demetallated	Ca^{II}, Sr^{II}, Ba^{II}

[a] The stability class of metalloporphyrin defined by Falk and Phillips, and detailed in references 17 and 18. [b] The stability class of various metal complexes of octa-alkyl-porphyrins.[17,19]

Mg > Cd > Sn > Ba,[17] and the comparable tendency was also reported in the demetallation of TPP complexes with lithium in refluxing ethylenediamine.[21] The low stability of ZnTPP obtained in the interfacial reaction agreed with the stability class.

The demetallation represented in equation 5.12 was observed from the significant spectral change, since λ_{max} at the Soret band was changed from 416 nm for ZnTPP to 466 nm for $(H_4TPP^{2+})_n$. The molar absorptivity of ZnTPP in dodecane was 4.98×10^5 dm^3 mol^{-1} cm^{-1} at 416 nm. The equilibrium constant of the interfacial demetallation of ZnTPP, K_{e2} (dm^9 mol^{-3}), was defined as

$$ZnTPP_i + 4H^+ \rightleftharpoons Zn^{2+} + (H_4TPP^{2+})_{ni} \quad (5.13)$$

$$K_{e2} = \frac{[Zn^{2+}][(H_4TPP^{2+})_n]_i}{[ZnTPP]_i[H^+]^4} \quad (5.14)$$

The logarithmic values of $[Zn^{2+}][(H_4TPP^{2+})_n]_i/[ZnTPP]_i$ were plotted against the acidity function of hydrochloric acid, $-H_0$,[22] as shown in Figure 5.6. The intercept, $\log K_{e2}$, and the slope of the linear plots were determined as –6.05±0.04 and 4.1±0.3, respectively.

In the initial concentrations of ZnTPP higher than *ca.* 1.3×10^{-5} mol dm^{-3} in the acidic conditions, $-H_0 \geq 0$, the final amount of $(H_4TPP^{2+})_n$ produced at the dodecane-water interface was saturated giving the value of absorbance of 0.067±0.004 at 466 nm. In this situation, the dodecane-water interface was completely occupied by the monolayer of the diprotonated aggregates and the remaining ZnTPP in the bulk organic phase can not be demetallated anymore. Therefore, this limiting value refers to the saturated interfacial concentration, a (mol cm^{-2}), of H_4TPP^{2+} forming the aggregate at the interface and the value of a can be evaluated from

$$a = \frac{A_{sat}}{2}\frac{1}{10^3\,\varepsilon} \quad (5.15)$$

where A_{sat} and ε are the saturated absorbance at 466 nm and the molar absorptivity of the monomer unit in $(H_4TPP^{2+})_n$ at 466 nm (3.06×10^5 dm^3 mol^{-1} cm^{-1}), respectively. The saturated

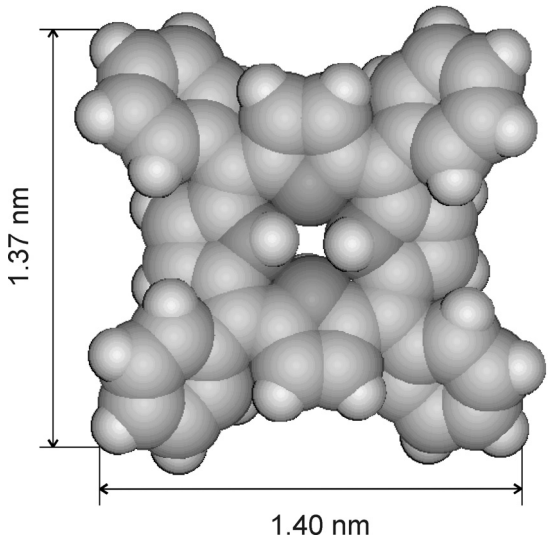

Figure 5.9. The molecular structure of H_4TPP^{2+} optimized by the molecular mechanics (MM2) calculation.

interfacial concentration and the occupied area per molecule were determined as (1.10±0.06) $\times 10^{-10}$ mol cm^{-2} and (1.51±0.08) nm^2, respectively. Taking into account that the area occupied by a molecule of H_4TPP^{2+} is predicted as *ca.* 1.9 nm^2 from the molecular mechanics (MM2) calculation, the experimental value is *ca.* 20 % smaller than the predicted value. The author has already observed that λ_{max} of the aggregate was red-shifted from 440 nm of H_4TPP^{2+} to 466 nm. Therefore, it was suggested that H_4TPP^{2+} is adsorbed as the J-aggregate at dodecane-hydrochloric acid interface. The tilting angle of the pyrrole ring plane from the interface, α, and the overlapped area of the monomers were estimated as less than 27 ° and 40 %, respectively. The configuration of H_4TPP^{2+} molecules adsorbed at the liquid-liquid interface is schematically drawn in Figure 5.10. The red-shift of the Soret band, which results from the J-aggregation of monomers, is detailed in Chapter 4.

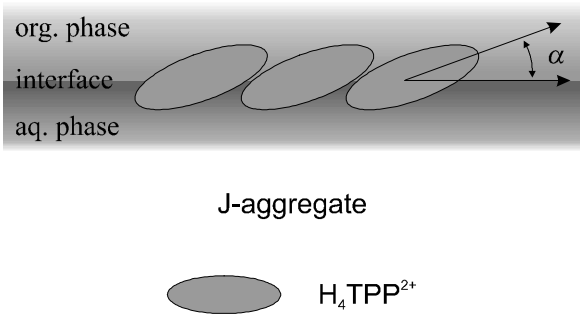

Figure 5.10. Schematic drawing of the presumed configuration of the J-aggregate at the liquid-liquid interface.(α < 27 °)

The absorbance decrease at λ_{max} of ZnTPP (*i.e.*, 416 nm) was analyzed as pseudo-first-order kinetics, since the concentration of hydrogen ion in the aqueous acid phase was in large excess. The rate law of the demetallation of ZnTPP represented by equation 5.12 was described as

$$-\frac{\mathrm{d}[\mathrm{ZnTPP}]_\mathrm{T}}{\mathrm{d}\,t} = k_{\mathrm{obs}}[\mathrm{ZnTPP}]_\mathrm{i}\frac{S_\mathrm{i}}{V_\mathrm{o}} \tag{5.16}$$

where k_{obs} (s^{-1}) is the observed rate constant and $[ZnTPP]_T$ is the total or initial concentrations of ZnTPP dissolved in the bulk organic phase, which equals the sum of the ZnTPP concentrations in the organic phase and at the interface.

$$[\mathrm{ZnTPP}]_\mathrm{T} = [\mathrm{ZnTPP}]_\mathrm{o} + [\mathrm{ZnTPP}]_\mathrm{i}\frac{S_\mathrm{i}}{V_\mathrm{o}} \tag{5.17}$$

The rate constants were obtained by a least-square curve-fitting of the absorbance change at λ_{max} of ZnTPP. The values of k_{obs} depended on the concentration of hydrochloric acid and the logarithmic values of k_{obs} were linearly correlated with the acidity function of hydrochloric acid as shown in Figure 5.11. The slope of the linear plots was calculated as 0.95 and the first-order reaction for the hydrogen ion was suggested. Since k_{obs} of the demetallation of

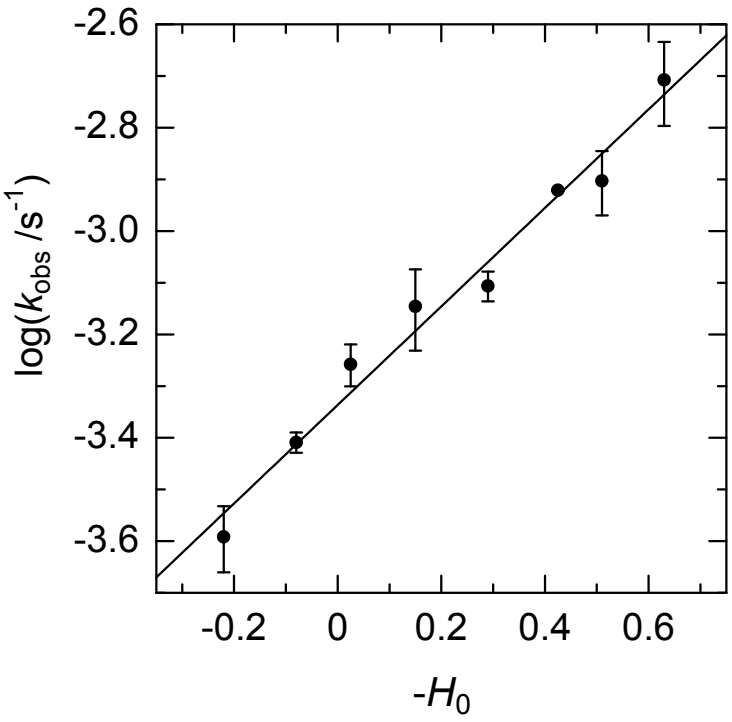

Figure 5.11. Logarithmic plot of the observed demetallation rate constants, k_{obs} (s^{-1}), *vs.* acidity function of hydrochloric acid, $-H_0$, at 298 K. The slope of the straight line is 0.95. The concentration of ZnTPP was 8.9×10^{-6} mol dm^{-3} and the ionic strength was kept at 2.0.

ZnTPP was very smaller than k_0 of the protonation of H_2TPP, it was suggested that the rate-determining step of the demetallation at dodecane-water interface is the protonation of the pyrrole ring as shown in equation 5.18.

$$[\mathrm{ZnTPP}]_\mathrm{i} + \mathrm{H}^+ \xrightarrow{k_1} [\mathrm{ZnTPPH}]^+{}_\mathrm{i} \qquad (5.18)$$

$$[\mathrm{ZnTPPH}]^+{}_\mathrm{i} + \mathrm{H}^+ \xrightarrow{k_2} \mathrm{Zn}^{2+} + \mathrm{H_2TPP_o} \qquad (k_2 >> k_1) \qquad (5.19)$$

Thus, it can be thought that the second attack of hydrogen ion shown in equation 5.19 is very fast process and the rate constant of the second step, k_2 (dm^3 mol^{-1} s^{-1}), is much larger than the rate constant of the first step, k_1 (dm^3 mol^{-1} s^{-1}). In this case, the rate law of the demetallation is described as follows,

$$-\frac{\mathrm{d}[\mathrm{ZnTPP}]_\mathrm{i}}{\mathrm{d}\,t}\frac{S_\mathrm{i}}{V_\mathrm{o}} = k_1[\mathrm{H}^+][\mathrm{ZnTPP}]_\mathrm{i}\frac{S_\mathrm{i}}{V_\mathrm{o}} \qquad (5.20)$$

From equations 5.16, 5.17 and 5.20, the value of k_1 can be calculated by

Table 5.4. The parameters of protonation and demetallation determined in the dodecane-hydrochloric acid system at 298 K

system	log K_e [a]	rate constant [b]	a / mol cm^{-2} [c]
interfacial protonation of H_2TPP	2.14±0.07	$(4.1\pm0.5)\times10^{-2}$ s^{-1}	—
interfacial demetallation of ZnTPP	-6.05±0.04	$(8.6\pm1.3)\times10^{-5}$ dm^3 mol^{-1} s^{-1}	$(1.10\pm0.06)\times10^{-10}$

[a] The logarithmic value of equilibrium constants, K_{e1} (dm^6 mol^{-2}) and K_{e2} (dm^9 mol^{-3}) refer to the diprotonation and the demetallation equilibria, respectively. [b] The rate constant of the interfacial protonation of H_2TPP was the mean value of rate constants determined in several concentrations of H_2TPP and HCl, in which the organic phase volume was 0.150 cm^3. [c] The saturated interfacial concentration determined by the direct spectrophotometric measurements.

$$k_1 = \frac{k_{obs}}{\left(1 + (1/K')(V_o/S_i)\right)[H^+]} \tag{5.21}$$

where the adsorption constant of ZnTPP in the dodecane-water system, K', is defined as

$$K' = \frac{[ZnTPP]_i}{[ZnTPP]_o} \tag{5.22}$$

and the value of K' in the dodecane-water system was determined as 2.1×10^{-4} dm.(*cf*. Chapter 2) Therefore, the rate law of the overall reaction can be rewritten as

$$-\frac{d[ZnTPP]_T}{dt} = k_1\left(1 + (1/K')(V_o/S_i)\right)[H^+][ZnTPP]_i \frac{S_i}{V_o} \tag{5.23}$$

The averaged value of k_1 was $(8.6\pm1.3)\times10^{-5}$ dm^3 mol^{-1} s^{-1} and the parameters obtained in the present study are summarized in Table 5.4.

The demetallation mechanism of ZnTPP in the dodecane-hydrochloric acid system was schematically shown in Figure 5.12. In the homogeneous systems, the second-order hydrogen ion dependence has been reported for the demetallation kinetics of various metalloporphyrins.[23-27] However, the first-order dependence of hydrogen ion concentration was obtained in this work. This difference suggests the unique property of the liquid-liquid interface as a reaction field. Since zinc atom is a relatively positive part in ZnTPP molecule and located out of the plane of pyrrole ring in its structure,[7] it is expected that the zinc atom side of the adsorbed complex is faced to the aqueous phase. The hydrogen ion may be difficult to approach the nitrogen atom of pyrrole ring in ZnTPP molecule which is somewhat solvated by dodecane. Once, a nitrogen atom of pyrrole ring is monoprotonated by a hydrogen

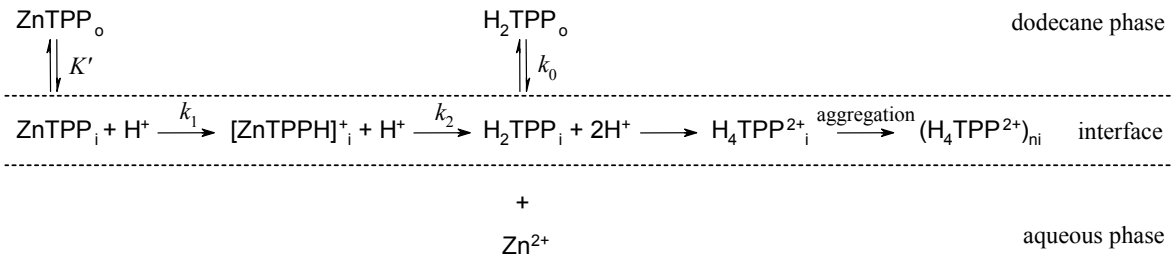

Figure 5.12. Schematic drawing of the demetallation mechanism of ZnTPP at the dodecane-water interface. The ZnTPP molecule distributes between the bulk dodecane phase and the interface with the adsorption constant defined as equation 5.22. At first, ZnTPP is monoprotonated at the interface and changed to the intermediate, $[ZnTPPH]^+$. Instantly, $[ZnTPPH]^+$ is further protonated and the free base H_2TPP is produced. The rate-determining step of the interfacial demetallation of ZnTPP is the first attacking step of a hydrogen. The diprotonation of H_2TPP in the present condition is much faster than the demetallation of ZnTPP, and at the end of reaction, the diprotonated aggregate, $(H_4TPP^{2+})_n$ is formed at the interface.

ion, the zinc complex will become more hydrophilic than the neutral compound, ZnTPP, and the produced intermediate, $[ZnTPPH]^+_i$, will be adsorbed at the interface more closely to the aqueous phase. Hence, the second protonation at the pyrrole ring can be easily proceeded. Thus, the rate-determining step of the demetallation of ZnTPP at the interface is ascribable to the first attacking step of a hydrogen ion.

5.4 CONCLUSIONS

A new spectrophotometric method to study the interfacial reaction, named the centrifugal liquid membrane (CLM) method, was established in this study. By using this method, a kinetic study of the demetallation of ZnTPP in the dodecane-hydrochloric acid system was carried out, and it was confirmed that the rate-determining step is the first attack process of hydrogen ion to ZnTPP at the interface. The specific interfacial area of the CLM method is constant value regardless of the kind of solute species. The values of the specific interfacial area summarized in Table 5.2, *i.e.* 68-170 cm^{-1}, are sufficiently large in comparison with other direct spectrophotometric methods to study the interfacial reaction in the liquid-liquid system, *e.g.*, 20 cm^{-1} of the Teflon capillary plate method, 67 cm^{-1} of the optical stir cell method[28] and 777 cm^{-1} of the two-phase stopped-flow method.[3] In addition, the sensitivity and selectivity of this method can be increased by the combination with absorption and fluorescence spectrometries. Thus, the CLM method is a sensitive and reliable method for the study of the interfacial kinetics and the adsorption equilibria. When the volume of organic phase is more reduced, the thickness of a liquid membrane becomes thinner and the specific interfacial area can readily be increased. Furthermore, the applicability of the CLM method is not restricted by the presence of surfactant and the properties of an organic solvent, *e.g.*, polarity, viscosity and refractive index. A difference in the densities of both phases is only necessary for the operation of the CLM method.

5.5 REFERENCES

(1) Watarai, H. *Trends Anal. Chem.*, **1993**, *12*, 313-318.

(2) Hanna, G. J.; Noble, R. D. *Chem. Rev.*, **1985**, *85*, 583-598.

(3) Nagatani, H.; Watarai, H. *Anal. Chem.*, **1996**, *68*, 1250-1253.

(4) Lavallee, D. K. *Coord. Chem. Rev.*, **1985**, *61*, 55-96.

(5) Hambright, P. In *Porphyrins and Metalloporphyrins*; Smith, K. M. Ed.; Elsevier: New York, 1975; Chapter 6.

(6) Berezin, B. D. *Russ. J. Inorg. Chem.*, **1992**, *37*, 634-648.

(7) Nagatani, H.; Watarai, H. *Chem. Lett.*, **1997**, 167-168.

(8) Nagatani, H.; Watarai, H. *J. Chem. Soc. Faraday Trans.*, **1998**, *94*, 247-252.

(9) Banks, C. V.; Bisque, R. E. *Anal. Chem.*, **1957**, *29*, 522-526.

(10) Riddick, J. A.; Bungel, W. B.; Sakano, T. K. *Organic Solvents*, 4th ed.; John Wiley & Sons: New York, 1986; pp 74, 132.

(11) Bohn, P. W. *Annu. Rev. Phys. Chem.*, **1993**, *44*, 37-60.

(12) Barber, D. C.; Freitag, R. A.; Whitten, D. G., *J. Phys. Chem.*, **1991**, *95*, 4074-4086.

(13) Maiti, N. C.; Mazumdar, S.; Periasamy, N. *J. Phys. Chem. B*, **1998**, *102*, 1528-1538.

(14) Ohno, O.; Kaizu, Y.; Kobayashi, H. *J. Chem. Phys.*, **1993**, *99*, 4128-4139.

(15) Akins, D. L.; Zhu, H.-R.; Guo, C. *J. Phys. Chem.*, **1996**, *100*, 5420-5425

(16) .Danesi, P.R. In *Principles and Practices of Solvent Extraction*; Rydberg, J., Musikas, C., Choppin, R. G., Eds.; Marcel Dekker: New York, 1992; Chapter 5.

(17) Buchler, J. W. Chapter 5 in reference 5.

(18) Phillips, J. N. *Rev. Pure Appl. Chem.*, **1960**, *10*, 35-60.

(19) Buchler, J. W.; Puppe, L.; Rohbock, K.; Schneehage, H. H. *Ann. N. Y. Acad. Sci.*, **1973**, *206*, 116-137.

(19) Hill, R. *Biochem. J.*, **1925**, *19*, 341-349.

(20) Eisner, U.; Harding, J. C. *J. Chem. Soc.*, **1964**, 4089-4101.

(21) Cox, R. A.; Yates, K. *Can. J. Chem.*, **1981**, *59*, 2116-2124.

(22) Sutter, T. P. G.; Hambright, P. *Inorg. Chem.*, **1992**, *31*, 5089-5093.

(23) Nwaeme, J.; Hambright, P. *Inorg. Chem.*, **1984**, *23*, 1990-1992.

(24) Thompson, A. N.; Krishnamurthy, M. *J. Inorg. Nucl. Chem.*, **1979**, *41*, 1251-1255.

(25) Cheung, S. K.; Dixon, F. L.; Fleischer, E. B.; Jeter, D. Y.; Krishnamurthy, M. *Bioinorg. Chem.*, **1973**, *2*, 281-294.

(26) Hambright, P.; Fleischer, E. B. *Inorg. Chem.*, **1970**, *9*, 1757-1761.

(27) Watarai, H.; Chida, Y. *Anal. Sci.*, **1994**, *10*, 105-107.

Chapter 6

Heterogeneous Fluorescence Quenching Reaction Between Zn^{II}TPP and Methylviologen at the Liquid-Liquid Interface

Abstract

The fluorescence quenching reaction of (5,10-15,20-tetraphenylporphyrinato)zinc(II) (ZnTPP) by methylviologen at the liquid-liquid interface was investigated by means of the centrifugal liquid membrane (CLM) method. The quenching reaction of ZnTPP at the interface could occur only in the presence of the anionic surfactant, *i.e.* sodium dodecyl sulfate (SDS). The quenching efficiency of ZnTPP depended on the concentration of SDS in aqueous phase. The quenching efficiency was approximately constant value, 13.5 %, which is less than one half value of the interfacial amount of ZnTPP evaluated from the interfacial adsorption constant. The quenching reaction was inhibited in the higher SDS concentration than *ca.* 10^{-4} mol dm^{-3}.

6.1 INTRODUCTION

The direct spectrophotometric method to determine the species adsorbed at the liquid-liquid interface has been required to study the solvent extraction system and the cell biology. As described in Chapters 4 and 5, we have devised *in situ* spectrophotometric methods, *i.e.* the two-phase stopped-flow method and the centrifugal liquid membrane (CLM) method, and investigated about the mechanisms of the interfacial adsorption reaction of the free base and the corresponding metal complex of 5,10,15,20-tetraphenyporphyrin (H_2TPP) in the liquid-liquid system by applying them.[1,2] The CLM method can form the two-phase liquid membrane system consisting of immiscible organic and aqueous phases in a rotating optical cell and it has high sensitivity for the interfacial species. The interfacial reaction could be directly measured from changes of the transmission absorption spectrum and/or the fluorescence spectrum.

Some of porphyrin compounds are known as strong phosphors.[3] In particular, as for zinc(II) complexes, the fluorescence quenching reaction and the electron transfer (ET) reaction in micellar, colloidal and homogeneous systems have been well studied as a model of the photosynthesis system.[4-9] Recently, the electron transfer between species dissolved in a nonpolar organic solvent and an aqueous solution was reported in the ternary system which

consists of electron donor, acceptor and porphyrin as catalyst.[10,11]

In this work, the author applied the CLM method for the investigation of the quenching reaction between (5,10,15,20-tetraphenyporphyrinato)zinc(II) in an organic phase and a cationic quencher, *i.e.* methylviologen (MV^{2+}), in an aqueous phase.

6.2 EXPERIMENTAL SECTION

Reagents. (5,10,15,20-tetraphenylporphyrinato)zinc(II) (ZnTPP) was prepared from 5,10,15,20-tetraphenylporphyrin (Dojindo Laboratories) and zinc(II) acetate dihydrate (Wako Chemicals, > 99.9 %) in refluxing *N,N′*-dimethylformamide.[12] Dodecane as an organic solvent was obtained from nacalai tesque and purified by distillation after being washed with a mixture of fuming sulfuric acid (nacalai tesque, E.P., 25 %) and sulfuric acid. The dichloride salt of methylviologen (TCI, G.R., > 98 %) as a quencher (Figure 6.1) was dissolved in an aqueous solution in the presence of an anionic surfactant, sodium dodecyl sulfate (nacalai tesque, S.P.). All aqueous solutions were prepared by Milli-Q water purified with a Millipore Milli-Q SP.TOC.

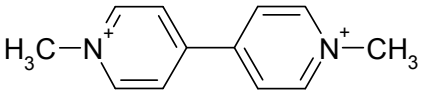

Figure 6.1. The molecular structure of methylviologen (MV^{2+}).

Measurement of Fluorescence Quenching Reaction. The centrifugal liquid membrane (CLM) method can form the stable ultra-thin two-phase liquid membrane by the centrifugal force produced by the rotation. The organic phase, 0.100 cm^3, and the aqueous phase, 0.250 cm^3, were put into the cylindrical glass cell as depicted in Figure 5.1. The optical cell was rotated by the high-speed motor (Nakanishi Inc., NK-260 with HG-200 attachment) and regulated at *ca.* 10000 rpm by a motor speed controller (Nakanishi Inc., NE-22E). The inner diameter and inner height of the cylindrical cell were 19 mm and 33 mm, respectively. When the densities of an organic and an aqueous phases are different, the two-phase system is spread out at the inner wall of the cylindrical glass cell by the high-speed rotation. The produced ultra-thin two-phase liquid membrane system was stable in the rotation speed above *ca.* 6000 rpm and the rotation speed was monitored by a digital tachometer (ONO SOKKI, HT-431). In the present system, the dodecane phase was spread as an inner liquid membrane of 56 μm film thickness and the aqueous phase as an outer liquid membrane of 128 μm thickness. The interfacial area between the two phases, S_i, was estimated as 19.6 cm^2 and the specific interfacial area, S_i/V_o, was calculated as 196 cm^{-1}. The thickness and the specific interfacial area can be controlled within 42 μm ≤ d_o ≤ 132 μm and 78 ≤ S_i/V_o ≤ 245 cm^{-1}, respectively, by changing the organic phase volume.(*cf.* Figure 5.2) The fluorescence spectrum of the two-phase liquid membrane system was measured by a Perkin Elmer LS50B luminescence spectrophotometer by the optical arrangement as shown in Figure 5.3.

Fluorescence Decay Measurement. The half life and the rate constant of the natural fluorescence decay of ZnTPP in dodecane were measured by the detecting system consists of a Hamamatsu Streak Scope C4334 and a Spectra-Physics Ti:Sappfire laser Tsunami (82 MHz) pumped by a cw visible laser Millennia V (5 W, 532 nm). The integration was 2000 times. All of measurements were carried out in the thermostated room at 298±1.5 K.

6.3 RESULTS AND DISCUSSION

Figure 6.2 shows a typical emission spectrum of ZnTPP in the two-phase liquid membrane system. ZnTPP has two characteristic emission peaks at 642 nm (strong), $Q(0,1)$, and 596 nm (medium), $Q(0,0)$.[4,5] The author found that the fluorescence quenching of ZnTPP takes place in the presence of a large excess of methylviologen and a slight amount of dodecyl sulfate anion (SDS^-). The fluorescence quenching did not take place without SDS^-. ZnTPP is an extremely hydrophobic reagent and specifically adsorbed at dodecane-water interface.[13] Since methylviologen is dissolved as a dication form in an aqueous phase, we expect that the transport of methylviologen from the aqueous phase into the dodecane phase is difficult, no matter how the ion pair with SDS^- can be formed. Moreover, preliminary experiments showed that the fluorescence quenching of the free base, which is not adsorbed at dodecane-water interface, could not occur in the same condition. Therefore, it can be predicted that the fluorescence quenching reaction of ZnTPP with methylviologen proceeds at dodecane-water interface.

Methylviologen is well known as an effective quencher for porphyrins and an electron

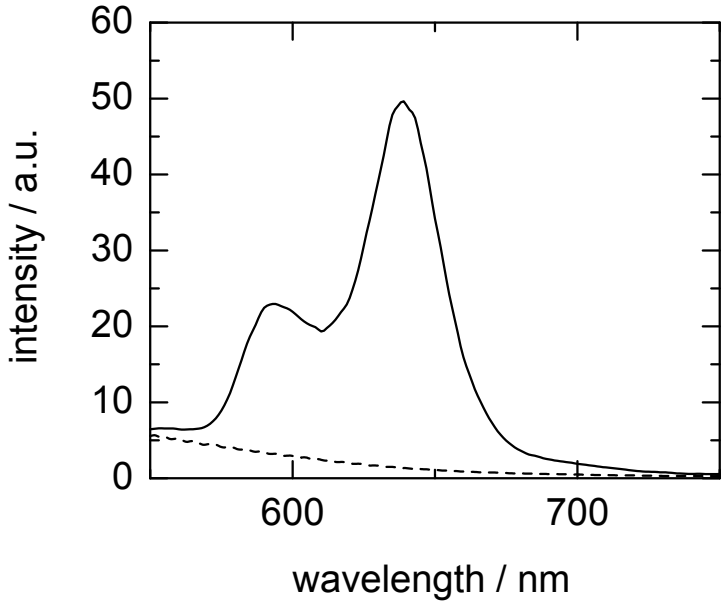

Figure 6.2. Typical emission spectra in the two-phase liquid membrane system. The solid line denotes emission spectrum of ZnTPP in the presence of MV^{2+} and the broken line is that of only MV^{2+} in an aqueous phase. The wavelength of excitation was 416.0 nm. The concentrations of ZnTPP in dodecane and MV^{2+} in aqueous solution were 3.7×10^{-6} mol dm^{-3} and 1.0 mol dm^{-3}, respectively.

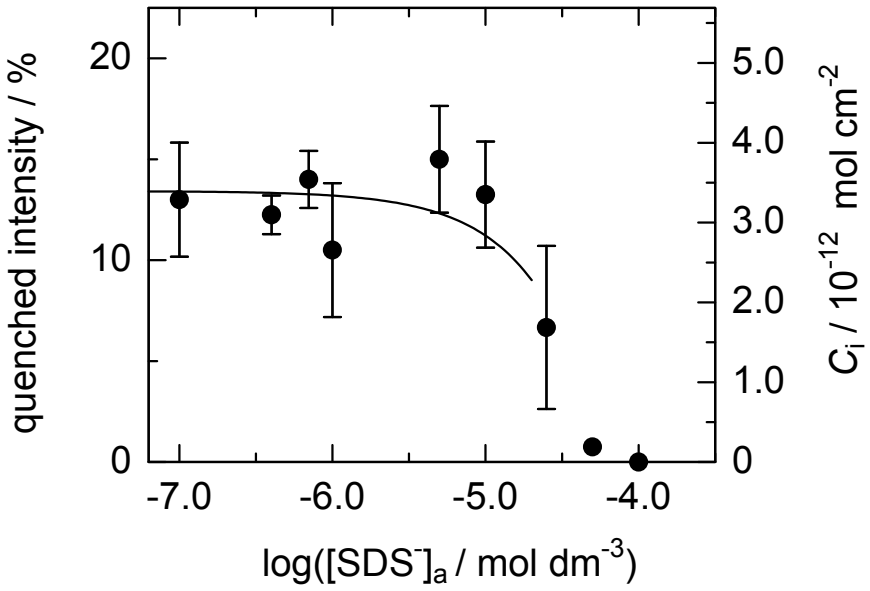

Figure 6.3. Plots of the relative quenched intensity of emission *vs.* the concentration of SDS^- in the aqueous phase. The wavelength of excitation was 416.0 nm. The concentrations of ZnTPP in dodecane and MV^{2+} in the aqueous solution were 4.1×10^{-6} mol dm^{-3} and 1.0 mol dm^{-3}, respectively.

acceptor.[4,7,14-16] It is thought that the fluorescence quenching reaction in the present system results from the electron transfer (ET) reaction from the singlet state of ZnTPP to methylviologen across the liquid-liquid interface.

$$ZnTPP_i + h\nu \rightarrow ZnTPP_i^* \quad (6.1)$$

$$ZnTPP_i^* + MV^{2+}{}_i \rightarrow ZnTPP^+{}_i\bullet + MV^+{}_i\bullet \quad (6.2)$$

The dependence of the relative quenching of emission on the concentration of SDS^- in an aqueous phase was evaluated from the intensity change at 642 nm which the emission peak is assigned to $Q(0,1)$ and plotted in Figure 6.3. The relative quenched intensity was approximately constant value, *i.e.* 13.5 % of the total amount of ZnTPP in the bulk dodecane phase and at the interface, in the lower concentration of SDS^- than *ca.* 10^{-5} mol dm^{-3}. This means that the interfacial concentration quenched is 2.8×10^{-12} mol cm^{-2}. The addition of minute amount of SDS^- effectively quenched even in very low concentration, *i.e.*, less than 10^{-7} mol dm^{-3}. However, the relative quenched intensity was decreased according to the increase of SDS^- in the higher concentration than 10^{-5} mol dm^{-3} and the quenching reaction was completely prevented in the higher concentration than *ca.* 5×10^{-5} mol dm^{-3}. Thus, the quenching reaction was controlled by the adsorption of SDS^-. The scheme of the

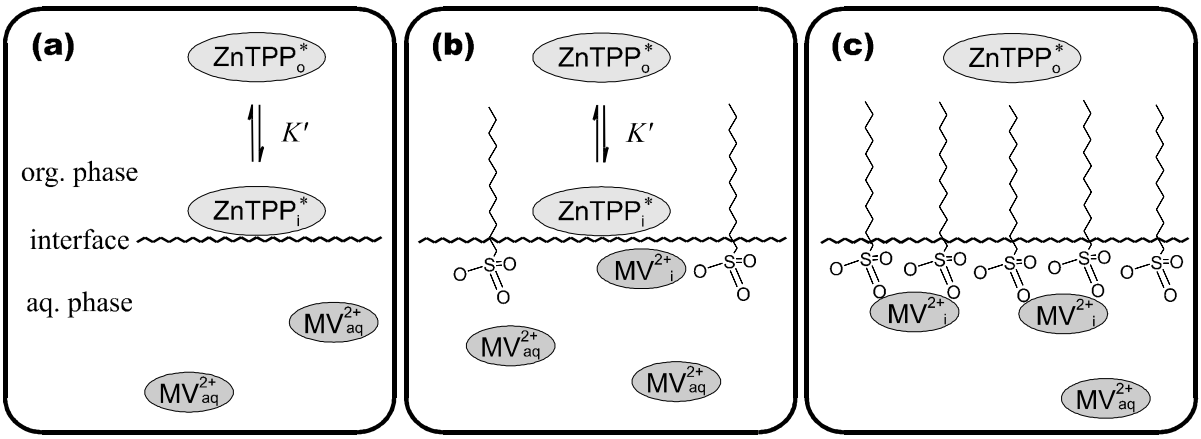

Figure 6.4. Schematic drawing of the fluorescence quenching mechanisms at the liquid-liquid interface. The concentrations of SDS^- in aqueous phase are $[SDS^-] = 0$ mol dm^{-3} (a), $[SDS^-] < 5\times10^{-5}$ mol dm^{-3} (b) and 5×10^{-5} mol $dm^{-3} < [SDS^-]$ (c), respectively.

heterogeneous quenching between ZnTPP in dodecane and methylviologen in an aqueous phase is shown in Figure 6.4. In the absence of SDS^-, ZnTPP is adsorbed at the liquid-liquid interface, but methylviologen dication dissolved in an aqueous phase can not be sufficiently provided to the interface.(Figure 6.4a) In the presence of SDS^-, the cationic quencher can be concentrated at the interface, which is negatively charged by the adsorbed surfactant anions, and the fluorescence quenching reaction takes place.(Figure 6.4b) In the presence of excess SDS^-, the interface is covered with the surfactant anions and the interfacial adsorption of ZnTPP is completely prevented.(Figure 6.4c) If it can be assumed that most of the surfactant molecules added into an aqueous phase is adsorbed at the liquid-liquid interface, the interfacial concentration of SDS can be roughly estimated as 6×10^{-10} mol cm^{-2} in the use of 5×10^{-5} mol dm^{-3} SDS solution. This value is similar to the saturated interfacial concentration reported in the interfacial tension measurement,[17] *i.e.*, 3.75×10^{-10} mol cm^{-2}. Hence, the fluorescence quenching reaction could occur effectively in the condition shown in Figure 6.4(b) in which the concentration of SDS^- in an aqueous phase was less than 5×10^{-5} mol dm^{-3}.

The interfacial adsorbed amount of ZnTPP can be estimated from the interfacial adsorption constant, *i.e.* $K' = 2.1\times10^{-4}$ dm, measured by means of the high-speed stirring method which is shown in Chapter 2. If all amount of ZnTPP at the liquid-liquid interface can be quenched by methylviologen, *ca.* 29 % of the emission should be decreased in the present system, however, the experimental value of the relative quenched intensity of emission was

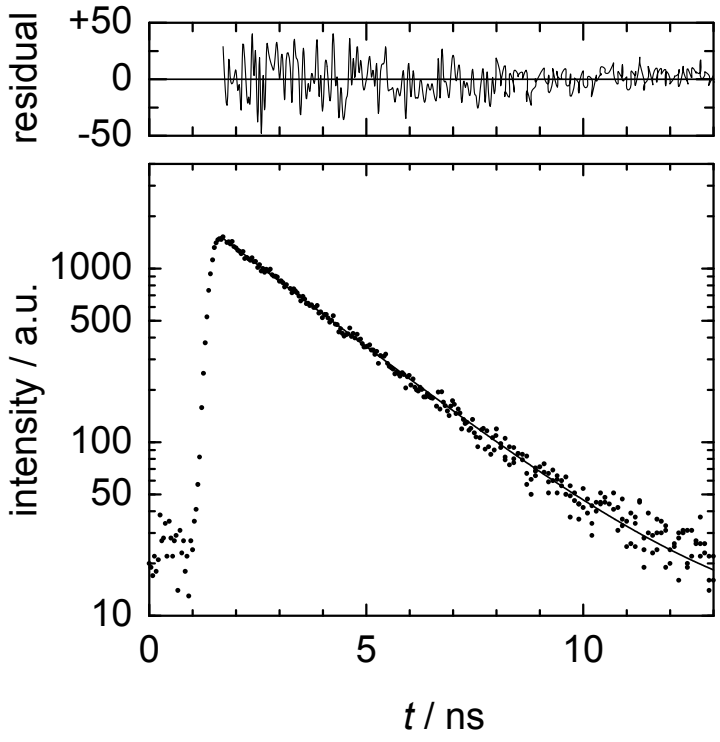

Figure 6.5. The natural fluorescence decay profile of ZnTPP in dodecane at 298 K. The solid line is the fitting curve obtained by the single exponential analysis. Upper figure shows the residual.

13.5 %. The difference between the experimental and evaluated values may be attributed to the limitation of the interfacial concentration of methylviologen. Since the quenching reaction is a bimolecular reaction and competes with the natural fluorescence decay of ZnTPP, the rate equation for the fluorescence decay can be described as

$$-\frac{\mathrm{d}[\mathrm{ZnTPP^*}]_\mathrm{i}}{\mathrm{d}\,t} = \left(k_0 + k_\mathrm{q}[\mathrm{MV}^{2+}]_\mathrm{i}\,\frac{S_\mathrm{i}}{V_\mathrm{o}} \right)[\mathrm{ZnTPP^*}]_\mathrm{i} \qquad (6.3)$$

where k_0, k_q, $[MV^{2+}]_i$ and S_i/V_o are the natural fluorescence decay constant (s^{-1}), the quenching rate constant ($dm^3\ mol^{-1}\ s^{-1}$), the interfacial concentration of methylviologen (mol dm^{-2}) provided by the ion-association with SDS^- and the specific interfacial area (1960 dm^{-1}), respectively. The half life, τ_0, and the rate constant, k_0, of the natural fluorescence decay of ZnTPP were determined as 2.3 ns and 4.4×10^8 s^{-1}, respectively, in the bulk dodecane phase. The observed value of τ_0 of ZnTPP is shorter than most of other phosphors and these results are similar to the reported values in other solvent systems, *e.g.*, 1.9 ns in benzene[4] and 1.7 ns in dichloromethane.[8] Furthermore, the product of k_q and $[MV^{2+}]_iS_i/V_o$ in equation 6.3 is a

finite value, since the maximum value of $[MV^{2+}]_i$ is the saturated interfacial concentration of that attracted by SDS^-. Even if the quencher in the bulk aqueous phase increases much more, the quenching rate, which is a function of the interfacial concentration of methylviologen, will not be able to increase. The value of k_q which is equal to the ET rate constant from the singlet state of Zn porphyrin to acceptor is reported between 10^{13} dm^3 mol^{-1} s^{-1} and 10^9 dm^3 mol^{-1} s^{-1} in various porphyrin systems.[4,7] Since the maximum value of $[MV^{2+}]_i S_i/V_o$ provided by adsorbed SDS^- is evaluated less than 10^{-5} mol dm^{-3} in the present system, it is impossible that the contribution of the bimolecular quenching reaction will be much larger than that of the natural fluorescence decay. This consideration agreed with the fact that the quenched intensity was one half of the predicted value in the present system.

In this study, the fluorescence quenching reaction at the liquid-liquid interface could occur in the presence of the anionic surfactant and the cationic quencher. On the other hands, the presence of excess surfactant also hindered the interfacial adsorption of ZnTPP. Therefore, the surfactant served as a catalyst for the heterogeneous fluorescence quenching reaction and an inhibitor for the interfacial adsorption of ZnTPP.

6.4 REFERENCES

(1) Nagatani, H.; Watarai, H. *Anal. Chem.*, **1996**, *68*, 1250-1253.

(2) Nagatani, H.; Watarai, H. *Anal. Chem.*, **1998**, *70*, 2860-2865.

(3) Hopf, F. R.; Whitten, D. G. In *Porphyrins and Metalloporphyrins*; Smith, K. M. Ed.; Elsevier: New York, 1975; Chapter 16.

(4) Costa, S. M. B.; Velázquez, M. M.; Tamai, N.; Yamazaki, I. *J. Luminescence*, **1991**, *48&49*, 341-351.

(5) Quimby, D. J.; Longo, F. R. *J. Am. Chem. Soc.*, **1975**, *97*, 5111-5117.

(6) Wasielewski, M. R. *Chem. Rev.*, **1992**, *92*, 435-461.

(7) Aota, H.; Araki, S.; Morishima, Y.; Kamachi, M. *Macromolecules*, **1997**, *30*, 4090-4096.

(8) Takahashi, K.; Hase, S.; Komura, T.; Imanaga, H.; Ohno, O. *Bull. Chem. Soc. Jpn.*, **1992**, *65*, 1475-1481.

(9) Harriman, A.; Poter, G.; Searle, N. *J. Chem. Soc. Faraday Trans 2*, **1979**, *76*, 1515-1521.

(10) Song, X.-Z.; Jia, S.-L.; Miura, M.; Ma, J.-G.; Shelnutt, J. A. *J. Photochem. Photobio. A: Chem.*, **1998**, *113*, 233-241.

(11) Volkov, A. G. *Anal. Sci.*, **1998**, *14*, 19-25.

(12) Adler, A. D.; Longo, F. R.; Kampas, F.; Kim, J. *J. Inorg. Nucl. Chem.*, **1970**, *32*, 2443-2445.

(13) Nagatani, H.; Watarai, H. *Chem. Lett.*, **1997**, 167-168.

(14) Astruc, D. *Electron Transfer and Radical Process in Transition-Metal Chemistry*; Wiley-VCH: New York, 1995.

(15) Scully, A. D.; Hirayama, H.; Fukushima, K.; Tominaga, T. *J. Phys. Chem.*, **1993**, 10524-10529.

(16) Harriman, A.; Porter, G.; Richoux, M.-C. *J. Chem. Soc., Faraday Trans 2*, **1982**, *78*, 1955-1970.

(17) Bonfillon, A.; Sicoli, F.; Langevin, D. *J. Colloid Interface Sci.*, **1994**, *168*, 497-504.

Chapter 7

Concluding Remarks

The adsorption and chemical reaction of porphyrin compounds at the liquid-liquid interface were investigated by means of conventional and new methods and the interfacial reaction mechanisms are revealed in this thesis. Their mechanisms are evidently different from those in the homogeneous system and the specificity of the liquid-liquid interface as a reaction field has been confirmed. The author considers that these results furnish valuable suggestions to understand the roles of the liquid-liquid interface in analytical chemistry and biochemistry.

On the promotion of studies, two kinds of *in situ* spectrophotometric methods which can directly measure the species and reaction kinetics at the liquid-liquid interface were proposed, *i.e.* the two-phase stopped-flow method and the centrifugal liquid membrane method, and their advantages were demonstrated. These methods make the kinetic measurement of the interfacial reaction more available in the many systems, which has some difficulties to be carried out by the conventional method. Moreover, the combination of new methods and the indirect method such as the high-speed stirring method can provide the information which is not able to be obtained by individual methods. The application of these methods will be very useful in studying various reaction systems at the liquid-liquid interface.

Acknowledgement

The author would like to express his greatest gratitude to Professor Hitoshi Watarai for his cordial guidance, discussion and support in coordinating this work.

The author also wishes to express his sincere thanks to all staffs of Watarai Laboratory for their helpful suggestion, kind instruction and encouragement in this work.

The author is grateful to all members of Watarai Laboratory, in both present and past, for their helpful advice, assistance and encouragement.

Finally, the author thanks all his friends and family for their help and encouragement.

Papers Relevant to the Present Study

(1) “Two-phase stopped-flow measurement of the protonation of tetraphenylporphyrin at the liquid-liquid interface”
Hirohisa Nagatani and Hitoshi Watarai
Analytical Chemistry, **1996**, *68*, 1250-1253.

(2) “Specific adsorption of metal complexes of tetraphenylporphyrin at dodecane-water interface”
Hirohisa Nagatani and Hitoshi Watarai
Chemistry Letters, **1997**, 167-168.

(3) “Formation and interfacial adsorption of the μ-oxo dimer of (5,10,15,20-tetraphenylporphyrinato)iron(III) in dodecane/aqueous acid system”
Hirohisa Nagatani and Hitoshi Watarai
Journal of the Chemical Society, Faraday Transactions, **1998**, *94*, 247-252.

(4) “Direct spectrophotometric measurement of demetalation kinetics of 5,10,15,20-tetraphenylporphyrinatozinc(II) at the liquid-liquid interface by a centrifugal liquid membrane method”
Hirohisa Nagatani and Hitoshi Watarai
Analytical Chemistry, **1998**, *70*, 2860-2865.

Paper Relate to the Present Study

(1) “Chelate formation and ion-association at liquid-liquid interface”
Hitoshi Watarai, Masashi Gotoh and Hirohisa Nagatani
ISEC96, Value Adding Through Solvent Extraction, Vol. I; Shallcross, D. C., Paimin R., Prvcic, L. M. Eds.; The University of Melbourne, **1996,** pp. 249-253.